ABSTRACT

Title of Document:	HISTORICAL EFFECTS OF FISHING ON AGE STRUCTURE AND STOCK MIXING IN NORTHWEST ATLANTIC BLUEFIN TUNA
	Matthew Ryan Siskey, Master of Science, 2015
Directed By:	Professor David H. Secor Marine Estuarine Environmental Sciences

Bluefin tuna support important fisheries in the Northwest Atlantic Ocean, which have declined in yield from intense, size-selective exploitation. Age structure, size-at-age, and stock composition were investigated as principal responses to exploitation, utilizing otolith microstructural and chemical analysis. To evaluate otoliths as ageing structures, annulus formation was compared to temperature-associated oscillations in otolith strontium:calcium. Evaluation of otolith stable isotope measures used in stock composition analyses indicated significant differences in $\delta^{18}O$ measurements between laboratories, but not $\delta^{13}C$ values. Comparisons of age structure, size-at-age, and stock composition over three periods (1974-1978, 1996-2002, 2009-2014) coinciding with the cycle of exploitation intensity suggest size-selective fishing caused (1) age truncation, where median age declined (14 to 6 years); (2) minor changes in size-at-age; and (3) fluctuating stock composition, with peak mixing in the 1990s (48% eastern stock contribution). Size-specific reductions in fishing mortality could contribute to recovery through more frequent production of strong year-classes.

HISTORICAL EFFECTS OF FISHING ON AGE STRUCTURE AND STOCK MIXING IN NORTHWEST ATLANTIC BLUEFIN TUNA

By

Matthew Ryan Siskey

Thesis submitted to the Faculty of the Graduate School of the
University of Maryland, College Park, in partial fulfillment
of the requirements for the degree of
Master of Science
2015

Advisory Committee:
Professor David H. Secor, Chair
Professor Michael J. Wilberg
Professor Lee W. Cooper

Acknowledgements

I would first like to thank my family. Dan, Kathy, Amanda, Ginny, and Unkie. Thank you for constantly motivating me to be the best that I can be, and supporting me as I pursue each adventure as they come.

Next, I would like to thank the members of the Secor Lab, past and present. In particular, I would like to acknowledge Ben Gahagan, who was elemental in teaching me the ways of tuna sampling and micromill wrangling; and Mike O'Brien, for convincing me, and subsequently teaching me, to use R. In addition, I would like to thank Alex Atkinson, Brian Gallagher, Gray Redding, and the rest of the students at the Chesapeake Biological Laboratory, for their advice and for providing an excellent arena for intellectual gymnastics.

Thanks goes to Derke Snodgrass and Julie Carter at NOAA, for their help acquiring data and otolith samples used in this thesis; to Phil Piccoli, for his guidance, support, and training on microprobe analyses; and to Slava Lyubchich, Dong Liang, David Dettman, and Dana Biasatti for your statistical and analytical guidance. I would also like to express my appreciation for Mike Wilberg and Lee Cooper, my committee members, whose guidance and persistence throughout the process of conducting this thesis was essential.

Finally, I would like to acknowledge my advisor, Dave Secor, and thank him for welcoming me into his lab and providing the opportunity to do this work. Dave, thank you for your unparalleled, seemingly-unlimited patience and support, for pushing me to become a better scientist, and for helping me realize what I am capable of.

Table of Contents

List of Tables

Table 2.1. Size classes, associated curved fork length (cm) for US Atlantic bluefin tuna, and fleet that targets each. Commercial limits are not presented because they are numerous and changing, varying by gear type, season, region, and fishery performance (Source: www.hmspermits.noaa.gov; www.iccat.int/en/RecsRegs.asp).

Table 2.2. Distribution of Atlantic bluefin tuna otolith samples by size (cm; curved fork length), region, and sample.

Table 2.3. Selectivity of Atlantic bluefin tuna age classes from 1970-2013, calculated from age-specific fishing mortality estimates generated in ICCAT's 2014 Atlantic bluefin tuna stock assessment via virtual population analysis (SCRS 2014). Age-16 references all ages >15 years.

Table 2.4. von Bertalanffy parameters of growth curves [L_{inf} (asymptotic length; cm CFL), K (rate at which asymptotic length is approached), and t_0 (length at age-0)] produced for Atlantic bluefin tuna samples landed in the 1970s, 1990s, and 2010s.

Table 2.5. Negative log likelihood contrasts for Atlantic bluefin tuna growth models, which include or exclude decadal effects. Full Model refers to models that incorporate separate decadal parameters; Reduced Model refers to models that use one set of parameters for both decades. Second-order Akaike Information Criteria (AIC_C) and AIC_C differences are reported for growth curves corresponding to the 1970s (N=350), 1990s (N=234), and 2010s (N=1359). Δ_I denotes the AIC_C difference between the full and reduced model.

Table 2.6. von Bertalanffy parameters of growth curves [L_{inf} (asymptotic length; cm CFL), K (rate at which asymptotic length is approached), and t_0 (length at age-0)] produced for assigned western stock Atlantic bluefin tuna samples landed in the 1970s (N=325), 1990s (N=132), and 2010s (N=1185).

Table 2.7. Negative log likelihood contrasts for assigned western stock Atlantic bluefin tuna growth models, which include or exclude decadal effects. Full Model refers to models that incorporate separate decadal parameters; Reduced Model refers to models that use one set of parameters for both decades. Second-order Akaike Information Criteria (AIC_C) and AIC_C differences are reported for growth curves corresponding to the 1970s (N=325), 1990s (N=132), and 2010s (N=1185). Δ_I denotes the AIC_C difference between the full and reduced model.

Table 2.8. Estimated population mixing levels in Atlantic bluefin tuna samples from Gulf of Mexico, New England, and Mid-Atlantic fisheries in the 1970s, 1990s, and 2010s.

Table 2.9. Juvenile and adult mixing levels in Atlantic bluefin tuna samples from Gulf of Mexico, New England, and Mid-Atlantic fisheries from the 1970s, 1990s, and 2010s.

Table 2.10. Estimated population mixing levels in Atlantic bluefin tuna samples from fisheries in the 1970s, 1990s, and 2010s by size class.

Table 2.11. Estimates of Atlantic bluefin tuna stock mixing for strong year classes.

List of Figures

Figure 2.2. Landings (in tonnes) of Atlantic bluefin tuna in the Western (red) and Eastern (blue) North Atlantic from 1950-2013. The Eastern North Atlantic includes the Mediterranean Sea.

Figure 2.3. Catch-at-size data for Atlantic bluefin tuna from fisheries operating in the 1970s (1974-1978), 1990s (1996-2002), and 2010s (2009), obtained via the ICCAT database (https://www.iccat.int/en/accesingdb.htm).

Figure 2.4. Size frequency data for Atlantic bluefin tuna individuals included in the 1970s (1974-1978), 1990s (1996-2002), and 2010s (2009-2014) samples obtained from NOAA.

Figure 2.5. Atlantic bluefin tuna otolith $\delta^{13}C$ values (‰) plotted against estimated year class (estimated age subtracted from year of capture). Regression line and 1 standard error limits are shown.

Figure 2.6. Corrected Atlantic bluefin tuna otolith $\delta^{13}C$values (‰) plotted against estimated year class (estimated age subtracted from year of capture). Regression line and 1 standard error limits are shown.

Figure 2.7. Atlantic bluefin tuna otolith $\delta^{18}O$ values (‰) plotted against estimated year class (estimated age subtracted from year of capture). Regression line and 1 standard error limits are shown.

Figure 2.8. Global sea surface (30 psu; $\leq$ 15 m) $\delta^{18}O$ values (‰) from 1967-2008. Data obtained from National Aeronautics and Space Administration's (NASA) Global Seawater Oxygen-18 database (Schmidt et al. 1999; http://data.giss.nasa.gov/o18data/). Regression line and 1 standard error limits are shown.

Figure 2.9. North Atlantic sea surface (30 psu; $\leq$ 15 m) $\delta^{18}O$ values (‰) from 1971-2004. Data obtained from National Aeronautics and Space Administration's (NASA) Global Seawater Oxygen-18 database (Schmidt et al. 1999; http://data.giss.nasa.gov/o18data/). Regression line and 1 standard error limits are shown.

Figure 2.10. Western North Atlantic sea surface (30 psu; $\leq$ 15 m) $\delta^{18}O$ values (‰) from 1973-2003. Data obtained from National Aeronautics and Space Administration's (NASA) Global Seawater Oxygen-18 database (Schmidt et al. 1999; http://data.giss.nasa.gov/o18data/). Regression line and 1 standard error limits are shown.

Figure 2.11. Mediterranean Sea surface (30 psu; $\leq$ 15 m) $\delta^{18}O$ values (‰) from 1973-2003. Data obtained from National Aeronautics and Space Administration's (NASA) Global Seawater Oxygen-18 database (Schmidt et al. 1999; http://data.giss.nasa.gov/o18data/). Regression line and 1 standard error limits are shown.

Figure 2.12. Atlantic bluefin tuna otolith $\delta^{13}C$ and $\delta^{18}O$ (‰; relative to V-PDB) baseline dataset, composed of age-1 juveniles collected in respective nursery grounds in the US

Mid-Atlantic Ocean (blue symbols) and Mediterranean Sea (red symbols) (1998-2011; N=264; data from Rooker et al. 2014). Dashed ellipses represent 90% confidence.

Figure 2.13. Annotated Atlantic bluefin tuna otolith image showing annuli (opaque bands; white dots), correct section type ("Y" section), measurement scale marker used for interpreting the first annulus.

Figure 2.14. Annotated Atlantic bluefin tuna otolith images showing two section types (A: "V" section; B: "Y" section.

Figure 2.15. Comparison of observed proportional length from ICCAT Atlantic bluefin tuna catch-at-size data (yellow bars) and proportional length from the ADMB model-derived proportional age matrix (blue bars).

Figure 2.16. Cumulative frequencies of Atlantic bluefin tuna otolith $\delta^{18}O$ (‰) for known western (red) and eastern (blue) captured juveniles. A discriminatory threshold for the western stock was determined at the 90th percentile $\delta^{18}O$ value ($\delta^{18}O$ = -0.925) (dashed line).

Figure 2.17. Relative size frequency distributions (cm, curved fork length) for Atlantic bluefin tuna individuals landed in the 1970s (blue; N=350), 1990s (yellow; N=234), and 2010s (green; N=1359). Bin width=10 cm.

Figure 2.18. Relative age frequency distributions (years) for Atlantic bluefin tuna individuals landed in the 1970s (blue; N=350), 1990s (yellow; N=234), and 2010s (green; N=1359). Bin width=1 year.

Figure 2.19. Relative age frequency distributions (years) for adult (age 8+) Atlantic bluefin tuna individuals landed in the 1970s (blue; N=350), 1990s (yellow; N=234), and 2010s (green; N=1359). Bin width=1 year.

Figure 2.20. Cumulative frequencies of size for Atlantic bluefin tuna individuals landed in the 1970s (blue; N=350), 1990s (yellow; N=234), and 2010s (green; N=1359).

Figure 2.21. Cumulative frequencies of age for Atlantic bluefin tuna individuals landed in the 1970s (blue; N=350), 1990s (yellow; N=234), and 2010s (green; N=1359).

Figure 2.22. Age frequency distributions (years) for western stock-categorized Atlantic bluefin tuna individuals landed in the 1970s (blue; N=350), 1990s (yellow; N=234), and 2010s (green; N=1359). Bin width=1 year.

Figure 2.23. Year class frequency distributions for juvenile (<8 years) Atlantic bluefin tuna landed in the 1970s (blue), 1990s (yellow), and 2010s (green). Bin width=1 year.

Figure 2.24. Year class frequency distributions for adult (> 7 years) Atlantic bluefin tuna landed in the 1970s (blue), 1990s (yellow), and 2010s (green). Bin width=1 year.

Executive Summary

Background

Atlantic bluefin tuna (*Thunnus thynnus*) is a highly-migratory, moderately long-lived (30-40 years) species consisting of two reproductive stocks (western and eastern stocks with spawning habitats in the Gulf of Mexico and Mediterranean Sea, respectively), which mix throughout the North Atlantic Ocean (Block et al. 2005; Rooker et al. 2008; Dickhut et al. 2009; Graves et al. 2015). Increased fishing pressure on the western stock in the mid-1900s led to its depletion in the late-1960s [Standing Committee on Research and Statistics (SCRS) 2014]. The stock remains depleted despite rebuilding efforts, leading to the hypothesis that a demographic shift to a reduced population state with diminished recruitment and age structure has occurred (Secor et al. 2015). In particular, the selective nature of both fisheries (market demand) and management (size limits) likely altered age structure by targeting specific demographic classes. The change in western stock yield may have also altered the relative contribution of the eastern stock to Northwest Atlantic fisheries (Rooker et al. 2008). Therefore, the primary goals of this thesis are to (1) further corroborate methods commonly used in age determination and stock mixing analysis; and (2) provide a comprehensive examination of age structure, growth rate, and stock mixing of bluefin tuna in the Northwest Atlantic over the past 40 years.

*Chapter 1: Validation of methods used in investigations of age structure and stock mixing for Atlantic bluefin tuna (*Thunnus thynnus*)*

Investigations of age structure, growth, and stock mixing depend on microstructural and chemical analysis of otoliths. These otolith-based techniques have undergone tests for accuracy and precision (Neilson and Campana 2008; Rooker et al. 2014; Secor et al. 2014) and offer fundamental information on life history, growth rate, mortality, production, spawning site fidelity, and stock mixing for assessment and management. Increasingly these approaches are being employed on an operational basis to improve assessments, requiring involvement of multiple laboratories engaged in the same otolith-based analyses and increased scrutiny on aspects of precision and bias. Here, I evaluate (1) the reproducibility of otolith stable isotope measurements across laboratories, which are used to estimate stock mixing; and (2) a previously untested assumption on the annual periodicity of annulus formation in Atlantic bluefin tuna otoliths.

Inter-laboratory calibration of the Chesapeake Biological Laboratory's (CBL) isotope ratio mass spectrometer (IRMS) and a similar instrument used for routine bluefin tuna otolith stable isotope analysis at University of Arizona's Environmental Isotope Laboratory was conducted using the same set of Atlantic bluefin tuna otoliths. Methods used between laboratory instruments render $\delta^{18}O$ values which are more sensitive to analytical error than $\delta^{13}C$ (Swart et al. 1991; Paul and Skrzypek 2007). Therefore, I hypothesized that measurement of $\delta^{13}C$ values would be more reproducible between laboratories than $\delta^{18}O$ values, and that no systemic bias between instruments would exist. This hypothesis was partially confirmed: $\delta^{18}O$ values measured by the two laboratories

were significantly different, while $\delta^{13}C$ values were not. The sensitivity of these differences in $\delta^{18}O$ values reported between laboratories (mean difference = -0.72 $\pm$ 0.21 per mil; *t*-test: $p < 0.001$) would generate moderate differences in stock mixing results when applied to a stock discrimination analysis, which estimates mixing of eastern and western ABFT stocks in a sample.

Periodicity of annulus formation was evaluated through time series analysis, which tested correspondence between visual annulus assignment (ageing) and oscillations of otolith strontium and calcium (Sr:Ca), which is thought to fluctuate in uptake with seasonal temperatures. The hypothesized periodicity of Sr:Ca fluctuations over annular cycles (1 period per annulus) was confirmed as the highest intensity periodicity using the Lomb-Scargle method of time series analysis, but two additional significant periodicities were identified as well (2 and 3 per annular cycle).

Chapter 1 findings indicate that estimates of stock mixing are sensitive to analytical differences between laboratories, which may reflect lack of accuracy relative to international standards, challenges pertaining to inter-laboratory reproducibility, and/or methodological differences. More work is needed to standardize isotopic analytical techniques between laboratories. In Chapter 1, the time series analysis of otolith Sr:Ca also corroborated visual assignment of annuli (rings) as a proxy for annual age.

*Chapter 2: Demographic changes to Northwestern Atlantic bluefin tuna (*Thunnus thynnus*) associated with size-selective fishing and long-term heightened exploitation*

Long-term and selective fishing was examined for its influence on age structure, growth, and stock composition of bluefin tuna in the Northwest Atlantic Ocean. I

examined three periods of exploitation – 1974-1978, 1996-2002, and 2009-2014 – utilizing otolith-based ageing and stable isotope-stock discrimination analysis to evaluate historical demographic changes. I expected that the combined effects of growth and recruitment overfishing resulted in age truncation, increased growth, less frequent production of strong year-classes, and decadal fluctuations in stock mixing with eastern stock fish. Age frequencies from the two more recent samples, adjusted for fishing selectivity over the 43 years of assessment history (SCRS 2014), showed considerable age truncation in comparison to the 1970s sample, with a decrease in median age from 14 to 6 years over the time period. Changes in growth (size-at-age) over the 40-year period were minor, although observed. Analyses of stock mixing using otolith stable isotope analysis showed a fluctuating pattern, with no apparent eastern contribution in the 1970s, a large eastern stock contribution (48% eastern stock fish) in the 1990s, and the 2010s returning to minimal levels of mixing (4% eastern fish). Despite the continued reliance on first- or second-time spawners, termed recruit spawners (age $\leq$ 12), age structure has expanded slightly in the most recent periods, perhaps owing to moderate stock recovery. Eastern stock contributions have returned to the minimal levels observed in the 1970s, mortality rates have declined, and several strong year classes of western stock origin were produced from 2000-2010. At the least, expansion of age structure and strong year class production indicate the potential for further recovery, especially in light of recent decreases in mortality (from 0.300 yr^{-1} to 0.035 yr^{-1} from the 1970s to the 2010s).

Conclusions

This study indicated that Atlantic bluefin tuna have undergone a demographic shift in age structure and stock mixing over the past 40 years, coinciding with exploitation intensity. Age structure remains diminished in the recent period in comparison to historical age structure observed in the 1970s. Further restoration of older age classes in the stock could contribute to increased resilience through the production of more frequent strong year classes. Conservation of older adults is feasible through the imposition of maximum size limits, or area closures where these large, old, western stock fish occur, but conservation benefits must be carefully assessed against economic costs. Interestingly, only minor changes in growth rate were observed over the 40 years of study despite substantial changes in age structure, suggesting that finer resolution investigations may be necessary, especially considering the continued scientific debate on stock-specific differences in growth and maturity (SCRS 2014).

Estimates of stock mixing are key inputs for Atlantic bluefin tuna assessment, especially when linked to information on age and size structure. Regional and size- or age-based mixing estimates are instrumental in testing the fundamental assessment assumption of no mixing between the two principal stocks and can inform more complex and spatially explicit stock assessment models that are currently under development (Taylor et al. 2011; Kerr et al. 2012).

A major limitation of the stock discrimination analysis presented in my thesis is the inability to unequivocally assign individuals to their natal stock. Development of a new individual-based assignment technique may require incorporation of additional

otolith tracers and more developed classification estimators. Additionally, the development of a new stock assignment approach that utilizes a Bayesian framework could be used to incorporate and simultaneously analyze complementary data types that are typically used in stock discrimination (e.g. otolith chemistry, genetics, tagging).

Chapter 1: Validation of methods used in investigations of age structure and stock mixing for Atlantic bluefin tuna (*Thunnus thynnus*)

Introduction

Otoliths are widely used in fisheries science to determine the ages of fish, information that is critical in evaluating life history parameters for fisheries assessment and management (e.g. growth rate, mortality rates, and production) (Campana 2001). Otoliths can also provide information on migration and stock composition through proxy indicators such as chemical and isotopic tracers which are incorporated into the growth of calcified structures (Elsdon et al. 2008; Secor 2010). For Atlantic bluefin tuna (ABFT; *Thunnus thynnus*), otolith-based ageing, growth rate estimation, and stock discrimination have provided key insights on how migration influences the population dynamics of two stocks which support interjurisdictional and high seas fisheries in the North Atlantic (Rooker et al. 2008; Secor et al. 2015; Chapter 2). In this chapter, I evaluate two important premises of otolith-based age estimation and stock discrimination procedures: the effects of inter-laboratory reproducibility on stock discrimination and the periodicity of annulus (ring) formation.

Inter-Laboratory Reproducibility of Otolith Stable Isotope Measures and Stock Discrimination

Eastern and Western stocks of Atlantic bluefin tuna originate from the Mediterranean Sea and Gulf of Mexico, respectively, and are managed under the assumption that no mixing occurs between them (SCRS 2014), despite significant

evidence to the contrary (Block et al. 2005; Rooker et al. 2008; Dickhut et al. 2009; Graves et al. 2015). Investigations of stock mixing that utilize stable isotope analyses of otolith core material rely on inherent differences in seawater $\delta^{18}O$ values between eastern (Mediterranean Sea) and western Atlantic nursery grounds; oxygen isotopes are incorporated into otolith growth in near-equilibrium to ambient seawater as new layers of calcium carbonate are precipitated onto the pre-existing otolith structure (Kalish 1991; Patterson et al. 1993; Radtke et al. 1996; Thorrold et al. 1997; Campana 1999). The semi-enclosed Mediterranean Sea is a more evaporative basin than western Atlantic shelf waters, so its surface waters contain more positive $\delta^{18}O$ values (LeGrande and Schmidt 2006), resulting in more positive $\delta^{18}O$ values in juvenile bluefin otoliths (Rooker et al. 2008; Rooker et al. 2014). Based on the oceanographic setting of the two nursery grounds, otolith core material extracted from individuals of unknown stock origin can indicate the nursery region of origin. This approach uses a baseline sample of age-1 juveniles collected from respective western and eastern nursery grounds (Rooker et al. 2014) and derives stock classification proportions for an unknown sample using maximum likelihood estimation.

The use of otolith stable isotope analyses in stock discrimination analysis is potentially powerful, and methodologies related to otolith preparation, extraction of material, and estimation of stock mixing have been standardized for Atlantic bluefin tuna across laboratories in the US, Canada, and Europe. As a result, >2000 $\delta^{18}O$ measurements have been used to estimate stock mixing across the North Atlantic (Secor 2015); however only one stable isotope laboratory (at the University of Arizona) is currently performing the stable isotope analyses. Therefore, a major objective of this study is to determine if

otolith isotopic values are reproducible between separate laboratories and mass spectrometry methods.

A previous inter-laboratory study on otolith stable isotopes demonstrated no significant differences in $\delta^{13}C$ values for paired otoliths analyzed at two different laboratories (University of Maryland College Park and University of Houston), but significant variation in $\delta^{18}O$ values. In the current study, I performed within-otolith comparisons to determine inter-laboratory analytical reproducibility and error in $\delta^{13}C$ and $\delta^{18}O$ values. Stock mixing was then estimated using data from the two analytical laboratories.

Sr:Ca Periodicity across Annular Zones

Otoliths contain ring-like structures (annuli), which are commonly used to determine the age of fish. However, the rate of annulus formation must be confirmed as annual to validate this technique. Annuli are composed of alternating opaque and translucent bands (Figure 1), which signify slow and fast growth segments of the year, respectively. Otolith-based ageing of ABFT has been initially validated by Neilson and Campana (2008) via bomb-radiocarbon dating, but this study was limited to verifying absolute age (i.e. longevity). At a recent international ageing workshop for this species held at the Chesapeake Biological Laboratory (CBL), a consensus was reached that more work was needed to establish rates of annulus formation across all age-classes (Secor et al 2014). Therefore, to evaluate rate or periodicity of annulus formation in ABFT, I evaluated whether optical features of annuli (opaque and translucent zones) coincide with oscillations in Sr:Ca measures, which relate to seasonal changes in growth and

temperature. Ratios of Sr:Ca in cod (*Gadus morhua*) and herring (*Clupea harengus*) otoliths, and in corals have been found to be inversely related to temperature, with incorporation presumably under temperature-regulated physiological control (Smith et al. 1979; Schneider and Smith 1982; Radtke 1984; Radtke et al. 1990). Therefore, in this study, the expectation was that Sr:Ca ratios would be associated with the temperature (season) of otolith deposition. In this study, Sr:Ca was measured across successive opaque and translucent zones of annuli spanning the juvenile and adult periods of individual Atlantic bluefin tuna otoliths utilizing an electron microprobe. These measurements of Sr:Ca were then evaluated for seasonal periodicity (Figure 1), which was subsequently compared to the frequency of opaque zone formation.

Methods

Inter-Laboratory Reproducibility of Otolith Stable Isotope Measures and Stock Discrimination

Otoliths (the sagittae of the three otolith pairs occurring in teleosts) were sampled from ABFT landed in North Carolina (USA) during February and March, 2011 (N=90). Otoliths were embedded in Struers epoxy resin (Struers A/S, Ballerup, Denmark) for sectioning. A 2.0-mm thick section containing the core region (the inner-most portion of the otolith, pertaining to the first year of life) was cut along a transverse plane using a Buehler IsoMet saw (Beuhler, Lake Bluff, Illinois). The otolith section was then attached to a glass slide using Crystalbond 509 mounting adhesive (SPI Supplies, West Chester, Pennsylvania) in preparation for milling.

The methods used to collect otolith material and perform stable isotope analysis follow Schloesser et al. (2010). A New Wave Research MicroMill (Freemont, California) was first used to extract carbonate. Using a 500-µm diameter Brasseler round carbide bit (Brasseler USA, Savannah, Georgia), a series of 55-µm passes was performed along a predetermined otolith milling template patterned after the shape of a yearling bluefin tuna otolith. After each sample was milled, otolith powder was collected with a microspatula and stored, and sampling equipment was cleaned with 100% pure USP-grade ethanol to prevent cross contamination.

Carbon ($\delta^{13}C/\delta^{12}C$) and oxygen ($\delta^{18}O/\delta^{16}O$) isotopic composition of the otolith carbonate samples are reported in δ notation (as $\delta^{13}C$ and $\delta^{18}O$, respectively), which - denotes the relative difference (in ‰) between the isotope ratio of the otolith carbonate (R_{Sample}) and the reference carbonate standard (R_{Standard}), as denoted by the equation

$$\delta_{Sample} = \left(\frac{R_{Sample}}{R_{Standard}} - 1\right) \times 10^3.$$

Measurements of $\delta^{13}C$ and $\delta^{18}O$ were made using two isotope-ratio mass spectrometers, one at the University of Arizona's Environmental Isotope Laboratory and the other at the University of Maryland Center for Environmental Science's Chesapeake Biological Laboratory. These two instruments differed in their mode of operation (continuous flow v. dual inlet).

At CBL, the unknown carbonate samples were converted to CO_2 gas (sample gas) by reaction with 100% phosphoric acid for 6 h at 60°C (modified from McCrea 1950). The carbon and oxygen isotope ratios of the resulting CO_2 were measured using a GasBench II peripheral preparation device (Thermo Fisher Scientific, Inc., Bremen, Germany) paired to an IRMS running in continuous flow mode (CF-IRMS) (Delta V

Plus; Thermo Fisher Scientific, Inc., Bremen, Germany). Isotope ratios were calibrated based on periodic measurements of international and laboratory standards (NBS-19, NBS-20, RoyCC, and YWCC) throughout the sequence of unknown samples and reported relative to the Vienna-Pee Dee Belemnite (V-PDB) standard (Brenna et al. 1997; Spotl and Vennemann 2003). The analytical precision (based on replicate analyses of the four international and laboratory standards) was calculated to be $\pm$ 0.06 per mil for $\delta^{13}C$ and $\pm$ 0.05 per mil for $\delta^{18}O$.

The University of Arizona instrument used an automated carbonate preparation device (Kiel-III; Thermo Fisher Scientific, Inc., Bremen, Germany) coupled to a dual-inlet IRMS (Finnigan MAT 252; Thermo Fisher Scientific, Inc., Bremen, Germany). Powered otolith carbonate samples were reacted with dehydrated phosphoric acid under vacuum at 70°C. Analytical precision of the mass spectrometer was determined to be $\pm$0.1 per mil for $\delta^{18}O$ and $\pm$0.08 per mil for $\delta^{13}C$ (1 standard deviation, SD) (Schloesser et al. 2010). In comparison to the CF-IRMS method, the dual-inlet isotope ratio mass spectrometry (DI-IRMS) method, which uses a single aliquot of gas, calibrated isotope ratio measurements by repeatedly alternating between sample gas and standard gas drawn by viscous flow out of a gas reservoir, here six times, so that numerous comparisons could be made between each sample and the standards used (NBS-19 and NBS-18) (Brenna et al. 1997; Spotl and Vennemann 2003). Isotope ratios are also reported relative to the V-PDB standard.

In prior general comparisons of the DI-IRMS (Kiel-III) and CF-IRMS (GasBench II) methods, it has been found that the Kiel device leads to isotopically more positive $\delta^{18}O$ values for carbonates when organic material is bound within the sample. Since fish

otoliths are generally 2-10% organic (Degens 1969), the presence of organic matter may pose some challenges. Additionally, the Kiel device may inaccurately measure $\delta^{13}C$ and $\delta^{18}O$ composition with decreasing carbonate content (increasing inorganic:organic content), which may have occurred here when minimum carbonate mass was barely met (Cui and Wang 2014).

Otolith core material was first analyzed at the University of Arizona. Additional otolith core material from the same individual samples was then analyzed at the Chesapeake Biological Laboratory in two separate analysis sequences. Between-sequence replicates were embedded in each sequence (N=10) and a single otolith carbonate sample was selected to be an internal replicate sample that was analyzed three times in each sequence (within-sequence replicate) to assess internal reproducibility in addition to the reproducibility determined from the international standards used.

The raw isotope data generated at CBL were corrected based upon adherence to international and laboratory standards using a linear regression of the differences between observed and expected values of the internal international and laboratory standards (NBS-19, NBS-20, RoyCC, and YWCC) (Tables 1 and 2). Following correction, otolith $\delta^{13}C$ and $\delta^{18}O$ values were compared between laboratories and between analytical sequences using *t*-tests and paired *t*-tests, respectively (H_0: no significant difference between laboratories). Between-sequence replicates were analyzed separately, because no comparable replicate analyses were undertaken at the University of Arizona, and inter-laboratory differences were estimated. To evaluate the sensitivity of stock discrimination procedures to analytical error, data generated at each laboratory were used in the maximum likelihood procedure that assigns stock origin to an unknown sample of ABFT

(Rooker et al. 2014) and results of this model were compared between datasets. This mixed-stock model (Millar 1990) estimated the variance using bootstrapping with 1000 simulations and otolith stable isotope data from a baseline of age-1 juveniles collected in the US Mid-Atlantic Ocean and Mediterranean Sea from 1998-2011 (Figure 2; N=265; data publicly available from Rooker et al. 2014, http://www.int-res.com/articles/suppl/m504p265_supp.xls).

Sr:Ca Periodicity across Annular Zones

Archived otoliths from older adult fish (age > 10 years) landed in the 1970s (N=32) were obtained from the National Marine Fisheries Service archive at the Southeast Fisheries Science Center in Miami, Florida (USA). A single otolith was randomly selected from each individual for analysis and cleaned of excess tissue. Otoliths were embedded and sectioned as described above.

To determine the rate of annulus formation in ABFT otoliths, coincidence of Sr:Ca oscillations with opaque zone locations (used as a visual indicator for each completed annulus; Figure 1) was evaluated. A power analysis was performed using the data from a preliminary analysis (N=1) to determine sample size. Here, Hartley's *F* test (Hartley 1949) was used to assess power:

$$F = \frac{\bar{p}_1(R - m + 1)}{SSE}$$

where $\bar{p}_1$ is the estimated magnitude of seasonal variation, $\bar{p}$ is the average magnitude across all frequencies, *R* equals half the length of the time series, *m* is the location of annual frequency in the periodogram, and *SSE* is the residual sum of squares. In this

analysis, it was assumed that 5 measurements of Sr:Ca would be obtained per annulus across the first 10 annuli of each otolith, so $R \approx 25$, and $m = 10$. For sample size calculations, power was assessed when $p_1 = 1.25\bar{p}$ and $p_1 = \bar{p}$. Accepting a Type II error of 0.2 at $\alpha=0.05$, a sample size of 26 otoliths was recommended when $p_1 = 1.25\bar{p}$ and 38 otoliths were recommended when $p_1 = \bar{p}$ (Figure 3). This information and the logistical feasibility of various sample sizes led to the sample size of 32 otoliths.

Intra-annular oscillations in Sr:Ca were measured across opaque and translucent zones using an electron probe micro-analyzer (EPMA) (N=32; JXA-8900 Superprobe, JEOL USA, Inc., Peabody, Massachusetts, USA) located in the Nanoscale Imaging Spectroscopy and Properties Laboratory at the University of Maryland, College Park. This instrument is a wavelength-dispersive X-ray spectrometer that uses an electron beam to generate characteristic x-ray intensities of Sr and Ca. Prior to analysis by EPMA, otolith samples were carbon-coated in a high-vacuum evaporator, and the instrument was calibrated using reference standards [calcite ($CaCO_3$) and strontianite ($SrCO_3$)].

Profile analysis has typically been used to quantify differences in chemical composition along an otolith axis from early to later lifetime periods, across daily increments or annular structures. Profiles relate different temporal periods (days, weeks, months, years, etc.) to environments experienced (Elsdon et a. 2008). Here, measurements of strontium and calcium were taken over ~50 30-µm increments for the first ~8 annuli, followed by ~40 20-µm increments for the following 4-6 annuli. This sampling design adjusted for decreasing annular width with age: annulus width in the adult period typically ranges from 80-100 µm, and the goal was to make at least four

probe measurements per annulus (20-µm is the spatial resolution limit). Measurements began proximal to the first annulus and ended distal to the 12th annulus.

The Sr:Ca measurements taken along the transect were then converted to un-equally spaced time series. Opaque bands were considered the start of an annulus, and measurement points within a cycle (opaque > translucent > opaque) were converted to fractional ages within the cycle. After the removal of one individual outlier point, attributed to a crack in the otolith, time series were detrended by extracting a parametric linear trend that was evident in the data (see Figure 4) so the subsequent analysis could focus on short-term oscillating trends. This positive linear trend was thought to be related to the increased thermal niche (more extreme warm and cool temperatures) that ABFT experience as they develop and expand their migratory behavior into higher latitudes and deeper waters. These colder-water habitats would be expected to amplify otolith Sr concentrations based upon the inverse relationship between Sr uptake and temperature.

The periodicities of the detrended time series of Sr:Ca measures were identified using a Lomb—Scargle periodogram that accounts for un-equally spaced measurements (V. Lyubchic, Chesapeake Biological Laboratory, pers. communication; Lomb 1976; Scargle 1982; Ruf 1999). Fourier series were then used for harmonic filtering to eliminate the identified periodic components and continue the search for other periodicities (Ferraz-Mello 1981):

$$y_t = \sum_{j=0}^{n} \{a_j \cos(w_j t) + \beta_j \sin(w_j t)\}$$

where y_t are the periodicities of the detrended Sr:Ca time series at time t, $w_j = \frac{2\pi j}{T}$ is the angular velocity and relates to a pair of trigonometrical components that undergo j cycles

over the length of the time series, *T* is the length of the time series, and $n = \frac{T}{2}$. Residual periodograms were constructed at each step to ensure that all significant periodicities were filtered out. Additionally, Hartley's F_{max} test was used to test the significance of the harmonic terms with the highest intensity (Hartley 1949):

$$F_{max} = \frac{\frac{1}{4} n S_{max}^2 (n - 2m - 1)}{R^2}$$

where n is the length of the time series, S_{max}^2 is the largest observed harmonic intensity, m is the number of harmonic terms tested, and R^2 is the residual sum of squares. The calculated F_{max} was then compared to the critical value from the ordinary *F*-distribution ($F_{\alpha/m,2,(n-2*m-1)}$). In addition, *F*-ratio was used to test the significance of multiple periodicities. Here, the calculated *F*-ratios were compared with a critical value ($F_{\alpha/m,2,(n-2*m-1)}$), and the search for significant periods ceased when an insignificant result was reached. The denominator *m* ensures that the familywise error rate (i.e., the probability of making any false discoveries in the multiple testing procedure) is maintained at the level $\alpha = 0.05$.

Results

Inter-Laboratory Reproducibility of Otolith Stable Isotope Measures and Stock Discrimination

Comparisons of corrected Atlantic bluefin tuna otolith $\delta^{13}C$ and $\delta^{18}O$ data between laboratories confirmed findings of previous work (Rooker et al. 2006; Rooker et al. 2008) that $\delta^{18}O$ values are less reproducible than $\delta^{13}C$ measurements. Between-laboratory comparisons showed no significant laboratory effect in the analysis of $\delta^{13}C$

(mean difference = -0.03 + 0.03 per mil; t-test: p = 0.69; Tables 3 and 4), while estimates of $\delta^{18}O$ were significantly different between laboratories (mean difference = -0.72 + 0.21 per mil; t-test: $p < 0.001$; Tables 3 and 4; Figure 5) with $\delta^{18}O$ values measured using Chesapeake Biological Laboratory's instrument systematically more negative. Replicates embedded in both CBL sequences (N=10) did not have significantly different $\delta^{13}C$ values (mean difference = 0.22 + 0.04 per mil; t-test: p = 0.11; Tables 3 and 4); however, $\delta^{18}O$ values were significantly different (mean difference = 0.86 + 0.03 per mil; t-test: $p < 0.001$; Tables 3 and 4). In comparisons of stock classification estimates that are based upon $\delta^{13}C$ and $\delta^{18}O$ values for the same sample measured by the two instruments, the isotope values from the Arizona instrument estimated an 89% contribution of the western stock to the sample, but the isotope values generated by the CBL instrument estimated that it was solely (100%) of western origin (Table 5). The results of this analysis reflect the tendency of the CBL instrument to report more negative $\delta^{18}O$ values for the same samples in comparison to the University of Arizona instrument.

Sr:Ca Periodicity across Annular Zones

Time series analysis of the data using the Lomb—Scargle method showed evidence of significant annular periodicity within otoliths, with the largest peak occurring at the period of 1 full annulus, as represented by the opaque zone (Figure 6). Additional Fourier series related to 0.5 and 0.33 annular periods were added to remove all significant periodicities in the detrended series (Figures 7 and 8). The Hartley's F-test for m = 5 confirmed significance of the annular periodicity (F_max> F_crit; F_max=112.7,

F_crit=4.1; $p < 0.001$). The F-ratio test of multiple periodicities found annular, bi-annular, and tri-annular periods to be significant (F-ratio > F_crit, F_crit=4.61; Table 6). The search for significance was ended after the third period, due to insignificance of a fourth period (criterion $p < 0.01$).

Discussion

Inter-Laboratory Reproducibility of Otolith Stable Isotope Measures and Stock Discrimination

To assess reproducibility of otolith stable isotope estimates between Chesapeake Biological Laboratory and University of Arizona instruments, I analyzed otolith material from the same individuals at both laboratories, and found that isotope ratio estimation of $\delta^{13}C$ was more reproducible between laboratories than $\delta^{18}O$. These differences in $\delta^{18}O$ values between laboratories caused subsequent deviations in the results of stock discrimination analysis, when using stable isotope measures from the two laboratories. Differences in fractionation between carbon and oxygen may explain the statistical differences observed in measured $\delta^{18}O$ values between laboratories. Typically, carbon from the otolith carbonate is completely converted to CO_2 via reaction with phosphoric acid, resulting in retention of the carbonate's $\delta^{13}C$ value in the CO_2 generated for mass spectrometric analysis. However, oxygen in the CO_2 analyzed is also sourced from other ions subjected to isotopic fractionation, leading to $\delta^{18}O$ values that are potentially more sensitive to analytical error (Swart et al. 1991; Paul and Skrzypek 2007).

The results of the analysis confirm my hypothesis that estimation of $\delta^{13}C$ was more reproducible than $\delta^{18}O$ between laboratories. The CBL instrument reported more

negative oxygen stable isotope values for the same samples in comparison to the University of Arizona instrument. These results indicate that analysis of stock mixing through otolith stable isotope composition is sensitive to the analytical method used. More work must be done to compare analytical techniques (e.g CF-IRMS v. DI-IRMS) between laboratories, determine the most appropriate technique for the application of stock discrimination analysis, and assess the potential limitations of analyses that depend upon relatively small variations in isotopic composition, as is the case here.

In this study, significant within-laboratory variation observed at CBL may have been a product of room temperature fluctuations (Figure 9), which can influence the isotopic content of water in equilibrium with carbon dioxide during analysis. The data correction performed on CBL data adjusted for drift of the data based on adherence of the international and laboratory standards to their true values, but did not adjust the data for the possible effects of fluctuating temperature in the analytical room housing the mass spectrometer. A separate correction for this effect was attempted but did not lead to satisfactory results. Here, the temperature correction may have confounded the differences observed between the analytical sequences and the differences documented between the laboratories. Future research could explore analytical improvements that would emphasize between-laboratory sequences of certified reference materials together with replicate otolith material.

Sr:Ca Periodicity across Annular Zones

Using an x-ray dispersive method to quantify and analyze Sr:Ca across annular cycles of Atlantic bluefin tuna otoliths, I confirmed that cycles of Sr:Ca, a proxy for

seasonal temperature, were associated with annulus formation. As expected, Sr:Ca fluctuated over annular cycles at the rate of 1 peak per annulus. However, 2 and 3 peaks per annular cycle were also identified as significant, although smaller in magnitude. The periodicity of 1 peak per annular cycle is consistent with seasonal temperature change; however, 2 or 3 peaks per annular cycle are not.

The lower-intensity periodicities observed could be the result of ageing inaccuracies, which, if systematic, could have led to significant sub-annular periodicities in Sr:Ca as observed here. However, this explanation is unlikely as it would require a consistent bias in mis-assignment. Further, the reader's ageing ability was calibrated using an ABFT otolith reference set and deemed precise to a level < 10% error (Secor et al. 2014).

An alternative explanation could be related to sub-seasonal temperature cycles and physiological responses. Radtke and Morales-Nin (1989) found "short-period" (sub-annular) cycles in otolith Sr:Ca across daily increments of juvenile Atlantic bluefin tuna otoliths and attributed these to short-term changes in temperatures that they encountered.

Otolith Sr:Ca ratios are influenced by the level of free Ca in the endolymph surrounding the otolith (Mugiya 1966; Mugiya and Takahashi 1985). Therefore, lower-intensity periodicities may be reflective of periodically increased calcium-binding proteins in the blood (Kalish 1989), which decrease free Ca in the blood and endolymph and increase Sr:Ca otolith uptake. Stress, physiology, condition, and reproduction can all influence the amount of calcium-binding proteins in the blood and, subsequently, otolith Sr:Ca concentrations. Nevertheless, regular periodicity in blood-bound Ca remains unclear.

This study complements previous validation of otolith-ageing for this species (Neilson and Campana 2006), which linked otolith-ageing to the absolute age of the otolith via bomb radiocarbon dating, and efforts to standardize otolith ageing techniques (Secor et al. 2014). Together, these three studies confirm that (1) ABFT otolith-ageing accurately captures the true age of ABFT (absolute age), (2) readers are able to visually resolve and identify individual annuli, and (3) annuli do in fact represent one year of otolith growth.

References

Block, B. A., L. L. H. Teo, A. Walli, A. Boustany, M. J.W. Stokesbury, C. J. Farwell, K. C. Weng, H. Dewar, and T. D. Williams. 2005. Electronic tagging and population structure of Atlantic bluefin tuna. Nature 434:1121-1127.

Brenna, J.T., T.N. Corso, H.J. Tobias, and R.J. Caimi. 1997. High-precision continuous-flow isotope ratio mass spectrometry. Mass Spectrometry Reviews 16: 227-258.

Campana, S.E. 1999. Chemistry and composition of fish otoliths: pathways, mechanisms, and applications. Marine Ecology Progress Series 1888: 263-297.

Campana, S.E. 2001. Accuracy, precision and quality control in age determination, including a review of the use and abuse of age validation methods. Journal of Fish Biology 59: 197-242.

Cui, L., and X. Wang. 2014. Determination of carbon and oxygen isotopes of geological samples with a complicated matrix: comparison of different analytical methods. Analytical Methods 6: 9173-9178.

Degens, E.T., W.G. Deuser, and R.L. Haedrich. 1969. Molecular structure and composition of fish otoliths. Marine Biology 2: 105-113.

Dickhut, R.M., A.D. Deshpande, A. Cincinelli, M.A. Cochran, S. Corsolini, R.W. Brill, D.H. Secor, and J.E. Graves. 2009. Atlantic bluefin tuna (*Thunnus thynnus*) population dynamics delineated by organochlorine tracers. Environmental Science & Technology 43: 8522-8527.

Elsdon, T.S., B.K. Wells, S.E. Campana, B.M. Gillanders, C.M. Jones, K.E. Limburg, D.H. Secor, S.R. Thorrold, and B.D. Walther. 2008. Otolith chemistry to describe movements and life-history parameters of fishes: hypotheses, assumptions, limitations and inferences. Oceanography and Marine Biology: An Annual Review 46: 297-330.

Ferraz-Mello, S. 1981. Estimation of periods from unequally spaced observations. The Astronomical Journal 86: 619-624.

Graves, J.E., A.S. Wozniak, R.M. Dickhut, M.A. Cochran, E.H. MacDonald, E. Bush, H. Arrizabalaga, and N. Goni. 2015. Transatlantic movements of juvenile Atlantic bluefin tuna inferred from analyses of organochlorine tracers. Canadian Journal of Fisheries and Aquatic Sciences 72: 1-9.

Hartley, H. 1949. Tests of significance in harmonic analysis. Biometrika 194-201.

Kalish, J.M. 1989. Otolith microchemistry: validation of the effects of physiology, age and environment on otolith composition. Journal of Experimental Marine Biology and Ecology 132: 151-178.

Kalish, J.M. 1991. ^{13}C and ^{18}O isotopic disequilibria in fish otoliths: metabolic and kinetic effects. Marine Ecology Progress Series 75: 191-203.

LeGrande, A.N., and G.A. Schmidt. 2006. Global gridded data set of the oxygen isotopic composition in seawater. Geophysical Research Letters 33: L12604.

Lomb, N.R. 1976. Least-squares frequency analysis of unequally spaced data. Astrophysics and Space Science 39: 447-462.

McCrea, J.M. 1950. On the isotopic chemistry of carbonates and a paleotemperature scale. The Journal of Chemical Physics 18: 849-857.

Millar, R.B. 1990. A versatile computer program for mixed stock fishery composition estimation. Canadian Technical Report of Fishery and Aquatic Science No. 1753.

Neilson, J.D., and S.E. Campana. 2008. A validated description of age and growth of western Atlantic bluefin tuna (*Thunnus thynnus*). Canadian Journal of Fisheries and Aquatic Sciences 65: 1523-1527.

Patterson, W.P., G.R. Smith, and K.C. Lohmann. 1993. Continental paleothermometry and seasonality using the isotopic composition of aragonitic otoliths of freshwater fishes. *Climate change in continental isotopic records*: 191-202.

Paul, D., and G. Skrzypek. 2007. Assessment of carbonate-phosphoric acid analytical technique performed using GasBench II in continuous flow isotope ratio mass spectrometry. International Journal of Mass Spectrometry 262: 180-186.

Radtke, R.L. 1984. Cod fish otoliths: information storage structures. In *The propagation of Cod* Gadus morhua *L*. (E. Dahl, D.S. Danielssen, E. Moksness, and P. Solemdal) 273-298.

Radtke, R.L., and B. Morales-Nin. 1989. Mediterranean juvenile bluefin tuna: life history patterns. Journal of Fish Biology 35:485-496.

Radtke, R.L., D.W. Townsend, S.D. Folsom, and M.A. Morrison. 1990. Strontium:calcium concentration ratios in otoliths of herring larvae as indicators of environmental histories. Environmental Biology of Fishes 27: 51-61.

Radtke, R.L., W. Showers, E. Moksness, and P. Lenz. 1996. Environmental information stored in otoliths: insights from stable isotopes. Marine Biology 127: 161-170.

Rooker, J.R., D.H. Secor, G. De Metrio, and E. Rodriquez-Marin. 2006. Evaluation of population structure and mixing rates of Atlantic bluefin tuna from chemical signatures in otoliths. ICCAT Collective Volume Science Papers 59: 813-818.

Rooker, J.R., D.H. Secor, G. D. DeMetrio, R. Schloesser, B.A. Block, and J.D. Neilson. 2008. Natal homing and connectivity in Atlantic bluefin tuna populations. Science 322: 742-744.

Rooker, J.R., H. Arrizabalaga, I. Fraile, D.H. Secor, D.L. Dettman, N. Abid, P. Addis, S. Deguara, F.S. Karakulak, A. Kimoto, O. Sakai, D. Macias, M.N. Santos. 2014. Crossing the line: migratory and homing behaviors of Atlantic bluefin tuna. Marine Ecology Progress Series 504: 265-276.

Ruf, T. 1999. The Lomb-Scargle periodogram in biological rhythm research: analysis of incomplete and unequally spaced time-series. Biological Rhythm Research 30: 178-201.

Scargle, J.D. 1982. Studies in astronomical time series analysis. II. Statistical aspects of spectral analysis of unevenly spaced data. The Astrophysical Journal 263: 835-853.

Schloesser, R.W., J.D. Neilson, D.H. Secor, and J.R. Rooker. 2010. Natal origin of Atlantic bluefin tuna (*Thunnus thynnus*) from Canadian waters based on otolith for $\delta^{13}C$ and $\delta^{18}O$. Canadian Journal of Fisheries and Aquatic Science 67: 563-569.

Schneider, R.C., and S.V. Smith. 1982. Skeletal Sr content and density in *Porites* spp. In relation to environmental factors. Marine Biology 66: 121-131.

Secor, D.H. 2010. Is otolith science transformative? New views on fish migration. Environmental Biology of Fishes 89: 209-220.

Secor, D.H. 2015. Migration ecology of marine fishes. Johns Hopkins University Press, Baltimore.

Secor, D.H., R. Allman, D. Busawon, B. Gahagan, W. Golet, E. Koob, P. Lastra Luque, and M. Siskey. 2014. Standardization of otolith-based ageing protocols for Atlantic bluefin tuna. ICCAT Collective Volume of Scientific Papers SCRS/2013/084.

Secor, D.H., J.R. Rooker, B.I. Gahagan, M.R. Siskey, and R. W. Wingate. 2015. Depressed resilience of bluefin tuna in the Western Atlantic and age truncation. Conservation Biology 29: 400-408.

Smith, S.V., R.W. Buddemeier, R.C. Redalje, and J.E. Houck. 1979. Strontium-calcium thermometry in coral skeletons. Science 204: 404-406.

Spotl, C. and T.W. Vennemann. 2003. Continuous-flow isotope ratio mass spectrometric analysis of carbonate minerals. Rapid Communications in Mass Spectrometry 17: 1004-1006.

Swart, P.K, S.J. Burns, and J.J. Leder. 1991. Fractionation of the stable isotopes of oxygen and carbon in carbon dioxide during the reaction of calcite with phosphoric acid

as a function of temperature and technique. Chemical Geology (Isotope Geoscience Section) 86: 89-96.

Thorrold, S.R., C.M. Jones, and S.E. Campana. 1997. Response of otolith microchemistry to environmental variations experienced by larval and juvenile Atlantic croaker (*Micropogonias undulatus*). Limnology and Oceanography 42: 102-111.

Tables

Table 1.1. Atlantic bluefin tuna otolith $\delta^{13}C$ and $\delta^{18}O$ values generated at the Chesapeake Biological Laboratory's (CBL) Stable Isotope Laboratory and the University of Arizona's Environmental Isotope Laboratory. CBL data was corrected based upon adherence to international and laboratory standards using linear regression of the differences between observed and expected values of the internal international and laboratory standards (NBS-19, NBS-20, RoyCC, and YWCC).

	$\delta^{13}C$		$\delta^{18}O$	
Sample ID	*CBL*	*AZ*	*CBL*	*AZ*
2011_NC_4	-9.04	-9.02	-1.57	-1.12
2011_NC_5	-8.77	-8.67	-1.73	-1.42
2011_NC_7	-8.72	-8.73	-1.81	-1.49
2011_NC_11	-7.95	-8.06	-1.35	-1.05
2011_NC_14	-8.86	-8.98	-1.42	-1.31
2011_NC_15	-8.52	-8.45	-1.15	-0.95
2011_NC_16	-7.98	-7.80	-1.56	-1.43
2011_NC_19	-8.61	-8.66	-1.80	-1.68
2011_NC_20	-8.85	-8.95	-1.35	-1.26
2011_NC_21	-9.25	-9.43	-1.44	-1.18
2011_NC_22	-9.36	-9.56	-1.45	-1.10
2011_NC_23	-8.62	-8.86	-1.19	-0.90
2011_NC_26	-9.05	-9.11	-1.68	-1.45
2011_NC_28	-8.95	-8.78	-1.49	-1.26
2011_NC_29	-8.28	-8.44	-1.25	-1.03
2011_NC_30	-8.86	-8.75	-1.43	-1.14
2011_NC_33	-8.55	-8.69	-1.04	-0.98
2011_NC_34	-8.59	-8.51	-1.22	-1.13
2011_NC_35	-9.71	-9.83	-1.43	-1.35
2011_NC_37	-8.88	-8.91	-1.45	-1.30
2011_NC_39	-8.76	-8.73	-1.23	-1.16
2011_NC_41	-9.22	-9.26	-1.41	-0.94
2011_NC_42	-8.95	-8.71	-1.28	-0.77
2011_NC_44	-8.92	-8.99	-1.76	-1.13

2011_NC_45	-8.44	-8.48	-1.37	-1.04
2011_NC_46	-9.18	-8.98	-1.84	-0.90
2011_NC_47	-8.57	-8.49	-1.72	-0.85
2011_NC_50	-8.43	-8.47	-1.11	-0.77
2011_NC_51	-7.79	-7.85	-1.58	-1.31
2011_NC_52	-8.60	-8.86	-1.85	-1.53
2011_NC_53	-8.87	-8.92	-1.67	-1.43
2011_NC_54	-9.49	-9.85	-1.11	-0.98
2011_NC_56	-8.72	-8.76	-0.96	-0.92
2011_NC_57	-8.91	-9.11	-1.08	-0.94
2011_NC_59	-8.87	-8.87	-2.18	-1.78
2011_NC_61	-8.75	-9.04	-1.33	-1.08
2011_NC_63	-9.40	-9.41	-1.64	-1.27
2011_NC_66	-9.20	-9.11	-2.01	-1.51
2011_NC_67	-9.07	-8.88	-2.53	-1.66
2011_NC_68	-7.78	-7.80	-0.64	-0.40
2011_NC_71	-9.05	-8.79	-2.72	-1.57
2011_NC_72	-8.91	-9.07	-2.64	-1.09
2011_NC_73	-9.15	-8.84	-2.32	-1.44
2011_NC_74	-8.64	-8.47	-2.32	-1.09
2011_NC_75	-8.80	-8.82	-2.29	-1.11
2011_NC_76	-8.92	-8.56	-2.29	-0.78
2011_NC_77	-8.24	-8.12	-2.72	-1.64
2011_NC_78	-8.84	-8.58	-2.59	-1.39
2011_NC_79	-8.61	-8.49	-2.09	-1.07
2011_NC_86	-9.37	-9.32	-2.35	-1.17
2011_NC_82	-8.81	-8.51	-2.14	-0.74
2011_NC_84	-8.91	-8.72	-2.36	-1.22
2011_NC_85	-8.96	-8.74	-2.34	-1.24
2011_NC_87	-8.59	-8.47	-2.10	-0.91
2011_NC_88	-8.68	-8.47	-2.13	-0.84
2011_NC_89	-9.08	-9.20	-2.24	-1.07
2011_NC_90	-8.51	-8.53	-2.30	-1.37
2011_NC_60	-8.86	-8.64	-2.28	-0.97
2011_NC_92	-8.20	-8.13	-2.44	-1.28
2011_NC_93	-9.40	-9.45	-2.43	-1.15

2011_NC_94	-8.47	-8.52	-2.52	-1.61
2011_NC_95	-8.76	-8.67	-2.27	-1.11
2011_NC_96	-8.74	-8.51	-2.22	-1.17
2011_NC_64	-8.13	-7.93	-3.08	-2.06
2011_NC_98	-9.37	-9.31	-2.41	-1.50
2011_NC_99	-8.87	-8.91	-2.20	-1.22
2011_NC_101	-8.93	-8.87	-2.22	-1.26
2011_NC_102	-8.53	-8.64	-1.38	-0.85
2011_NC_65	-9.10	-8.94	-2.31	-1.01
2011_NC_104	-8.59	-8.40	-2.23	-1.31
2011_NC_105	-8.75	-9.04	-2.21	-1.11
2011_NC_106	-8.96	-9.08	-2.45	-1.53
2011_NC_108	-8.40	-8.55	-2.60	-1.64
2011_NC_109	-8.57	-8.67	-3.01	-1.93
2011_NC_110	-8.67	-8.71	-2.75	-1.61
2011_NC_81	-8.14	-8.24	-1.89	-0.88
2011_NC_83	-8.82	-8.77	-2.22	-0.79
2011_NC_100	-9.42	-9.01	-2.69	-1.41
2011_NC_107	-9.26	-9.18	-2.79	-1.45
2011_NC_9	-9.52	-9.21	-2.37	-1.14

Table 1.2. $\delta^{13}C$ and $\delta^{18}O$ values from between-sequence replicate Atlantic bluefin tuna otolith samples, generated at the Chesapeake Biological Laboratory's (CBL) Stable Isotope Laboratory.

	$\delta^{13}C$		$\delta^{18}O$	
Sample ID	*Sequence 1*	*Sequence 2*	*Sequence 1*	*Sequence 2*
2011_NC_2	-8.64	-8.84	-1.26	-1.99
2011_NC_10	-8.07	-8.31	-1.80	-2.68
2011_NC_18	-8.80	-8.81	-1.32	-2.13
2011_NC_24	-8.60	-8.75	-1.70	-2.50
2011_NC_32	-8.55	-8.51	-1.38	-2.07
2011_NC_36	-8.67	-8.72	-0.94	-1.80
2011_NC_43	-8.27	-8.54	-1.58	-2.39
2011_NC_49	-9.02	-9.38	-1.59	-2.26
2011_NC_55	-8.19	-8.81	-0.72	-1.86
2011_NC_70	-8.69	-8.99	-1.11	-2.31

Table 1.3. Absolute mean differences of corrected $\delta^{13}C$ and $\delta^{18}O$ values (per mil) for between-sequence replicates of Atlantic bluefin tuna otolith samples, generated at the Chesapeake Biological Laboratory's (CBL) Stable Isotope Laboratory, and corrected international standard measurements. Data was corrected based upon adherence to international and laboratory standards using a linear regression of the differences between observed and expected values of the internal international and laboratory standards (NBS-19, NBS-20, RoyCC, and YWCC) during each analysis sequence. International standard values used in calculation of the difference are averaged values from three replicates in each sequence.

	Replicates	*NBS-19*	*NBS-20*	*RoyCC*	*YWCC*
$\delta^{13}C$ (per mil)	0.22	0.11	0.15	0.26	0.00
$\delta^{18}O$ (per mil)	0.86	0.18	0.11	0.17	0.09

Table 1.4. P-values for t-tests of between-laboratory and between-sequence comparisons (CBL only) of Atlantic bluefin tuna otolith $\delta^{13}C$ and $\delta^{18}O$ values generated at the Chesapeake Biological Laboratory's (CBL) Stable Isotope Laboratory and the University of Arizona's Environmental Isotope Laboratory. Between-lab comparisons used t-tests and were performed utilizing all of the non-replicated data analyzed at each laboratory (N=80). Between-sequence comparisons used paired t-tests to compare replicates of the same samples (N=10) analyzed in each sequence of the CBL machine. CBL_1 refers to the samples analyzed in the first analysis sequence for the instrument at CBL. Data was corrected based upon adherence to international and laboratory standards using linear regression of the differences between observed and expected values of the internal international and laboratory standards (NBS-19, NBS-20, RoyCC, and YWCC). * = significant p-value.

	CBL v. Arizona	*CBL_1 v. CBL_2*
$\delta^{13}C$ (per mil)	0.692	0.113
$\delta^{18}O$ (per mil)	< 0.001*	< 0.001*

Table 1.5. Estimates of stock mixing of Atlantic bluefin tuna in the 2011 North Carolina winter fishery using corrected $\delta^{13}C$ and $\delta^{18}O$ values from paired analyses conducted at the University of Arizona's Environmental Isotope Laboratory and the Chesapeake Biological Laboratory's Stable Isotope Laboratory.

Years sampled	*Location*	*Laboratory*	*n*	*Population*	*MLE%*	*MLE SD*
2011	North Carolina	Arizona	80	west	89	6.8
				east	11	
2011	North Carolina	CBL	80	west	100	0.2
				east	0	

Table 1.6. *F*-ratio test of multiple periodicities in Atlantic bluefin tuna otolith Sr:Ca time series data. The search for significance was ended after the first insignificant ($p > 0.01$) result.

Periodicity (per annulus)	F-*ratio*	*Critical Value*	*p*
1	90.77	4.61	< 0.001
2	28.25	4.61	< 0.001
3	21.90	4.61	< 0.001
4	3.59	4.61	0.028
5	5.51	4.61	< 0.01

Figures

Figure 1.1. Annotated Atlantic bluefin tuna otolith micrograph image showing opaque and translucent zones combined to form annuli (opaque zones = yellow dots). Also shown are microprobe transects (white squares) used to evaluate the periodicity of annulus formation.

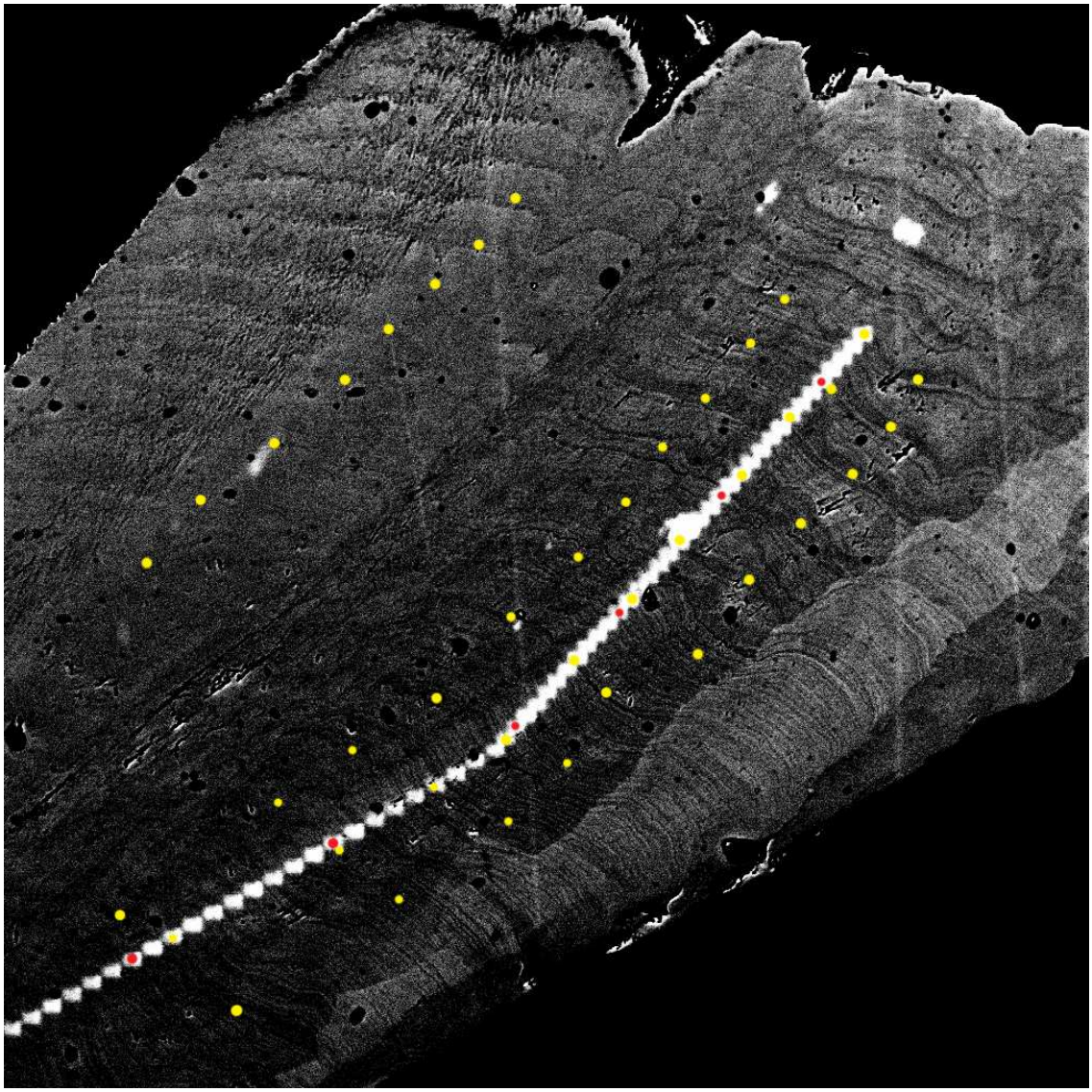

Figure 1.2. Atlantic bluefin tuna otolith $\delta^{13}C$ and $\delta^{18}O$ (‰; relative to V-PDB) baseline dataset, composed of age-1 juveniles collected in respective nursery grounds in the US Mid-Atlantic Ocean (blue symbols) and Mediterranean Sea (red symbols) (1998-2011; N=264; data from Rooker et al. 2014). Dashed ellipses represent 90% confidence.

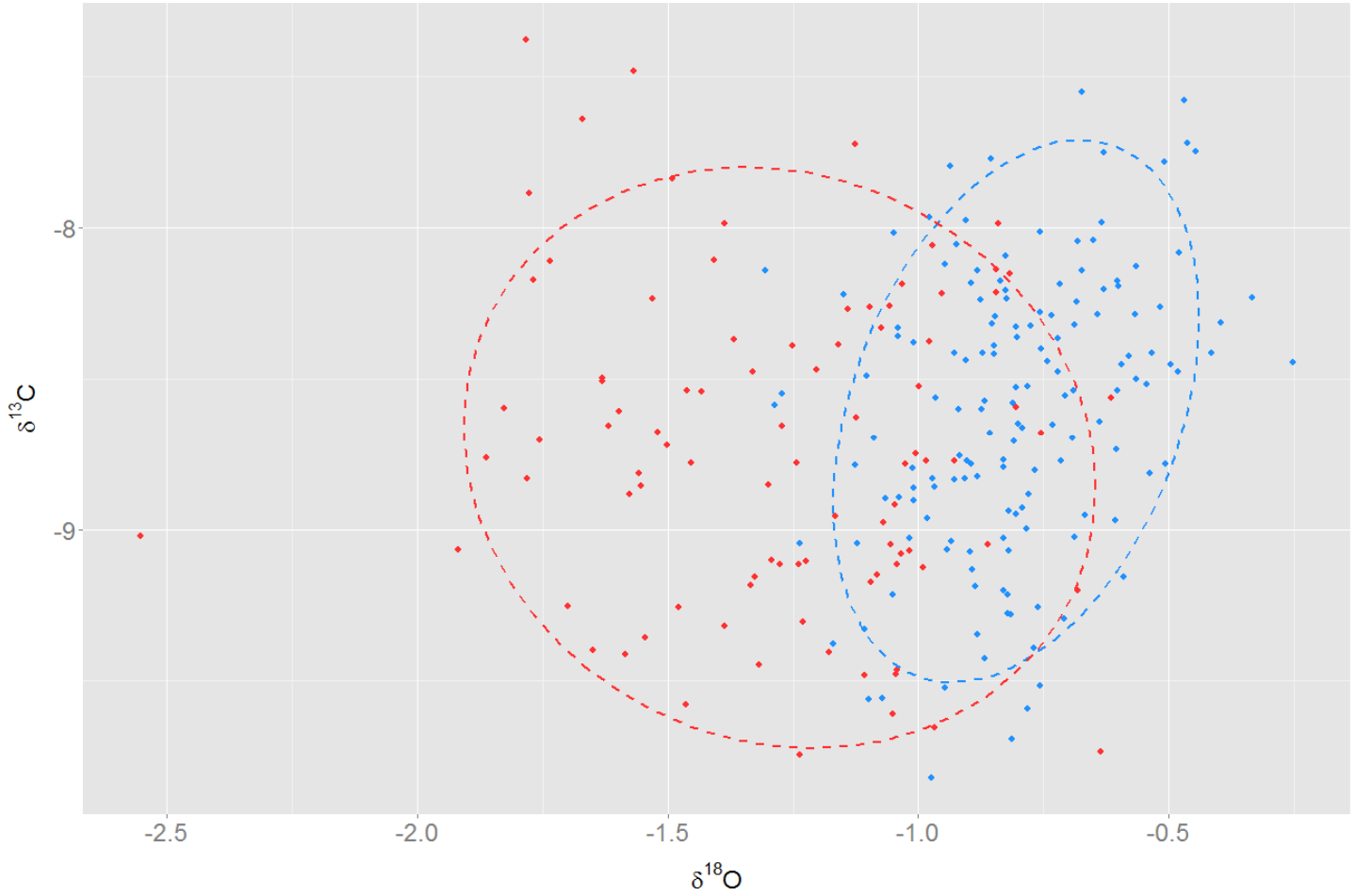

Figure 1.3. Power analysis to determine sample size for investigation of Sr:Ca periodicity across annular zones. Type II error of Hartley's *F* test at α=0.05, R=25, m=10 and λ=1 or 1.25.

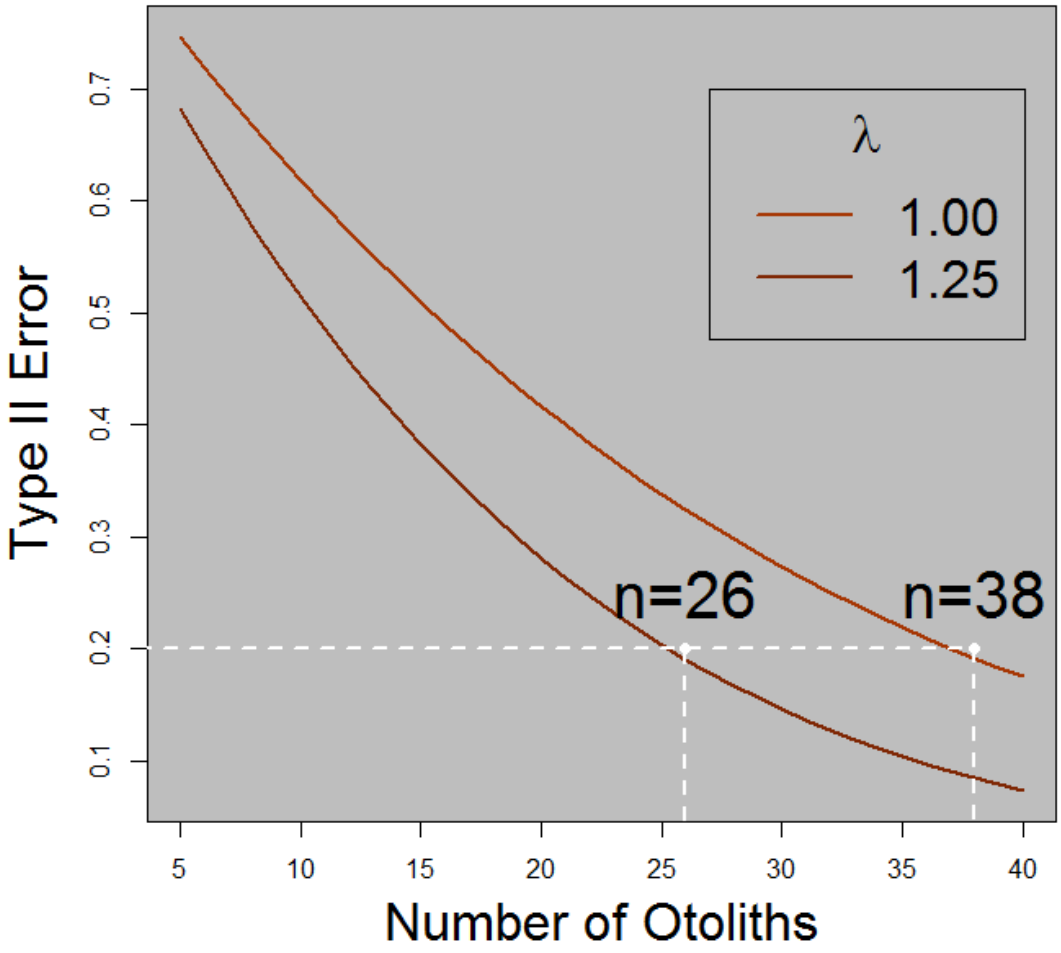

Figure 1.4. Measurements of Sr:Ca along profiles of Atlantic bluefin tuna otoliths with individual outlier removed. Integers correspond to opaque zones. A positive linear trend in the data is apparent across annuli.

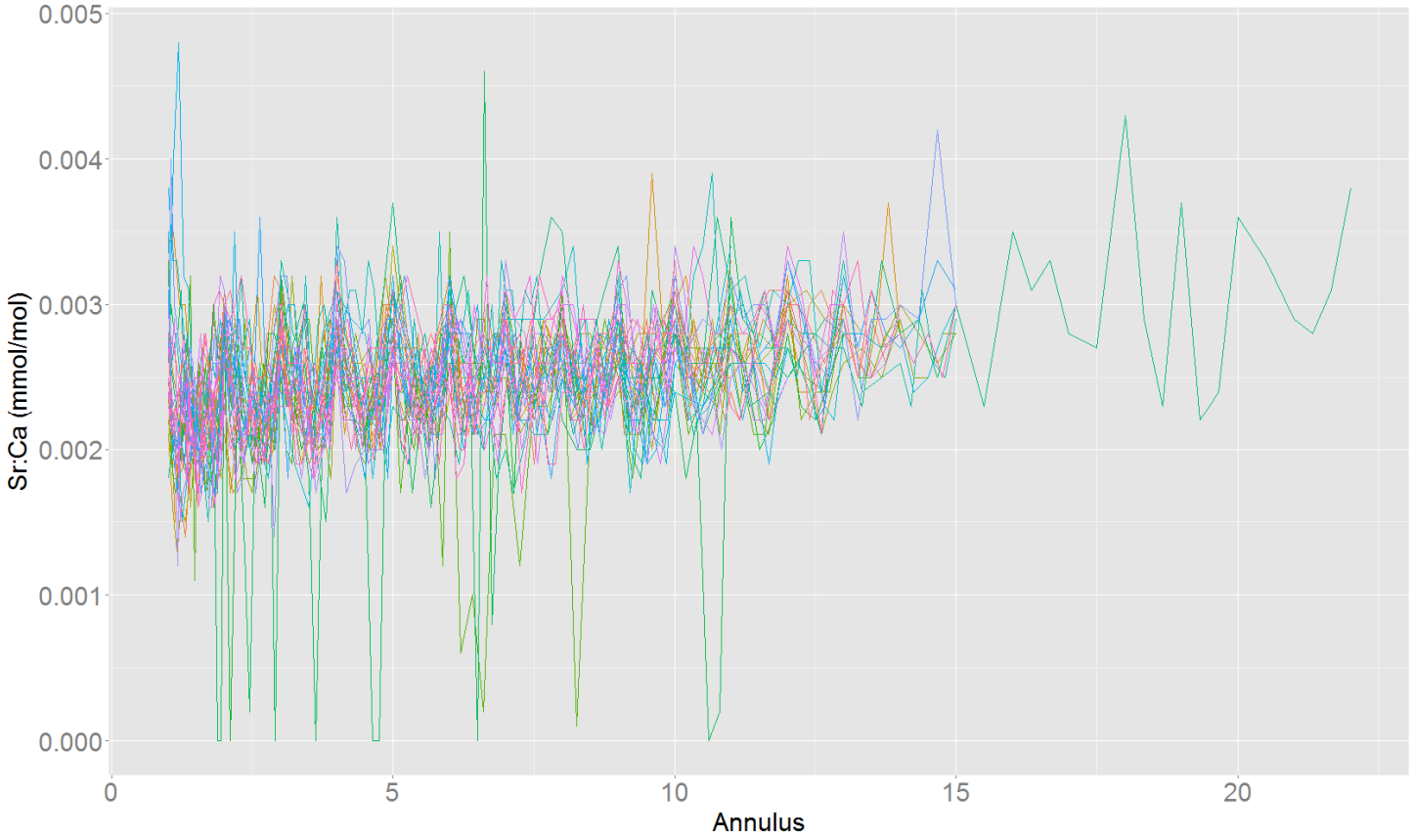

Figure 1.5. Comparison of raw $\delta^{18}O$ values measured at both laboratories with corrected $\delta^{18}O$ values. Also shown is the 1:1 line (blue diamond = corrected data; red box = raw data; green triangle = 1:1 line).

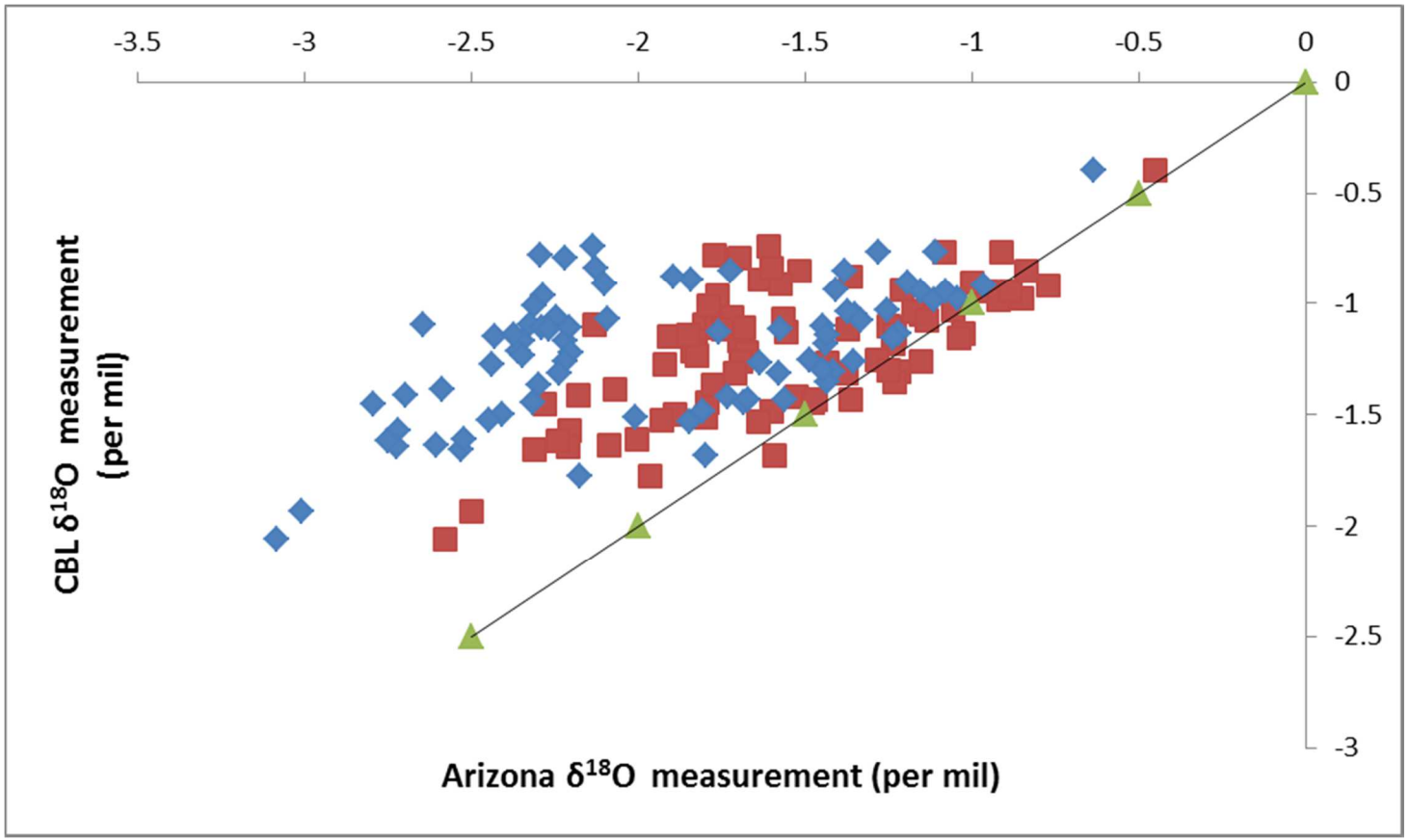

Figure 1.6. Lomb-Scargle periodogram of Atlantic bluefin tuna Sr:Ca time series data (N=31) from otolith transects (Figure 1) showing significant periodicities in the data. Significance ($p<0.05$) is indicated by the dotted line.

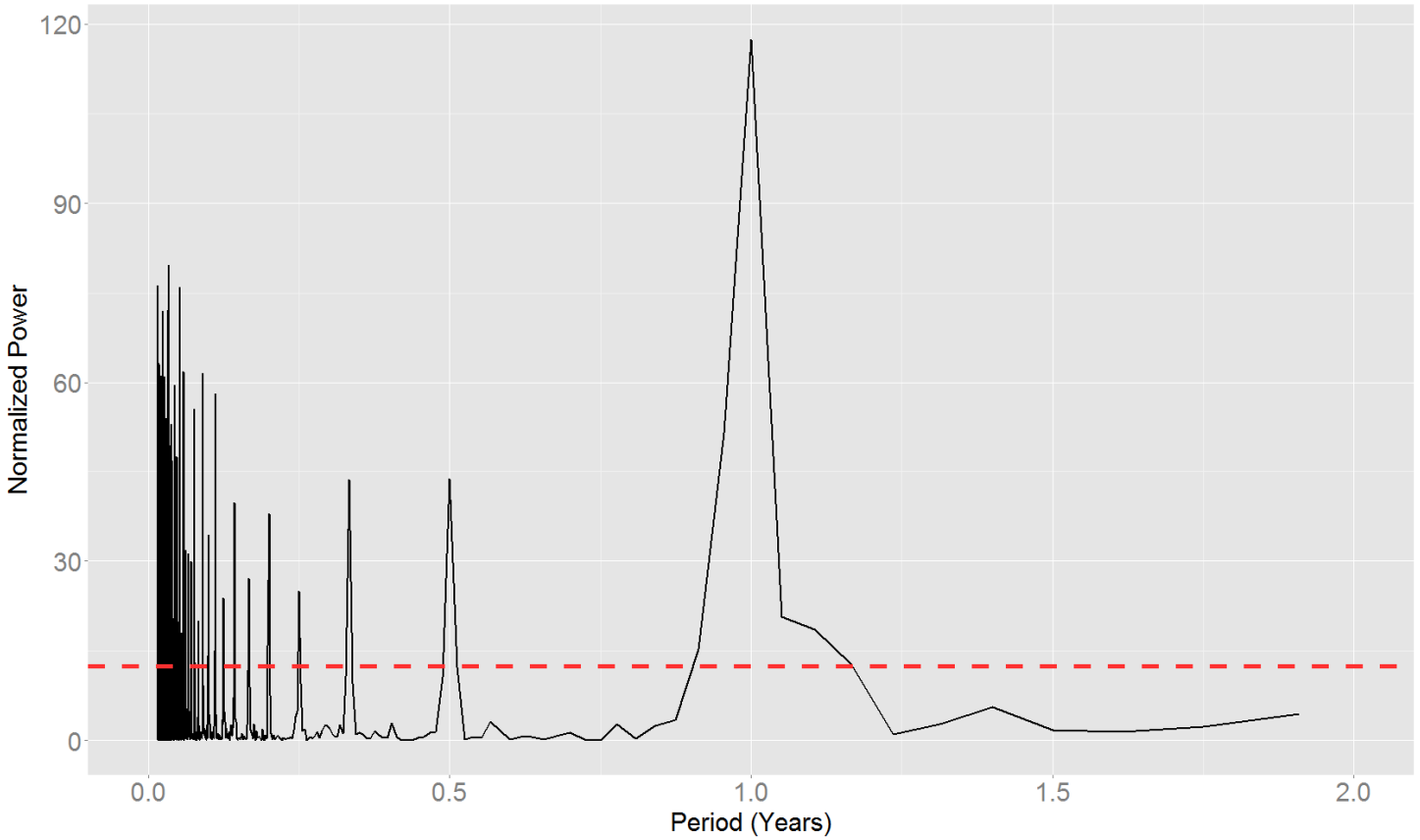

Figure 1.7. Lomb-Scargle periodogram of Atlantic bluefin tuna Sr:Ca time series data (N=31) from otolith transects (Figure 1) showing significant periodicities remaining after annual periodicity was filtered out. Significance ($p<0.05$) is indicated by the dotted line.

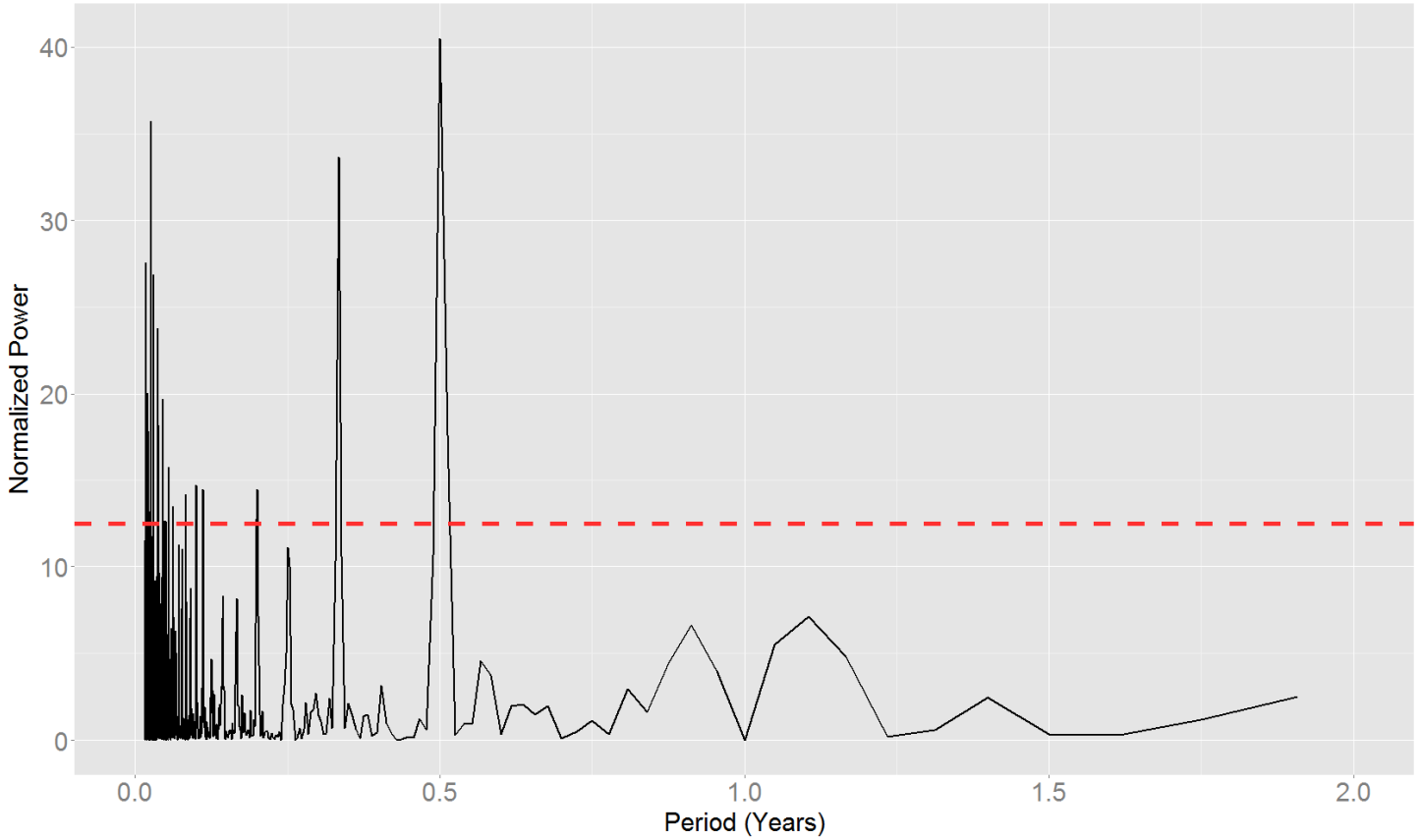

Figure 1.8. Lomb-Scargle periodogram of Atlantic bluefin tuna Sr:Ca time series data (N=31) from otolith transects (Figure 1) showing no significant periodicities remaining after annual, biannual, and triannual periodicities were filtered out. Significance ($p<0.05$) is indicated by the dotted line.

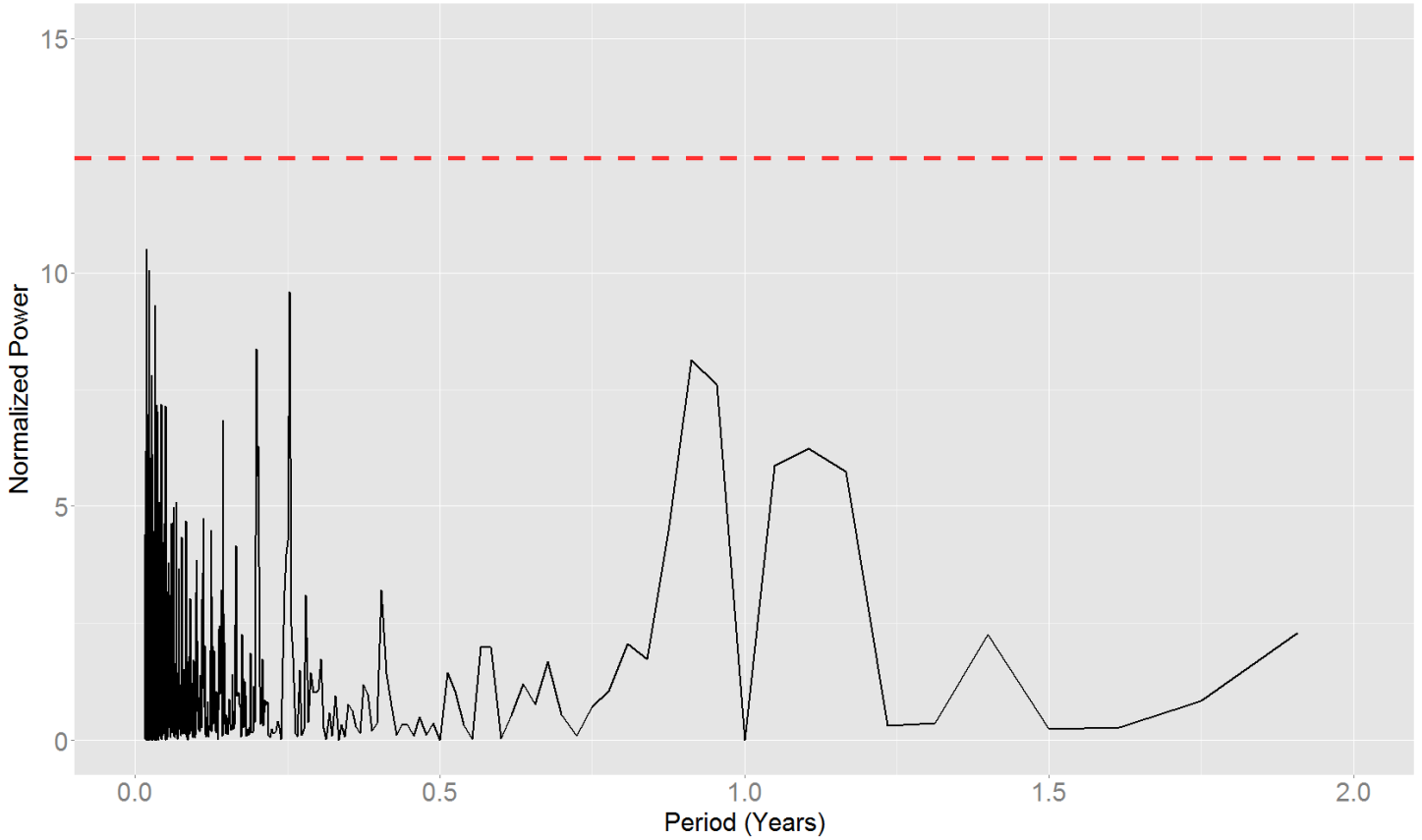

Figure 1.9. Ambient temperature (°C) in the Chesapeake Biological Laboratory's analytical room housing the isotope ratio mass spectrometer used in the study over the two analytical sequences (sequence 1 unknown samples = blue diamonds; sequence 2 unknown samples = red squares; sequence 1 standards = green triangles; sequence 2 standards = purple circles).

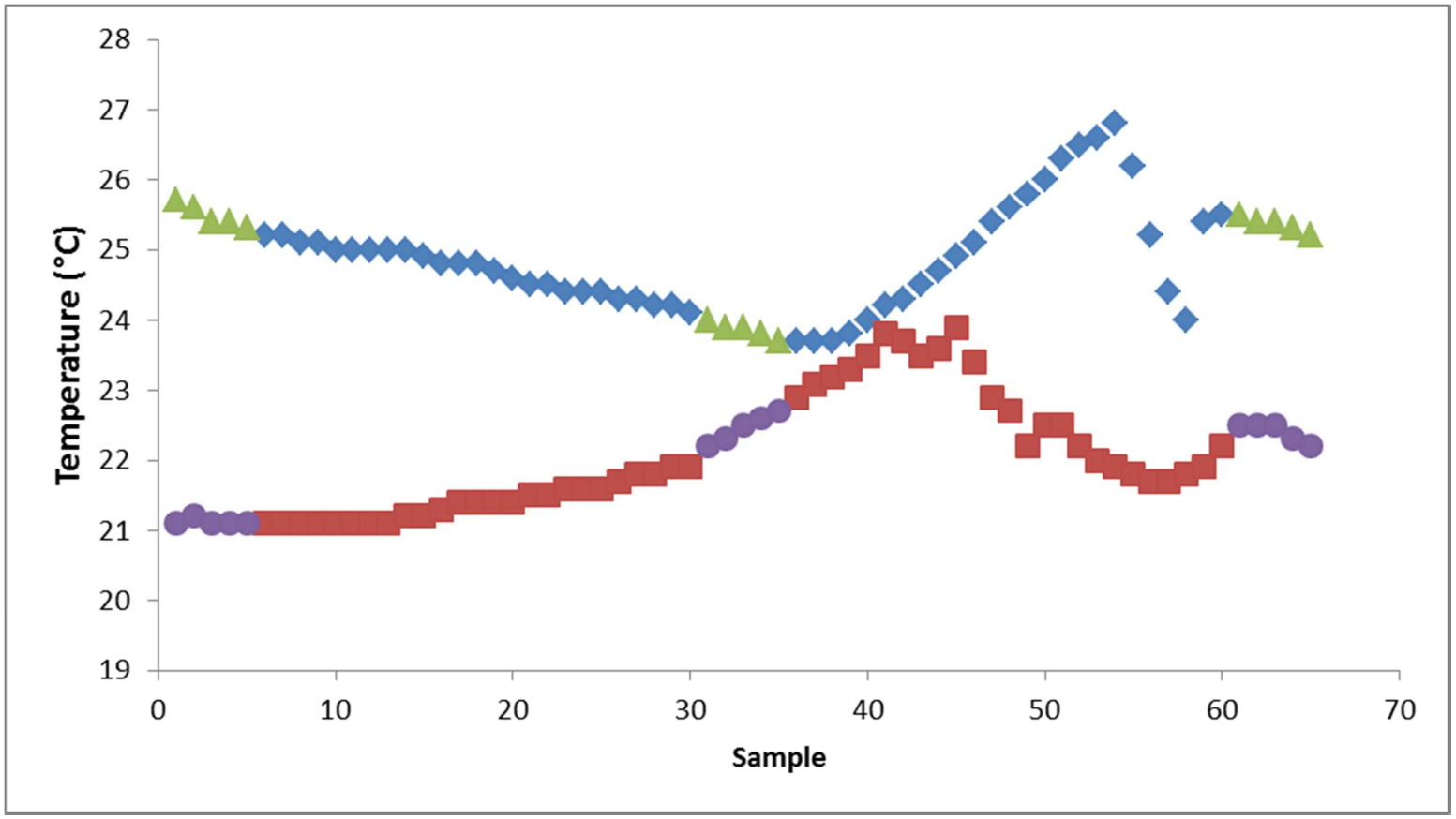

Chapter 2: Demographics changes to Northwestern Atlantic bluefin tuna (*Thunnus thynnus*) associated with size-selective fishing and long-term heightened exploitation

Introduction

Steep declines in commercially important fish populations during the past 50 years are well documented (Hutchings 2000; Myers and Worm 2003), as are the effects of fishing on ecosystems and population production (Pikitch 2004; Worm et al. 2009). Long-term exploitation of marine fishes has the potential to change the overall structure of food webs as well as individual populations (Jennings et al. 1999). Beyond declines in overall abundance, fishing can increase population variability over time in comparison to unexploited species, particularly for size-selective fisheries (Hsieh et al. 2006; Garcia et al. 2012), which can be a result of both market demand and management actions. With gear that specifically targets certain size (and age) categories, fisheries can lead to near-term demographic changes. Over generations, fishing can select for phenotypic variants, and induce genetic changes and evolutionary changes in life history traits (e.g. growth rate, mean maximum size, age-at-maturity, or size-at-maturity) of a species or population (Jennings et al. 1998; Allendorf et al. 2008; Jorgensen et al. 2007; Edeline et al. 2007; Swain et al. 2007). In turn, these changes can affect fisheries through loss of yield, and ecosystems through loss of ecosystem services (Trippel 1995; Jennings et al. 1999; Law 2000; Jorgensen et al. 2007). However, evidence suggests that the effects of fisheries-induced evolution takes decades (many generations) to develop (Law 2007) and may be reversible (Conover et al. 2009).

Historical changes in age structure and growth rate associated with fishing are found across diverse taxa. Long-term exploitation and selection of larger individuals in a cohort has been associated with reductions of size, age, size-at-maturity, and reproductive capacity (Hutchings 2000; Hixon et al. 2014). In the Northeast Pacific, fishing has been associated with decreased size in rockfishes (Harvey et al. 2006), and decreased size and age in Chinook salmon (*Oncorhynchus tshawytscha*) (Ricker 1981). In the Atlantic, sustained fishing pressure on red porgy (*Pagrus pagrus*) reduced mean size-at-age, growth rate, and size-at-maturity over a 20 year period (Harris and McGovern 1997) – a result of the selective removal of faster-growing individuals that ultimately would attain a larger size, thus leaving slower-growing and smaller individuals in the reproductive population. Alternatively, changes in temperature and consumption rate can also prompt changes in growth rates to varying degrees (Conover and Munch 2002; Sinclair et al. 2002).

Increased adult mortality and decline in mean age of spawners may lead to higher-frequency fluctuations in the population as a result of a diminished ability to buffer recruitment responses to environmental variability. Recruitment variance is expected to be higher in populations that undergo age truncation, driven by a reduction in storage effect (Secor 2007), which describes the degree to which age structure and overlapping generations allow populations to sample across years that vary in conditions favoring early larval and juvenile survival (Warner and Chesson 1985; Anderson et al. 2008; Rouyer et al. 2012). Age truncation and a compromised storage effect is especially detrimental to periodic strategists, such as Atlantic bluefin tuna (ABFT), who live moderately long lives, mature late, reproduce many times over their life span, and have

low early survival. These fish depend on a broad and diverse adult age structure to sample multiple reproductive seasons for favorable spawning and larval conditions in order to produce strong, successful year-classes (Winemiller and Rose 1992; Secor 2007).

Atlantic bluefin tuna is a large teleost fish (maximum size = 330 cm; Cort et al. 2013) with a moderate longevity (>30 years) that consists of two spawning populations, or stocks: a Gulf of Mexico-spawning (western) stock in the Northwest Atlantic, and a Mediterranean-spawning (eastern) stock in the Northeast Atlantic (Figure 1; Rooker et al 2007; Fromentin et al. 2014). The highly migratory nature of this species results in trans-oceanic movements and stock mixing in regions of principal fisheries, particularly those in the Northwest Atlantic (Block et al. 2005; Rooker et al. 2008; Secor et al. 2015). Divergent life history characteristics and productivity levels exist between the stocks, with the eastern stock maturing at an earlier age (age-4 vs. age-9) and being 5 to 10 times more productive than the western stock [Fromentin and Powers 2005; Standing Committee for Research and Statistics (SCRS) 2012]. The slow maturation rate and relatively low production of the western stock may cause it to be more susceptible to overexploitation (Safina and Klinger 2008; Secor et al. 2015).

The development of selective fishing in the western ABFT fishery from growth overfishing (exploitation of younger age categories with the purse seine fisheries of the 1950s and 1960s) to recruitment overfishing (targeting larger individuals in the 1960s and 1970s) paired with chronic, long-term exploitation and subsequent low levels of abundance may have caused a substantial reduction in age structure (age truncation) and a shift to a lower production level, resulting in less frequent production of strong year-

classes by the western stock (SCRS 2012; Secor et al. 2015). Further, under scenarios of moderate stock mixing, perceived strong year-classes in the Northwest Atlantic may in fact be due to eastern stock subsidy (i.e. migrants)(Rooker et al. 2008; Graves et al. 2015). Accordingly, I posited that long-term fishing on Northwest Atlantic bluefin tuna (*Thunnus thynnus*; ABFT) has resulted in age truncation and increased mixing with Northeast Atlantic bluefin tuna originating in the Mediterranean Sea (eastern stock).

Here, the combined influences of prolonged exploitation, fishing selectivity, and changing selectivity on age structure, growth rates, and stock mixing of Atlantic bluefin tuna are investigated over the past 40 years. In an initial comparison of historical and recent age structure, Secor et al. (2015) showed that a substantial reduction in the number of age-20+ fish occurred between the 1970s and 1990s, but sample sizes were moderate and changes in selectivity were not incorporated into the analysis. A major goal of this work is to provide a more robust comparison of age structure for Northwest Atlantic bluefin tuna over the past 40 years in the context of major shifts in selectivity over the time period.

Size selectivity has been evident throughout the history of the Northwest ABFT fishery. In the late 1950s and 1960s, small schooling juveniles [50-125 cm curved fork length (CFL); age 1-4 yr] were caught by purse seine and utilized in pet food canneries; in the mid-1960s and 1970s, medium- to large-sized [150-250 cm curved fork length (CFL); age> 5 yr] fish were landed by Japanese longliners, primarily for sashimi markets (Mather et al. 1995; Fromentin et al. 2014). Over time, imposition of size limits and gear types, which both selectively target certain demographic classes of tuna, has resulted in

management-based selectivity, as exemplified by current size restrictions for US fisheries (Table 1).

Atlantic bluefin tuna fisheries are appreciably smaller in the Northwest Atlantic than in the Northeast Atlantic and Mediterranean Sea (Figure 2). Total landings in the Northwest Atlantic Ocean peaked at ~19,000 tons in 1964, followed by a rapid decline to 3,000-7,000 tons between 1966-1981 (Figure 2; SCRS 2014). Following the Law of the Sea Convention (1982), the International Commission for the Conservation of Atlantic Tuna (ICCAT; established in 1969) evolved a stronger assessment and regulatory capacity to manage high sea fisheries for bluefin tuna and other highly migratory fishes in the Atlantic Ocean. In 1980, ICCAT erected bluefin tuna management boundaries, separating fishing areas (stock boundaries) on either side of the 45-degree Meridian (Figure 1). In response to the depressed status of the western stock, a conservative "scientific monitoring quota" of 1,160 tons was set in 1981. This action was taken to allow continued assessment of the stock, which was expected to recover (Porch 2005). Since then, the western stock has remained relatively stable but depleted, despite the efforts by ICCAT to rebuild the stock. In 2010, the SCRS for ICCAT concluded that the stock was still overfished and that overfishing was occurring. Reductions in total allowable catch (TAC) followed, yet the stock remains depleted (SCRS 2014).

The two stocks of Atlantic bluefin tuna are assessed under the restrictive assumption that no mixing occurs between them (SCRS 2014). However, ample evidence of migration across the international management boundary now exists via tagging, genetics, and otolith chemistry studies (Block et al. 2005; Rooker et al. 2008; Dickhut et al. 2009; Graves et al. 2015). Otolith stable isotope analysis of $\delta^{13}C$ and $\delta^{18}O$ values has

greatly expanded our understanding of stock separation (natal homing) and mixing (trans-oceanic migration) (Rooker et al. 2008; Rooker et al. 2014; Secor et al. 2015), and has revealed key elements of stock structure including, (1) no mixing occurs between the two stocks in principal spawning areas; (2) at times, a variable but considerable eastern stock subsidy to North American (US and Canadian) fisheries has existed [0-57%; 1997-2000, 2011-2013 (Rooker et al. 2008; Secor et al. 2015)]; and (3) contributions of the western stock to Northeast Atlantic and Mediterranean fisheries is minimal [<7%; 2003-2007, 2010-2011 (Rooker et al. 2008; Rooker et al. 2014)].

Mixing levels likely vary through time, possibly influenced by stock-specific production and trans-oceanic migrations; however, the degree of these fluctuations is not well known (Secor et al. 2015). As a result of the decline in abundance observed in the western stock, I hypothesized that mixing in the Northwest Atlantic has increased over the past four decades, with larger contributions of eastern fish from the 1980s to present day. This hypothesis is consistent with the findings of Rooker et al. (2008), who estimated substantial mixing of stocks in the US Mid-Atlantic Bight region during 1997-2000, particularly in recreational fisheries targeting small- to medium-sized fish. This increased eastern stock contribution to smaller-category fish could indicate that dominant strong year-classes present in the 1990s may have been due to eastern stock subsidy (Rooker et al. 2008; Graves et al. 2015). Finally, I hypothesized that the Gulf of Mexico samples would show little or no eastern stock contribution, which has been inferred from past otolith stable isotope, tagging, and size-frequency analyses (Nemerson et al. 2000; Block et al. 2005; Rooker et al. 2008).

To evaluate historical changes in stock mixing, age structure, and growth rate in western stock Atlantic bluefin tuna, I examined three periods during which the National Marine Fisheries Service actively collected biological information, including otoliths, from US fisheries: 1974-1978, 1996-2002, and 2009-2014. Age frequency was compiled through direct ages estimated from otoliths and adjusted for fishing selectivity over the 43 years of assessment history (SCRS 2014). Mixing levels (contribution of each stock to US fisheries) were evaluated using otolith stable isotope analysis. Pooled and stock-specific life-time growth rates (size-at-age) were also evaluated for any changes during this period. Because estimates of stock-specific growth and age structure can be confounded by stock mixing in fishery samples, western stock growth curves and age structures for the three samples were reconstructed using an individual stock assignment method which selected individuals that had a high probability of western stock origin.

Methods

Archived sagittal otolith samples used in investigations of age structure and stock mixing were obtained from the National Marine Fisheries Service (Table 2), which port-sampled and archived these Atlantic bluefin tuna otoliths through a directed biological sampling effort for pelagic fishes. Port samplers were trained to remove otoliths and typically extracted otoliths from fish carcasses at weigh stations. The sample of otoliths from fish landed in the 1970s was taken from the archive at the National Oceanographic and Atmospheric Administration's (NOAA) Southeast Fisheries Science Center in Miami, FL (1974-1978; N=350); the 1990s sample was taken from the Marine Forensics Archive at the NOAA Center for Coastal Environmental Health and Biomolecular

Research in Charleston, SC (1996-2002; N=234); and the sample from fish landed in the 2010s was collected by the NOAA Southeast Fisheries Science Center and Chesapeake Biological Laboratory (2009-2014; N=1359; R. Allman, National Marine Fisheries Service, Panama City Laboratory, unpublished data; Secor et al. 2015). Individuals chosen for each sample were selected based on size-class and region of capture in an effort to show demographic changes to the western stock (Table 2). When compared to catch-at-size data from the three time periods, these samples do appear broadly representative of size range and modes in the size distribution, but are biased towards larger individuals (Figures 3 & 4). These strata supported hypothesis tests on mixing levels among (1) decadal periods, (2) size-classes, and (3) regions; however, no analysis occurred for some size class-region strata due to lack of samples (e.g. Gulf of Mexico in the 1990s). Regions for which samples were obtained included New England (Maine, New Hampshire, Massachusetts, and Rhode Island), the Mid-Atlantic (New York, New Jersey, Delaware, Maryland, Virginia, and North Carolina), and the Gulf of Mexico (western Florida, Louisiana, and Texas).

A single sagittal otolith was randomly selected from each individual for analysis and cleaned of excess tissue. Otoliths were embedded in Struers epoxy resin (Struers A/S, Denmark) for sectioning. A 2.0-mm thick section containing the core region was taken along a transverse plane using a Buehler IsoMet saw (Beuhler, Lake Bluff, Illinois). The otolith section was then attached to a glass slide using Crystalbond 509 mounting adhesive (SPI Supplies, West Chester, Pennsylvania) in preparation for milling. After milling, section thickness was reduced and the surface was polished for ageing.

Investigations of stock mixing relied on stable isotope analysis of otolith core material, which corresponds to early life growth and residence on natal nursery grounds. Discrimination between reproductive stocks is primarily based on differences in $\delta^{18}O$ values between the Mediterranean Sea and western-Atlantic shelf waters, south of the Gulf of Maine. Because the Mediterranean Sea is a more evaporative basin than western-Atlantic shelf waters, cumulative evaporation leads to more positive $\delta^{18}O$ values in surface seawater, resulting in more positive $\delta^{18}O$ values uptaken by juvenile bluefin otoliths (LeGrande and Schmidt 2006; Rooker et al. 2008). In this work, otolith core material extracted from individuals of unknown stock origin was compared to material previously extracted and analyzed from juveniles of known stock origin (baseline data). The methods used in the collection of otolith material and subsequent stable isotope analysis closely follow Schloesser et al. (2010). To extract core material, a New Wave Research MicroMill (Freemont, California) was used. Using a 500-µm diameter Brasseler round carbide bit (Brasseler USA, Savannah, Georgia), a series of 55-µm passes occurred along a predetermined otolith milling template patterned after the shape of a yearling bluefin tuna otolith. After each sample was milled, otolith powder was collected with a microspatula and stored, and sampling equipment was cleaned with 100% pure USP-grade ethanol to prevent cross contamination.

Otolith core material was analyzed for $\delta^{13}C$ and $\delta^{18}O$ using an automated carbonate preparation device (Kiel-III; Thermo Fisher Scientific, Inc., Bremen, Germany) coupled to an isotope ratio mass spectrometer (Finnigan MAT 252; Thermo Fisher Scientific, Inc., Bremen, Germany) at the University of Arizona's Environmental Isotope Laboratory. Analytical precision of the mass spectrometer was determined to be $\pm$0.1‰

for $\delta^{18}O$ and $\pm$0.08‰ for $\delta^{13}C$ (1 standard deviation, SD) (Schloesser et al. 2010). Otolith $\delta^{13}C/\delta^{12}C$ became more depleted over the last several decades, likely due to $\delta^{13}C$-depleted fossil fuel emissions (termed the Suess effect) (Figure 5; Keeling 1979; Verburg 2007; Schloesser et al. 2009). In addition, because carbon in otoliths is partially derived from metabolic processes (Solomon et al. 2006), increased variation of otolith $\delta^{13}C$ observed over the time period may be due to changing prey abundance, which may have subsequently caused a change in prey species consumed by young-of-the-year and yearling Atlantic bluefin tuna (Eggleston and Bochenek 1990; Estrada et al. 2005; Logan et al. 2011). Based on these considerations, raw otolith core $\delta^{13}C$ values were corrected for these effects following methods from Schloesser et al. (2009). $\delta^{13}C$ estimates were plotted over the individual's year of birth (year-class; Figure 5) and the slope (β_{13C}) of this relationship was used to correct the data across all year-classes, as follows:

$$Suess\ Effect_{13C} = \beta_{13C} \times (Year\ of\ Baseline - (Year\ of\ Capture - Age))$$

where Year of Baseline (2006) was chosen as the modal year over which the baseline sample was collected (1998-2011). Here, $\beta_{13C} = -0.039$ (N=1953; R^2=0.62). I confirmed that the Suess effect was filtered from the isotope data, and that a linear rate of decrease adequately modeled this effect, by plotting corrected $\delta^{13}C$ data against year-class (Figure 6). The Suess effect correction is not entirely satisfactory, because, in comparison, Schloesser et al. (2009) estimated $\beta_{13C} = -0.026$ (N=369; R^2=0.57). The difference in slopes between these two samples may have been due to sample size and regional representation (61% of Schloesser et al.'s sample was from the Gulf of St. Lawrence, and regional variation in the Suess effect exists). Nevertheless, the slopes are

comparable in some respects, and when used to estimate mixing levels of my samples, the Schloesser et al. (2009) slope gives similar results (Appendix 1).

Otolith $\delta^{18}O$ showed a slight ($\beta_{18O} = 0.0015$) but significant ($R^2 = 0.005$; $p = 0.001$) long-term trend, prompting inquiry of whether correction of the data was necessary (Figure 7). Global seawater $\delta^{18}O$ data were acquired from the National Aeronautics and Space Administration's (NASA) Global Seawater Oxygen-18 database (Schmidt et al. 1999; http://data.giss.nasa.gov/o18data/) for examination of temporal global- and basin-wide trends that could subsequently bias otolith $\delta^{18}O$ estimates. Seawater $\delta^{18}O$ data were selected for depth 0-15 m, salinity >30 PSU, and locations (latitude, longitude) where young juvenile ABFT are known to occur (Fromentin and Powers 2005). Global-, North Atlantic-, and nursery-specific changes in seawater $\delta^{18}O$ were examined (Figures 8, 9, 10, and 11). When the slopes of these temporal seawater $\delta^{18}O$ trends were applied for possible correction of the otolith $\delta^{18}O$ data, sensitivity analyses revealed they had no effect on the outcome of stock discrimination analyses (Appendix 2). Therefore, isotope data used in stock discrimination analysis consisted of adjusted $\delta^{13}C$ data, but $\delta^{18}O$ data was not corrected due to the negligible changes observed in ocean surface water $\delta^{18}O$.

Isotope data for individual samples of unknown origin were compared with yearling baseline data composed of age-1 juveniles collected in the US Mid-Atlantic Ocean and Mediterranean Sea from 1998-2011 (N=265; Figure 12; data publically available from Rooker et al. 2014, http://www.int-res.com/articles/suppl/m504p265_supp.xls) and assigned to eastern or western nursery categories using a maximum likelihood approach with the FORTRAN program HISEA

(Millar 1990). Historical (1974-1978; 1996-2002) and recent (2009-2014) levels of stock mixing were estimated by region (New England, Mid-Atlantic, and Gulf of Mexico), size-class, year-class (determined via otolith-based ageing techniques) and life history stage (juvenile: age < 8 years; adult: age ≥ 8 years; Restrepo et al. 2010; Heinisch et al. 2014). Here, the adult size-class also corresponds to the approximate length limit for the commercial fishery (183 cm CFL).

The same otoliths analyzed for population assignment were used in direct age estimation through counts of annuli. After milling, section thickness was reduced to ~750-1000 μm with a lapping wheel and then hand-polished with a Buehler microcloth to increase visibility of annuli. Images were taken under transmitted light using an Olympus SZX12 dissecting microscope (Olympus America, Center Valley, Pennsylvania) fixed with a Lumenera Infinity 1 camera (Infinity Corporation, Ottawa, Ontario). Age determination employed standardized otolith ageing protocols (Rodriguez-Marin et al. 2006; Secor et al. 2014a). Visual enhancement and notation techniques of otolith images using Adobe Photoshop CS6, a "Y" section type (Figure 13), interpretation criteria for the first annulus, and calibration of the reader to a reference collection. Two blind counts of annuli were conducted for each image. If counts differed by <2 years, the second count was accepted. If counts differed by ≥2 years, the image was read a third time, consulting the first two count estimates for a final age estimate. In some instances, only a "V" section type was available for ageing. In these instances, a single year was added to the direct age estimate based on the findings of Secor et al. (2014a) that a 0.77 year age bias exists between "V" and "Y" section types (Figure 14). In addition, I assumed that the completion of each annulus (opaque zone) occurred during the second half of the

calendar year. Therefore, if the fish was landed within the first six months of the year (January-June), 1 year was added to the estimated age, assuming a spawning time of April-June (Baglin 1982).

Changes in age structure between the sample periods were initially evaluated through graphical depictions of frequency histograms. Age-specific fishing mortality estimates were drawn from the 2014 ICCAT SCRS assessment's virtual population analysis (VPA; SCRS 2014), and for each year, age-specific fishing mortality estimates were converted to selectivity by dividing the fishing mortality by the maximum age-specific mortality within that year ($S_{age} = \frac{F_{age}}{F_{max}}$). To account for the shift in fisheries selectivity that occurred in the late 1960s, decadal age-specific selectivity was calculated by averaging age-specific selectivities across years within each sample, and these sample-specific selectivities were then used to adjust age frequency in the three samples by dividing each age by the corresponding average age-specific selectivity.

Selectivity-adjusted decadal mortality estimates for Atlantic bluefin tuna were calculated using catch-at-size data and a global age-length key. Here, the catch-at-size data were obtained from ICCAT for the years 1974-1978, 1996-2000, 2002, and 2009; and length-bins 5-300 cm CFL, corresponding to study samples. No catch-at-size data were available for 2010-2014, so all subsequent reports of 2010s mortality only correspond to the year 2009. The use of length bins 50-300 cm CFL resulted in exclusion of < 1% of the available data. The age-length key was constructed using direct age estimates and corresponding length data from individuals in this study. The catch-at-size and age-length key matrices were used to generate proportions-at-length and proportions-at-age in AD Model Builder (ADMB Version 11.2; Fournier et al. 2012). Estimated

annual proportions-at-length from the ADMB output were first compared to the observed annual proportions-at-length from the catch-at-size data to check model fit and ensure the validity of proportions-at-age estimated by ADMB that were used in subsequent calculations of mortality (Figure 15). Following confirmation of model fit, annual proportions-at-age estimated by ADMB were converted to annual numbers-at-age by multiplying them by annual catch from the ICCAT catch-at-size database. Decadal numbers-at-age were generated by summing annual numbers-at-age for each decade. This matrix was then adjusted for selectivity by dividing decadal numbers-at-age by decadal age-specific selectivities calculated from age-specific mortalities generated by the ICCAT VPA $\left(S_{age} = \frac{F_{age}}{F_{max}}\right)$. Decadal total instantaneous mortality (*Z*; combined fishing and natural mortality) was estimated from the selectivity-adjusted decadal numbers-at-age matrix (i.e. age-year matrix) using the function glmer provided by the lme4 library in R (Version 3.1.2) with the line of code:

glmer(Decade~Age+(1|Age),family=poisson,data=data)

where Decade and Age corresponds to decade- and age-vectors in the age-decade matrix of selectivity-adjusted numbers-at-age (Millar 2015). This function fits a generalized linear mixed model via maximum likelihood and incorporates both fixed-effects parameters and random effects in a linear predictor (Bates et al. 2014).

To investigate possible changes in growth rate over time, von Bertalanffy growth curves were constructed for the three periods (1970s, 1990s, and 2010s) from size-at-age data following the equation:

$$L_t = L_\infty \times [1 - \exp(-K \times (t - t_0))]$$

where L_{inf} is the asymptotic length, K is the rate at which the asymptotic length is approached, and t_0 is the length at age-0. If CFL was not recorded, CFL was estimated from straight fork length or snout length, using conversions from Secor et al. (2014b) or ICCAT (ICCAT 2000). Differences in growth rate (size-at-age) between pairs of samples (1970s v. 1990s, 1990s v. 2010s, and 1970s v. 2010s) were investigated by comparing corrected Akaike's Information Criterion (AIC_C; Burnham and Anderson 2002):

$$AIC_C = -2\log\left(\mathcal{L}(\hat{\theta})\right) + 2K\left(\frac{n}{n-K-1}\right)$$

where $\mathcal{L}(\hat{\theta})$ is the likelihood function, K is the number of model parameters, and n is the sample size. Here, AIC_C values of full models, which estimated decade-specific parameters for combined data from two decades being compared (e.g. separate L_{inf} estimates for the 1970s and 1990s), were compared to AIC_C values of reduced models, which only estimated one parameter for the pooled data (e.g. one L_{inf} estimated for the combined 1970s and 1990s data) to select the best model and determine differences in growth between samples. Full models used a dummy variable (0 or 1) to distinguish which decadal sample each individual belonged to:

$$L_t = L_{\infty,D} \times [1 - \exp\left(-K_D \times \left(t - t_{0,D}\right)\right)]$$

where D pertains to a decadal sample-specific parameter. Reduced models used the traditional von Bertalanffy model (above) for all the data in a comparison.

Estimating a growth function for only the western stock required that individuals obtained from the mixed stock samples be assigned to their respective stocks. Because the maximum likelihood approach used to assess the degree of mixing in a sample does not allow for individual assignment to a stock, I undertook an approach that reduced the

likelihood of eastern stock inclusion. Among the two stable isotopes used to discriminate stocks, $\delta^{18}O$ is much more influential (Rooker et al. 2014), I used this tracer to isolate those individuals most likely to be of western stock origin (lower $\delta^{18}O$ values) from the remainder of the sample. Cumulative frequencies of known western and eastern fish from the baseline sample were plotted and a threshold was determined at the 90th percentile $\delta^{18}O$ value of the western stock ($\delta^{18}O$ = -0.925; Figure 16). Using this threshold, individuals below the threshold were assigned to the western stock. These individuals were then selected to reconstruct growth curves for the western stock. A sensitivity analysis was performed to identify the effect of reducing the resolution of the stock discrimination threshold (from $\delta^{18}O$ = -0.925 to $\delta^{18}O$ = -0.9). Using this reduced threshold did not change the results of AIC_C model selection, so the original 90th percentile threshold was used in this decadal comparison of western stock growth.

Results

Age structure

Individuals from the 1970s sample (1974-1978; N=350) ranged from 50 – 306 cm CFL with strong modes at 70 and 250 cm, while individuals from the more recent samples had similar, but smaller ranges: 53 – 274 cm and 63—296 cm for the 1990s and 2010s samples (Figure 17). Modes occurred at 80, 190, and 230 cm for the 1990s, and 110, 190, and ~250 cm for the 2010s. In comparison, age distributions were markedly different over the time period. Individuals landed in the 1970s ranged 1—34 years, while individuals landed in the 1990s only ranged from 1—21 years (Figure 18). The age structure of the 2010s sample was similar to the 1990s sample, although ages ranged

from 3—34 years, with only 12 individuals over age 21 (0.9% of the sample). Strong modes at ages 2 and 19 in the 1970s, ages 2 and 10 in the 1990s, and age 6 in the 2010s indicate of potentially strong year-classes during each sampling period. Considering adult age structure only (Figure 19), ages spanned 26 years (age 8-34) in the 1970s with a mode centered on ages 18-25. In contrast, adult ages in the 1990s and 2010s were skewed to the right with a modal age centered between 9 and 11 years. Cumulative frequency distributions of curved fork length (cm) across samples show that the median length has decreased considerably over time: 240 cm in the 1970s, 185 cm in the 1990s, and 147 cm in the 2010s (Figure 20). Similarly, the median age of the 1990s sample (age 7) was half that of the historical sample (age 14) and the median age for the 2010s sample declined further to age 6 (Figure 21). Application of the $\delta^{18}O$ threshold to exclude most eastern stock individuals did not substantially alter age structure. Trends in diminished age structure remained except for the 2010s period, for which only 0.01% of the sample consisted of individuals above age 21 (Figure 22).

Large changes in juvenile and adult year-class structure were also observed across decades. In the earliest period, a very strong year-class was observed in 1973 in juvenile age-classes (< 8 years), but no similarly dominant year-classes were detected in the two more recent samples (Figure 23). In the most recent decade, 2007 and 2008 juvenile year-classes were most dominant. Historically, year-class frequency estimated from the adult sample (Figure 24) appeared normally distributed with a span of 25 years (1944-1969), but moving forward to the 1990s, the distribution of year-classes became narrower (19 years) with 98% of the distribution spanning 11 years (1984-1994). In the 2010s sample, the distribution is skewed to the left (more recent year-classes), and spans 28 years with

99% of the distribution occurring within a 19 year period (1987-2006) (Figure 24). Dominant adult year-class modes occur in 1988 and 2004 for the 1990s and 2010s samples.

Age-specific selectivities from the ICCAT assessment showed a shift in age-classes targeted over time (Table 3; Figure 25). In the 1970s age 2-5 fish were heavily selected. In the 1980s, age 2 and 3 fish were still heavily selected, but age 15 and 16+ fish were also strongly selected. In the 1990s, selection of the youngest ages fell and, in general, selectivity began to spread more evenly across adult age-classes. Over the past 30 years, adult age-classes represent the most highly selected component of the stock. Between 2000 and 2013, some years show strong selectivity for juvenile fish (ages 3 to 6), and the observed diagonal pattern of full selectivity potentially indicates the selection of a strong year-class over the time period. Alternatively, this could be an artifact of inaccurate age determination in the assessment's virtual population analysis, which uses a cohort slicing method to determine age frequency from length frequency data. Following adjustments for decadal changes in selectivity, estimated age distributions still supported a diminished age structure for the recent periods (Figure 26). These distributions show a much more dispersed age structure in the 1970s in comparison to the 1990s and 2010s. In particular, the age distribution in the 1990s exhibited the highest bias towards the youngest age-classes and sharp deterioration of older age-classes. The 2010s sample is unimodal and more normally-distributed, with higher abundances of intermediate age-classes (ages 4-10).

Estimates of total instantaneous mortality (Z) across the sampling periods exhibited the pattern expected. Estimates of Z peaked at 0.300 yr^{-1} in the 1970s, fell to 0.265 yr^{-1} in the 1990s, and fell again to 0.035 yr^{-1} in the 2010s (Figure 27).

Growth

Length-at-age followed a similar, overlapping trajectory for all three samples (Figure 28). von Bertalanffy growth curves fit to the three samples overlapped considerably (Figure 29), with similar values for L_{inf} (asymptotic length), K (rate at which asymptotic length is approached), and t_0 (length at age-0) parameters in the 1970s and 1990s samples (Table 4). Differences between these two curves and the 2010s curve were largely influenced by t_0 and L_{inf}, which may have been inaccurately estimated due to lack of age-1, age-2, and age-21+ individuals in the 2010s. AIC_C model selection consistently chose curves that incorporated decade-specific model parameters (Table 5). Based on AIC_C differences, reduced models received little support.

Western stock-specific growth curves constructed based on the 90th percentile $\delta^{18}O$ threshold were very similar between decadal periods, yet AIC_C again supported curves that incorporated sample-specific parameters for each decade (Figure 30; Tables 6 and 7). Western stock-specific growth curves all largely overlapped with each other. They were also similar to the western stock growth curve accepted by ICCAT and used in management of this species (the Restrepo growth curve, described in Restrepo et al. 2010). The 1970s and 1990s curve more closely matched each other than the 2010s curve. The 2010s curve more closely resembled the Restrepo growth curve, but differences in t_0 and lengths predicted for intermediate ages still existed between the two

curves (Table 6). Observed differences between the 1970s/1990s and the 2010s/Restrepo pairs of curves are likely influenced by L_{inf}, which may have been inaccurately estimated in the 2010s sample due to very low sample sizes for ages > 21 (Table 6).

Stock mixing

Stock discrimination analyses using otolith stable isotope data showed virtually no contribution of the eastern stock in the 1970s sample (0%), a large increase in eastern stock subsidy in the 1990s sample (48%), and a return to low-level eastern contribution in the 2010s sample (4%) (Table 8). In the 1970s, New England, Mid-Atlantic, and Gulf of Mexico had 0% contribution of eastern fish, respectively. In contrast, the 1990s sample showed considerable eastern stock subsidy across regions: New England and Mid-Atlantic regions showed 41% and 64% contribution of eastern stock fish, respectively. Interestingly, the contribution of eastern fish to the 2010s sample declined across regions, with New England, Mid-Atlantic, and Gulf of Mexico samples estimated to include 1%, 10%, and 0% eastern fish.

Mixing of both juveniles and adults was more prevalent in the 1990s sample than for other periods (Table 9). Over all regions, the eastern stock contributed substantially more to juveniles than adult portions of the sample (juveniles: 65% eastern stock fish; adults: 26% eastern stock fish). Juvenile mixing levels were minimal and similar to adult levels during the 1970s and 2010s, with the exception of adults sampled from the Mid-Atlantic during 2011-2014 (18% eastern origin fish). This moderate level of mixing was influenced by the inclusion of samples from the North Carolina winter fishery, which is known to have strong connectivity to Mediterranean-spawning bluefin tuna (Block et al.

2005; Secor et al. 2015). Alone, 24% of this North Carolina sample (2011-2014; N=350) was of eastern-stock contribution.

Parsed by size-class, mixing trends were similar to those observed in life history stage analyses, but showed finer scale separation (Table 10). Regardless of size-class, the eastern stock contribution was minimal in the 1970s (maximum: 1% eastern stock fish; 50-100 cm CFL category). In contrast, the highest contribution of eastern stock fish was observed in the smallest size-class in the 1990s (73% eastern stock fish; 50-100 cm CFL category). In this decade, as size increased eastern stock contribution declined (51%, 100-200 cm; 32%, 200-250 cm; 0%, 250-300 cm). This shows a clear trend of decreased mixing with increased fish size. In the 2010s, mixing levels were minimal ($\leq$ 8% eastern stock fish), but did show size-dependent changes with higher levels of eastern stock contribution in smaller-category fish (7%, 50-100 cm; 8%, 100-200 cm; 0%, 200-250 cm; 0%, 250-300 cm).

Strong year-classes produced from 1952-1974 were estimated to be 94.8-100.0% western origin, while those produced from 1986-1997 were much more variable in origin (Table 11). Out of these later strong year-classes, only 1988 was estimated to be largely of western origin (98% western stock) while 1986, 1987, 1989, 1995, and 1997 had major contributions from the eastern stock (47, 61, 83, 65, 68% western stock). After the turn of the century, strong year-classes from 2001-2008 were estimated to be mostly western origin (2004: 85%; other years: 92-100% western stock).

Discussion

Using a large, representative sample, I analyzed age and size structure, growth, year-class strength, and stock mixing – providing evidence for a reduced age structure after intensive fishing in the 1970s and 1990s and a modest recovery in age structure in the most recent decade. Samples over-represented larger fish in each decade, indicating that inferences related to diminished representation of older age-classes were conservative. Under the dual influences of growth overfishing (overfishing juveniles) and recruitment overfishing (overfishing adults), I expected to see age truncation and increased growth. Size and age distributions provided clear evidence of diminished age structure in the 1990s, which is consistent with trends in abundance of the age-16+ age-class as reported in the most recent ICCAT stock assessment (Figure 31; SCRS 2014). Despite evidence of diminished age structure in the 1990s, only moderate changes in growth were observed. Age structure has recovered slightly in the recent period (2010s): the span of age and year-classes increased, but the adult population is still predominantly comprised of first- or second-time spawners, termed recruit spawners (young adult spawners, age < 12). Associated with diminished age structure, I expected to observe lower incidence of strong year-classes, which was supported by age structure and fishing selectivity analyses (Figures 23 and 24).

Mixing levels were inversely related to landings observed over time (Figure 2). Stock mixing increased from minimal levels in the 1970s to large-scale eastern subsidy in the 1990s. The recent return to low mixing in the 2010s could be an indicator of western stock recovery or decline of the eastern stock over the past 20 years. Variable western stock contribution in identified "strong" year-classes, particularly in the 1990s, could

indicate that recruitment levels were less than predicted for this period (SCRS 2012). Still, a modest increase in age structure, broader year-class structure, dominant western stock year-classes, and the reduction in mortality (Figure 27) support the overall inference of partial recovery in the western stock. This perspective is consistent with the recent ICCAT assessment, which supports moderate recovery in spawning stock biomass from the low levels observed in the 1990s (SCRS 2014).

The declining yield and age structure, as evidenced in the ICCAT stock assessment (Figure 31; SCRS 2014) and confirmed in this study using empirically-derived age composition over the past 40 years, is likely a response to sequential growth and recruitment overfishing. Together, growth and recruitment overfishing had the potential to induce a severe depletion in abundance, decrease the potential to produce strong year-classes, and cause age truncation, as has been seen in other species (Pauly 1983; Berkeley et al. 2004). Fisheries for bluefin tuna in the Northwest Atlantic in the 1970s primarily targeted juveniles with purse seines and, to a smaller degree, adults with longlines and rod-and-reel. As evidenced by age-specific selectivity, targeted age-classes principally included those <5 years (Figure 25). Reduced catch in the purse seine fishery in the mid-1970s generated concern for declines in recruitment (Fromentin and Powers 2005). Further, heavy exploitation by the Japanese longline fleet on medium- to large-sized individuals in the western Atlantic Ocean depleted this demographic component of the stock. The resulting reduction in adult catch in the western Atlantic Ocean caused Japanese longline fisheries to expand into the eastern Atlantic Ocean and Mediterranean Sea, while remaining longline effort in the western Atlantic Ocean was focused in the northern Gulf of Mexico in May and June and south of the Grand Banks in

Newfoundland over most of the year. These US and Canadian fleets were primarily targeting large individuals (> 185 cm CFL) spawning in the Gulf of Mexico and giants (> 205 cm CFL) foraging in Canadian waters (Mather et al. 1995). The increased selectivity for ages > 12 in the early 1980s (Figure 25) is consistent with expansion of the longline fleet. With recruitment dwindling and the focus of commercial fisheries shifting, the removal of old individuals would have had both direct and indirect effects on the population.

High estimates of total instantaneous mortality (Z) in the 1970s and 1990s (Figure 27) indicate the scale of these historical fisheries. Considering the age-independent natural mortality used in assessment of ABFT is 0.14 yr^{-1} (SCRS 2014), estimates of Z in the current study (0.300 yr^{-1} and 0.265 yr^{-1} in the 1970s and 1990s, respectively) suggest fishing mortality rates more than double the natural mortality rate (where Z = F + M). Together, size-selective fishing (Figure 25) and high total instantaneous mortality (Figure 27) could facilitate a demographic shift in the western stock of ABFT, resulting in the large changes in age structure, year-class production, and stock composition observed in this study.

The shift in fishing selectivity on western-stock Atlantic bluefin tuna from the 1970s (juveniles) to the 1980s (large adults) likely prevented strong year-classes produced in the 1950s and 1960s (e.g. 1952, 1956, 1957, 1958; Table 11) from maturing into adult spawning stock biomass (SCRS 2012; Secor et al. 2015). Therefore, older cohorts observed in the 1970s sample (1974-1978) were quite possibly already diminished in abundance (Mather et al. 1995). The strongest year-class observed in this study occurred in 1973, and presumably supported exploitation rates on older adults in

the subsequent two decades. High fishing mortality on older individuals (age ≥ 13 years; BFT-Figure 29 in SCRS 2014) and the lack of substantial management action to protect larger, old individuals in the late 1970s and 1980s very likely resulted in recruitment overfishing, and may explain the loss of old age structure and diminished storage effect observed for this species.

Old individuals are thought to supply unique attributes to fish populations. In their comprehensive, multi-species review, Hixon et al. (2014) found that a more widely distributed age structure which includes big, old, fat, fecund female fish ("BOFFFFs") contributes to population stability, yield, and persistence. They also found that BOFFFFs often produce larger and sometimes higher quality eggs and larvae (Hislop 1988; Marteinsdottir and Steinarsson 1998; Birkeland and Dayton 2005; Hixon et al. 2014), spawn more batches (Fitzhugh et al. 2012), and may spawn more frequently (Hixon et al. 2014). In addition, BOFFFFs ensure that bet-hedging strategies are more effectively employed by contributing to a more protracted spawning season and range of spawning habitats. In turn, this increases the chances that offspring (larvae) will encounter favorable conditions (more food encounters, less predation) (Wright and Trippel 2009; Hsieh et al 2010; Hixon et al. 2014).

Evidence that older Atlantic bluefin tuna contribute disproportionately to population reproductive rates and recruitment remains unstudied. Effects of female size on egg size, quality, and viability, and spawning frequency and duration remain unknown. Interestingly, loss of larger individuals could mean proportionally higher loss of males because male ABFT attain slightly larger sizes than females (L_∞: males, 286.64 cm; females, 277.315 cm; Caddy et al. 1976). Although it's possible that selective

fisheries could alter sex ratios in ABFT, how this in turn would influence mating systems is uncertain. The overall sex ratio of large ABFT is unclear, as it has been found to fluctuate spatially, with females more than twice as prevalent than males in the Straits of Florida (near the spawning ground) but males almost seven times more prevalent than females in waters of the Gulf of Maine and north (Rivas 1976).

In other species, the loss of BOFFFFs and adult age structure has been attributed to higher recruitment variability, a decreased capacity to produce strong year-classes, and higher susceptibility to population collapse. Periodic-strategists such as bluefin tuna, cod, and striped bass (Winemiller and Rose 1992), which rely on an intact age structure to buffer against unproductive years, are particularly susceptible to age truncation (Rouyer et al. 2012). For Northwest Atlantic cod (*Gadus morhua*), Myers et al. (1996, 1997) found that the loss of older fish was related to increasing levels of fishing mortality in the 1980s and 1990s. This depletion of the stock's age structure subsequently may have contributed to the lack of recovery observed for this species. Alternatively, conserved age structure may have been the root of recovery in Chesapeake Bay striped bass (*Morone saxatilis*). A sustained period of poor early survival and recruitment overfishing of striped bass resulted in a 10-year gap in age structure (Secor 2000a). Ultimately, the imposition of a fishing moratorium and the contribution of old females, which hadn't been selected historically in the striped bass fishery, led to successful recovery (Secor 2015). Thus, loss and recovery of age structure can cause populations to cross nonlinear thresholds as they move from one abundance state to another (Dixon et al. 1999; Hsieh et al. 2005; Secor et al. 2015). Similarly, reduced age structure may have enabled ABFT to cross a threshold,

which is curtailing the population from returning to the high abundance state observed historically.

Remarkably, Atlantic bluefin tuna have been targeted for centuries, but not deemed threatened until recently (Safina and Klinger 2008). In the Mediterranean Sea, bluefin tuna have been caught using handlines, seines, and traps since the 7th millennium BC (Fromentin and Powers 2005). Although speculative, this long-term exploitation of the eastern stock possibly explains its earlier maturation schedule compared to the western stock (age 4 v. age 8; SCRS 2014), whereby long-term fishing and size-selective adult mortality have reduced age-at-maturity in the eastern stock. Similarly, these mechanisms may be acting on western stock fish, but have not occurred over the many generations required to cause evolutionary change in life history traits.

Using endocrine profiling, an alternative method to determine sexual maturity, Heinisch et al. (2014) has suggested that western stock individuals may be spawning earlier than previously thought (> 134 cm; age ~5 years). In comparison, the congeners Pacific bluefin tuna (*Thunnus orientalis*) and southern bluefin tuna (*Thunnus maccoyii*) show similar maturation schedules to the eastern and western stocks, respectively, with the former maturing at age 3-5 years and the latter at age 10-12 years (Tanaka 2006; Gunn et al. 2008). Therefore, both early and later maturation schedules for the reproductively separate ABFT stocks seem realistic, but the maturation schedule for the western stock remains poorly studied, prompting a need for a comprehensive evaluation of age-at-maturity which employs all available tools, including endocrine profiling, histology, careful age determination, and further direct observations of spawning behaviors (e.g., Walli et al. 2009)

The decadal changes observed in stock mixing may result from the combined influence of (1) changing migration behavior by the eastern stock, (2) changing biomass (production) of the eastern stock, and (3) changing biomass (production) of the western stock. One view is that the increased mixing detected in the 1990s may be representative of an expansion of the eastern stock's range in response to depletion of the western stock. The relative recovery of forage abundance (Atlantic herring, Atlantic mackerel) from the mid- to late-1980s in the Northwest Atlantic may have facilitated this expansion of the eastern stock into Northwest Atlantic waters (Overholtz 1989; Overholtz and Friedland 2002; Overholtz 2006). Range expansion for the highly migratory bluefin tuna is certainly not farfetched: oceanographic changes (temperature and salinity), shifts in trophic dynamics (forage fluctuations), and fishing have been offered as explanations for the sudden emergence of bluefin tuna aggregations off Brazil (termed the "Brazilian Episode") and the collapse of the Norwegian and North Sea fisheries in the 1960s (Fromentin 2009; Fromentin et al. 2014). Recently, Atlantic bluefin tuna have also followed irruptions of Atlantic mackerel and herring into boreal waters off Greenland and Iceland (MacKenzie et al. 2014).

Alternatively, fluctuations in stock mixing could be attributed to changes in production. Nemerson et al. (2000) posited that due to large inherent differences in stock size, westward migration by eastern stock fish would have a relatively larger effect on observed dynamics in the western fishery. Because the eastern stock is substantially larger than the western stock (~5-10 times larger), a reduction in western stock abundance could amplify the level of the eastern stock's contribution. This would explain why substantially higher levels of eastern contribution were observed in the 1990s, a time

when abundance of the western stock was extremely low. Because there is no definitive means to separate the relative influence of changing migration and abundance, I propose a compromise: western stock depletion and a recovering forage base triggered the westward expansion of the eastern stock in the 1980s, accounting for the increased mixing observed in the 1990s. Since then, moderate recovery of the western stock and diminishing abundance of the eastern stock since the 1990s (SCRS 2014), has likely resulted in a diminished eastern stock signal in the 2010s sample.

Because this species may undergo long-term fluctuations due to forage and oceanographic conditions (Ravier and Fromentin 2001; Ravier and Fromentin 2004; Overholtz 2006; MacKenzie et al. 2014) and fishing, there is a need for long-term monitoring of population demographics. The large-scale return of the forage base in the mid- to late-1980s (Overholtz 1989; Overholtz and Friedland 2002; Overholtz 2006) could have resulted in increased somatic growth as a result of increased food availability and consumption rate. AIC_C model selection chose models that were specific to sampling periods (Table 5), but the von Bertalanffy growth curves (predicted size-at-age) were quite similar in shape and amplitude (Figure 29). If data was selected to only include ages used in the assessment (age-1 to age-16+) smaller differences occurred between the sampling periods (Appendix 3). Comparing curves derived from age 1-16, western-origin designated fish (Figure 30; Restrepo et al. 2010), even larger similarities are observed when considering AIC_C differences for the 1970s v. 2010s and 1990s v. 2010s contrasts (Appendix 4). Thus, the original rejection of reduced models was possibly driven by differences in sample-specific maximum length, absence of the oldest age-classes in the 1990s sample, and low frequencies of the old age-classes in the 2010s.

Size-at-age growth models provide a coarse representation of individual growth rates and therefore may be relatively insensitive to decadal changes in growth (Mulligan and Leaman 1992). In contrast, tagging studies may offer a better approach for resolving stock and decadal patterns in growth, although bluefin tuna tagging studies have formidable challenges obtaining reliable estimates of size increment during the period the fish is at large (Restrepo et al. 2010). In particular, problems arise due to short time-at-large increments and error in measured length increments. Lengths are frequently estimated instead of measured, and are inconsistently recorded (Ailloud et al. 2014). Further, tagging studies may not span sufficient periods to evaluate decadal changes in growth.

This investigation confirmed some of the key elements of stock structure and behavior: (1) substantial levels of eastern stock subsidy have existed in the Northwest Atlantic (Table 8), (2) little to no mixing occurs on spawning grounds (Gulf of Mexico; Table 8), (3) the Mid-Atlantic region hosts the highest mixing levels (Table 8), and (4) eastern stock contribution decreases with fish size (Table 10). The observed fluctuation in stock mixing does not support the assumptions of constant stock composition (no mixing) made in the ICCAT stock assessments (see also Rooker et al. 2008; Secor 2014; Secor et al. 2015) and indicates that the assessment model should be revised to include these dynamics of stock mixing. To understand the role of migration and production on fluctuations of stock mixing, simulation modeling and sensitivity analyses are needed (Taylor et al. 2011; Kerr et al. 2012).

The return to majority western-origin year-classes in the 2000s (Table 11) offers evidence of population stabilization and possible recovery, yet the continued reliance on

recruit spawners may be curtailing the magnitude of strong year-classes and inhibiting further recovery. Thus, management reference points should also incorporate conservation of older age-classes in the Northwest Atlantic, allowing young adults to grow old. This could possibly be enacted using a maximum size limit or size-based fishing mortality reference points that explicitly track exploitation of specific year classes.

Recovery of age structure will require conservation of all age classes, but if ABFT BOFFFFs indeed offer the reproductive attributes described above (Hixon et al. 2014), a more focused conservation plan may be required to protect these fish. Size limits are one potential management strategy to achieve this, yet economic and technical constraints merit careful attention. Often, the relationship between price per kilogram and individual body size is positive, owing to fishery selectivity, and industry and market preferences (Mullon et al. 2012). However, in the case of Atlantic bluefin tuna, price is primarily related to quality metrics: freshness, fat content, color, and shape (Carroll et al. 2001). Quality metrics and a price plateau at sizes between 150-250 kg (CFL 198.2 – 233.2 cm; ages 10 – 14; Restrepo et al. 2010), suggest the price-size relationship of Atlantic bluefin tuna is parabolic (Mylonas et al. 2010). This supports the hypothesis offered by Mullon et al. (2012), that targeting smaller adults is economically and ecologically viable, where the industry and market remain productive, and BOFFFFs are kept in the spawning stock.

Conservation of older fish would require release of large fish following their capture. However, gears used to capture large adults are not selective enough to discriminate among size ranges: rod-and-reel and longline hooks are not size-selective and size of a hooked individual is typically not known until it surfaces. Although

Hoolihan et al. (2011) observed irregular post-release behavior (i.e. changes in vertical movement patterns) in Atlantic bluefin tuna, Stokesbury et al. (2011) provided evidence that catch-and-release should, in fact, be an option for management and protection of larger individuals, reporting a low post-release mortality of 3.4% for individuals caught in southern Gulf of St. Lawrence. Marcek and Graves (2014) performed a similar study on school-size (69-119 cm CFL) individuals and estimated a post-release mortality of 0%, although this extremely low mortality was likely related to their small sample size (N=19) and the specific fishing method used (recreational gear and tackle, short handling time). Based on market preference for individuals 150-250 kg (198.2-233.2 cm CFL; ages 10-14), I would suggest a maximum size limit of 240 cm CFL. This size limit, corresponding to individuals age-15+, would protect large, old spawning individuals that may not be particularly favored by the Japanese market. Concerns that maximum size limits only work if individuals survive to reach that size are valid; however, in this study, individuals $\geq$ 240 cm CFL comprised 15% of the 2010s sample, so ABFT are indeed surviving to enter this size class.

Alternatively, restoring the age structure of western-stock Atlantic bluefin tuna could be addressed using marine reserves to implement size class-directed reductions in fishing mortality. Large, old western-stock Atlantic bluefin tuna are known to show strong site fidelity to Gulf of Mexico spawning grounds (April-June) and Gulf of St. Lawrence foraging grounds (July-November) with little or no mixing with eastern stock fish (Mather et al. 1995; Rooker et al 2008; Neilson et al 2009; Schloesser et al 2010; Rooker et al 2014). These areas are prime locations for closures, as they would ensure a decreased effort and fishing mortality on large, old fish. In fact, targeted bluefin tuna

fisheries in the Gulf of Mexico are prohibited, with small levels of incidental bycatch comprising the only permitted landings. On the other hand, Canadian maritime fishing communities will face economic hardships if fishing is completely prohibited on giant ABFT. Obviously, improved information on price structure and catch-and-release mortality will be needed to balance conservation benefits against economic costs.

References

Ailloud, L.E., M.V. Lauretta, J.M. Hoenig, J.F. Walter, and A. Fonteneau. 2014. Growth of Atlantic bluefin tuna determined from the ICCAT tagging database: a reconsideration of methods. ICCAT Collective Volume of Scientific Papers 70: 380-393.

Allendorf, F.W., P.R. England, G. Luikart, P.A. Ritchie, and N. Ryman. 2008. Genetic effects of harvest on wild animal populations. Trends in Ecology and Evolution 23: 327-337.

Allman, R. 2015. Unpublished data. NOAA Southeast Fisheries Science Center.

Anderson, C.N.K., C. Hsieh, S.A. Sandin, R. Hewitt, A. Hollowed, J. Beddington, R.M. May, and G. Sugihara. 2008. Why fishing magnifies fluctuations in fish abundance. Nature 452: 835-839.

Baglin, R.E. Jr. 1982. Reproductive biology of western Atlantic bluefin tuna. Fishery Bulletin 80: 121-134.

Bates, D., M. Maechler, B.M. Bolker, and S. Walker. 2014. lme4: Linear mixed-effects models using Eigen and S4. Journal of Statistical Software, URL: http://arxiv.org/abs/1406.5823.

Berkeley, S.A., M.A. Hixon, R.J. Larson, and M.S. Love. 2004. Fisheries sustainability via protection of age structure and spatial distribution of fish populations. Fisheries 29: 23-32.

Birkeland, C., and P.K. Dayton. 2005. The importance in fishery management of leaving the big ones. Trends in Ecology and Evolution 20: 356-358.

Block, B. A., L. L. H. Teo, A. Walli, A. Boustany, M. J.W. Stokesbury, C. J. Farwell, K. C. Weng, H. Dewar, and T. D. Williams. 2005. Electronic tagging and population structure of Atlantic bluefin tuna. Nature 434:1121-1127.

Burnham, K.P. and D.R. Anderson. 2002. Model selection and multimodel inference: A practical information-theoretic approach. Second Edition.

Caddy, J.F., C.A. Dickson, and J.A. Butler. 1976. Age and growth of giant bluefin tuna (*Thunnus thynnus*) taken in Canadian waters in 1975. Journal of the Fisheries Research Board of Canada MS Rep. No. 1395.

Carroll, M.T., J.L. Anderson, J. Martinez-Garmendia. 2001. Pricing US North Atlantic bluefin tuna and implications for management. Agribusiness 17: 243-254.

Conover, D.O., and S.B. Munch. 2002. Sustaining fisheries yields over evolutionary time scales. Science 297:94-96.

Conover, D.O., S.B. Munch, and S.A. Arnott. 2009. Reversal of evolutionary downsizing caused by selective harvest of large fish. Proceedings of the Royal Society: Biological Sciences 276: 2015-2020.

Cort, J.L., S. Deguara, T. Galaz, B. Mèlich, I. Artetxe, I. Arregi, J. Neilson, I. Andrushchenko, A. Hanke, M. Neves dos Santos, V. Estruch, M. Lutcavage, J. Knapp, G. Compeán-Jiménez, R. Solana-Sansores, A. Belmonte, D. Martínez, C. Picinetti, A. Di Natale, A. Kimoto, P. Addis, M. Velasco, J.M. de la Serna, D. Godoy, T. Ceyhan, A. López, O. Ribalta, N. Abid, M. Idrissi, and L. Nøttestad. 2013. Searching for the giant Atlantic bluefin tuna (*Thunnus thynnus*). ICCAT Collective Volume of Scientific Papers SCRS/2012/114.

Dickhut, R.M., A.D. Deshpande, A. Cincinelli, M.A. Cochran, S. Corsolini, R.W. Brill, D.H. Secor, and J.E. Graves. 2009. Atlantic bluefin tuna (*Thunnus thynnus*) population dynamics delineated by organochlorine tracers. Environmental Science & Technology 43: 8522-8527.

Dixon, P.A., M.J. Milicich, G. Sugihara. 1999. Episodic fluctuations in larval supply. Science 283: 1528-1530.

Edeline, E., S.M. Carlson, L.C. Stige, I.J. Winfield, J.M. Fletcher, J.B. James, T.O. Haugen, L.A. Bollestad, and N. Stenseth. 2007. Trait changes in a harvested population are driven by a dynamic tug-of-war between natural and harvest selection. Proceedings of the National Academy of Sciences 104: 15799-15804

Eggleston, D.B., E.A. Bochenek. 1990. Stomach contents and parasite infestation of school bluefin tuna *Thunnus thynnus* collected from the middle Atlantic Bight, Virginia. Fishery Bulletin 88: 389-395.

Estrada, J.A., M. Lutcavage, S.R. Thorrold. 2005. Diet and trophic position of Atlantic bluefin tuna (*Thunnus thynnus*) inferred from stable carbon and nitrogen isotope anlaysis. Marine Biology 147: 37-45.

Fitzhugh, G.R., K.W. Shertzer, G.T. Kellison, and D.M. Wyanski. 2012. Review of size- and age-dependence in batch spawning implications for stock assessment of fish species exhibiting indeterminate fecundity. Fishery Bulletin 110: 413-425.

Fournier, D.A., H.J. Skaug, J. Ancheta, J. Ianelli, A. Magnusson, M.N. Maunder, A. Nielson, and J. Sibert. 2012. AD Model Builder: using automatic differentiation for statistical inference of highly parameterized complex nonlinear models. Optimization Methods and Software 27: 233-249.

Fromentin, J.M. 2009. Lessons from the past: investigating historical data from bluefin tuna fisheries. Fish and Fisheries 10: 197-216.

Fromentin, J.M., and J.E. Powers. 2005. Atlantic bluefin tuna: population dynamics, ecology, fisheries and management. Fish and Fisheries 6:281-306.

Fromentin, J.M., H. Arrizabalaga, V.R. Restrepo, and J. Ortiz de Urbina. 2007. Estimates of total mortality of Eastern Atlantic bluefin tuna abased on year-class curves. ICCAT Collective Volume of Scientific Papers 60: 928-936.

Fromentin, J.M., and V.R. Restrepo. 2009. A year-class curve analysis to estimate mortality of Atlantic bluefin tuna caught by the Norwegian fishery from 1956 to 1979. ICCAT Collective Volume of Scientific Papers 64: 480-490.

Fromentin, J.M., G. Reygondeau, S. Bonhommeau, and G. Beaugrand. 2014. Oceanographic changes and exploitation drive the spatiotemporal dynamics of Atlantic bluefin tuna. Fisheries Oceanography 23:147-156.

Garcia, S.M., J. Kolding, J. Rice, M.-J. Rochet. S. Zhou, T. Arimoto, J.E. Beyer, L. Borges, A. Bundy, D. Dunn, E.A. Fulton, M. Hall, M. Heino, R. Law, M. Makino, A.D. Rijnsdorp, F. Simard, and A.D.M. Smith. 2012. Reconsidering the consequences of selective fisheries. Science. 335:1045-1047.

Graves, J.E., A.S. Wozniak, R.M. Dickhut, M.A. Cochran, E.H. MacDonald, E. Bush, H. Arrizabalaga, and N. Goni. 2015. Transatlantic movements of juvenile Atlantic bluefin tuna inferred from analyses of organochlorine tracers. Canadian Journal of Fisheries and Aquatic Sciences 72: 1-9.

Gunn, J.S., N.P. Clear, T.I. Carter, A.J. Rees, C.A. Stanley, J.H. Farley, J.M. Kalish. 2008. Age and growth in southern bluefin tuna, *Thunnus maccoyii* (Castelnau): Direct estimation from otoliths, scales, and vertebrae. Fisheries Research 92: 207-220.

Harris, P.J., and J.C. McGovern. 1997. Changes in the life history of red porgy, *Pagrus pagrus*, from the southeastern United States, 1972-1994. Fishery Bulletin 95: 732-747.

Harvey, C.J., N. Tolimieri, and P.S. Levin. 2006. Changes in body size, abundance, and energy allocation in rockfish assemblages of the Northeast Pacific. Ecological Applications 16: 1502-1515.

Heinisch, G., H. Rosenfeld, J.M. Knapp, H. Gordin, and M.E. Lutcavage. 2014. Sexual maturity in western Atlantic bluefin tuna. Scientific Reports 4, 7205; DOI:10.1038/srep07205.

Hislop, J.R.G. 1988. The influence of maternal length and age on the size and weight of the eggs and the relative fecundity of the haddock, *Melanogrammus aeglefinus*, in British waters. Journal of Fish Biology 32: 923-930.

Hixon, M.A., D.W. Johnson, and S.M. Sogard. 2014. BOFFFFs: on the importance of conserving old-growth age structure in fishery populations. ICES Journal of Marine Science 71: 2171-2185.

Hoolihan, J.P., J. Luo, F.J. Abascal, S.E. Campana, G. De Metrio, H. Dewar, M.L. Domeier, L.A. Howey, M.E. Lutcavage, M.K. Musyl, J.D. Neilson, E.S. Orbesen, E.D. Prince, and J.R. Rooker. 2011. Evaluating post-release behaviour modification in large pelagic fish deployed with pop-up satellite archival tags. ICES Journal of Marine Sciences 68: 880-889.

Hsieh, C.H., S.M. Glaser, A.J. Lucas, and G. Sugihara. 2005. Distinguishing random environmental fluctuations from ecological catastrophes for the North Pacific Ocean. Nature 435: 336-340.

Hsieh, C.H., C.S. Reiss, J.R. Hunter, J.R. Beddington, R.M. May, and G. Sugihara. 2006. Fishing elevates variability in the abundance of exploited species. Nature 443: 859-862.

Hsieh, C.H., A. Yamauchi, T. Nakazawa, and W. Wang. 2010. Fishing effects on age and spatial structures undermine population stability of fishes. Aquatic Sciences 72: 165-178.

Hutchings, J. A. 2000. Collapse and recovery of marine fishes. Nature 406:882-885.

ICCAT. 2000. ICCAT Conversion Factors. http://www.iccat.int/documents/stats/convers.pdf.

Jennings, S., J.D. Reynolds, and S.C. Mills. 1998. Life history correlates of responses to fisheries exploitation. Proceedings of the Royal Society: Biological Sciences 265: 333-339.

Jennings, S., P.R. Greenstreet, and J.D. Reynolds. 1999. Structural change in an exploited fish community: a consequence of differential fishing effects on species with contrasting life histories. Journal of Animal Ecology 68: 617-627.

Jorgensen, C. K. Enberg, E.S. Dunlop, R. Arlinghaus, D.S. Boukal, K. Brander, B. Ernande, A. Gardmark, F. Johnson, S. Matsumara, H. Pardoe, K. Raab, A. Silva, A. Vainikka, U. Dieckmann, M. Heino, A.D. Rijnsdorp. 2007. Managing evolving fish stocks. Science 318: 1247-1248.

Keeling, C.D. 1979. The Suess effect: ^{13}Carbon-^{14}Carbon interrelations. Environment International 2: 229-300.

Kerr, L.A., S.X. Cadrin, and D.H. Secor. 2012. Evaluating population effects and management implications of mixing between eastern and western Atlantic bluefin tuna stocks. ICES CM 2012/N:13.

Knapp, J.M., G. Aranda, A. Medina, and M. Lutcavage. 2014. Comparative assessment of the reproductive status of female Atlantic bluefin tuna from the Gulf of Mexico and the Mediterranean Sea. PLoS One 9: e98233.

Law, R. 2000. Fishing, selection, and phenotypic evolution. ICES Journal of Marine Science 57: 659-668.

Law, R. 2007. Fisheries-induced evolution: present status and future directions. Marine Ecology Progress Series 335: 249-251.

Logan, J.M., E. Rodriquez-Marin, N. Goni, S. Barreiro, H. Arrizabalaga, W. Golet, and M. Lutcavage. 2011. Diet of young Atlantic bluefin tuna (*Thunnus thynnus*) in eastern and western Atlantic foraging grounds. Marine Biology 158: 73-85.

MacKenzie, B.R., M.R. Payne, J. Boje, J.L. Hoyer, and H. Siegstad. 2014. A cascade of warming impacts brings bluefin tuna to Greenland waters. Global Change Biology 20: 2484-2491.

Marcek, B.J., and J.E. Graves. 2014. An estimate of post-release mortality of school-size bluefin tuna in the U.S. recreational troll fishery. North American Journal of Fisheries Management 34: 602-608.

Marteinsdottir, G. and A. Steinarsson. 1998. Maternal influence on the size and viability of Iceland cod *Gadus morhua* egs and larvae. Journal of Fish Biology 52: 1241-1258.

Mather, F.J., J.M. Mason, and A.C. Jones. 1995. Historical document: life history and fisheries of Atlantic bluefin tuna. National Oceanic and Atmospheric Agency Technical Memorandum NMFS-SEFSC 370.

Millar, R.B. 1990. A versatile computer program for mixed stock fishery composition estimation. Canadian Technical Report of Fishery and Aquatic Science No. 1753.

Millar, R.B. 2015. A better estimator of mortality rate from age-frequency data. Canadian Journal of Fisheries and Aquatic Sciences 72: 364-375.

Mulligan, T.J, and B.M. Leaman. 1992. Length-at-age analysis: can you get what you see? Canadian Journal of Fisheries and Aquatic Sciences 49: 632-643.

Mullon, C., J.G. Field, O. Thebaud, P. Cury, and C. Chaboud. 2012. Keeping the big fish: economic and ecological tradeoffs in size-based fisheries management. Journal of Bioeconomics 14: 267-285.

Myers, R.A., J.A. Hutchings, and N.J. Barrowman. 1996. Hypotheses for the decline of cod in the North Atlantic. Marine Ecology Progress Series 138: 293-308.

Myers, R.A, J.A. Hutchings, and N.J. Barrowman. 1997. Why do fish stocks collapse? The example of cod in Atlantic Canada. Ecological Applications 7: 91-106.

Myers, R.A., and B. Worm. 2003. Rapid worldwide depletion of predatory fish communities. Nature 423:280-283.

Mylonas, C.C., F. De La Gandara, A. Corriero, and A.B. Rios. 2010. Atlantic bluefin tuna (*Thunnus thynnus*) farming and fattening in the Mediterranean Sea. Reviews in Fisheries Science 18: 266-280.

Neilson, J.D., S. Smith, M. Ortiz, and B. Lester. 2009. Indices of stock status obtained from the Canadian bluefin tuna fishery. ICCAT Collective Volume Science Papers 64: 380-404.

Nemerson, D., S. Berkeley, and C. Safina. 2000. Spawning site fidelity in Atlantic bluefin tuna, *Thunnus thynnus*: the use of size-frequency analysis to test for the presence of migrant east Atlantic bluefin tuna on Gulf of Mexico spawning grounds. Fishery Bulletin 98: 118-126.

Overholtz, W.J. 1989. Density-dependent growth in the Northwest Atlantic stock of Atlantic mackerel (*Scomber scombrus*). Journal of Northwest Atlantic Fisheries Science 9: 115-121.

Overholtz, W.J. and K.D. Friedland. 2002. Recovery of the Gulf of Maine—Georges Bank Atlantic herring (*Clupea harengus*) complex: perspectives based on bottom trawl survey data. Fishery Bulletin 100: 593-608.

Overholtz, W.J. 2006. Estimates of consumption of Atlantic herring (*Clupea harengus*) by bluefin tuna (*Thunnus thynnus*) during 1970-2002: an approach incorporating uncertainty. Journal of Northwest Atlantic Fisheries Science 36: 55-63.

Pauly, D. 1983. Some simple methods for the 1983 assessment of tropical fish stocks. FAO Fish.Tech.Pap 234: 52..

Pikitch, E.K., C. Santora, E.A. Babcock, A. Bakun, R. Bonfil, D.O. Conover, P. Dayton, P. Doukakis, D. Fluharty, B. Heneman, E.D. Houde, J. Link, P.A. Livingston, M. Mangel, M.K. McAllister, J. Pope, and K.J Sainsbury. 2004. Ecosystem-based fishery management. Science 305:346-347.

Porch, C.E. 2005. The sustainability of western Atlantic bluefin tuna: a warm-blooded fish in a hot-blooded fishery. Bulletin of Marine Science 76: 363-384.

Ravier, C. and J.-M. Fromentin. 2001. Long-term fluctuations in the Eastern Atlantic and Mediterranean bluefin tuna population. ICES Journal of Marine Science 58: 1299-1317.

Ravier, C. and J.-M. Fromentin. 2004. Are the long-term fluctuations in Atlantic bluefin tuna (*Thunnus thynnus*) population related to environmental changes? Fisheries Oceanography 13: 145-160.

Restrepo, V.R., G.A. Diaz, J.F. Walter, J.D. Neilson, S.E. Campana, D. Secor, and R.L. Wingate. 2010. Updated estimate of the growth curve of Western Atlantic bluefin tuna. Aquatic Living Resources 23: 335-342.

Ricker, W.E. 1981. Changes in the average size and average age of Pacific salmon. Canadian Journal of Fisheries and Aquatic Sciences 38: 1636-1656.

Rivas, L.R. 1976. Variation in sex ratio, size differences between sexes, and change in size and age composition in western North Atlantic giant bluefin tuna (*Thunnus thynnus*). ICCAT Collective Volume of Scientific Papers 5: 297-301.

Rodriguez-Marin, E. N. Clear, J.L. Cort, P. Megalofonou, J.D. Neilson, M. Neves dos Santos, D. Olafsdottir, C. Rodriguez-Cabello, M. Ruiz, and J. Valeiras. 2006. Report of the 2006 ICCAT workshop for bluefin tuna direct ageing. ICCAT Collective Volume Science Papers 60(4): 1349-1392.

Rooker, J.R., J.R. Alvarado-Bremer, B.A. Block, J.L. Cort, H. Dewar, G. DeMetrio, R.T. Kraus, E.D. Prince, E. Rodriquez-Marin, D.H. Secor. 2007. Life history and stock structure of Atlantic bluefin tuna (*Thunnus thynnus*). Reviews in Fisheries Science 15:265-310.

Rooker, J.R., D.H. Secor, G. D. DeMetrio, R. Schloesser, B.A. Block, and J.D. Neilson. 2008. Natal homing and connectivity in Atlantic bluefin tuna populations. Science 322:742-744.

Rooker, J.R., H. Arrizabalaga, I. Fraile, D.H. Secor, D.L. Dettman, N. Abid, P. Addis, S. Deguara, F.S. Karakulak, A. Kimoto, O. Sakai, D. Macias, M.N. Santos. 2014. Crossing the line: migratory and homing behaviors of Atlantic bluefin tuna. Marine Ecology Progress Series 504:265-276.

Rouyer, T., A. Sadykov, J. Ohlberger, and N.C. Stenseth. 2012. Does increasing mortality change the response of fish populations to environmental fluctuations? Ecology Letters 15: 658-665.

Safina, C., and D.H. Klinger. 2008. Collapse of bluefin tuna in the Western Atlantic. Conservation Biology 22: 243-246.

Schloesser, R.W., J.R. Rooker, P. Louchuoarn, J.D. Neilson, and D.H. Secor. 2009. Interdecadal variation in seawater for $\delta^{13}C$ and $\delta^{18}O$ recorded in fish otoliths. Limnology and Oceanography 54(5): 1665-1668.

Schloesser, R.W., J.D. Neilson, D.H. Secor, and J.R. Rooker. 2010. Natal origin of Atlantic bluefin tuna (*Thunnus thynnus*) from Canadian waters based on otolith for $\delta^{13}C$ and $\delta^{18}O$. Canadian Journal of Fisheries and Aquatic Science 67:563-569.

Schmidt, G.A., G.R. Bigg, and R.J. Rohling. 1999. Global Seawater Oxygen-18 Database – v1.21. http://data.giss.nasa.gov/o18data/

SCRS (Standing Committee on Research and Statistics, International Commission for the Conservation of Atlantic Tunas). 2012. Report of the 2012 Atlantic bluefin tuna stock assessment session. Madrid. Available from http://www.iccat.es/en/assess.html.

SCRS (Standing Committee on Research and Statistics, International Commission for the Conservation of Atlantic Tunas). 2014. Report of the 2014 Atlantic bluefin tuna stock assessment session. Madrid. Available from http://www.iccat.es/en/assess.html.

Secor, D.H. 2000a. Longevity and resilience of Chesapeake Bay striped bass. ICES Journal of Marine Science 57: 808-815.

Secor, D.H. 2000b. Spawning in the nick of time? Effect of adult demographics on spawning behavior and recruitment in Chesapeake Bay striped bass. ICES Journal of Marine Science 57: 403-411.

Secor, D.H. 2007. The year-class phenomenon and the storage effect in marine fishes. Journal of Sea Research 57:91-103.

Secor, D.H. 2014. Synopsis of regional mixing levels for Atlantic bluefin tuna estimated from otolith stable isotope analysis, 2007-2014. ICCAT Collective Volume Science Papers.

Secor, D.H. 2015. Migration ecology of marine fishes. Johns Hopkins University Press, Baltimore.

Secor, D.H., R. Allman, D. Busawon, B. Gahagan, W. Golet, E. Koob, P. Lastra Luque, and M. Siskey. 2014a. Standardization of otolith-based ageing protocols for Atlantic bluefin tuna. ICCAT Collective Volume of Scientific Papers SCRS/2013/084.

Secor, D.H., D. Busawon, B. Gahagan, W. Golet, E. Koob, J. Neilson, and M. Siskey. 2014b. Conversion factors for Atlantic bluefin tuna fork length from measures of snout length and otolith mass. ICCAT Collective Volume of Scientific Papers 70: 364-367.

Secor, D.H., J.R. Rooker, B.I. Gahagan, M.R. Siskey, and R. W. Wingate. 2015. Depressed resilience of bluefin tuna in the Western Atlantic and age truncation. Conservation Biology 29: 400-408.

Sinclair, A.F., D.P. Swain, and J.M. Hanson. 2002. Disentangling the effects of size-selective mortality, density, and temperature on length-at-age. Canadian Journal of Fisheries and Aquatic Sciences 59: 372-382.

Solomon, C.T., P.K. Weber, J.J. Cech Jr., B.L. Ingram, M.E. Conrad, M.V. Machavaram, A.R. Pogodina, and R.L. Franklin. 2006. Experimental determination of the sources of otolith carbon and associated isotopic fractionation. Canadian Journal of Fisheries and Aquatic Sciences 63: 79-89.

Stokesbury, M.J.W., J.D. Neilson, E. Susko, and S.J. Cooke. 2011. Estimating mortality of Atlantic bluefin tuna (*Thunnus thynnus*) in an experimental recreational catch-and-release fishery. Biological Conservation 144: 2684-2691.

Swain, D.P., A.F. Sinclair, and J.M. Hanson. 2007. Evolutionary response to size-selective mortality in an exploited fish population. Proceedings of the Royal Society B 274: 1015-1022.

Tanaka, S. 2006. Maturation of bluefin tuna in the Sea of Japan. ISC PBF-WG/06/Doc.9.

Taylor, N.G., M.K. McAllister, G.L. Lawson, T. Carruthers, B.A. Block. 2011. Atlantic bluefin tuna: a novel multistock spatial model for assessing population biomass. PLoS One 6: e27693.

Trippel, E.A. 1995. Age at maturity as a stress indicator in fisheries. BioScience 45: 759-771.

Verburg, P. 2007. The need to correct for the Suess effect in the application of $\delta^{13}C$ in sediment of autotrophic Lake Tanganyika as a productivity proxy in the Anthropocene. Journal of Paleolimnology 37: 591-602.

Walli, A., S.L.H. Teo, A. Boustany, C.J. Farwell, T. Williams, H. Dewar, E. Prince, and B.A. Block. 2009. Seasonal movements, aggregations and diving behavior of Atlantic bluefin tuna (*Thunnus thynnus*) revealed with archival tags. PLoS One 4: e6151.

Warner, R.R. and P.L. Chesson. 1985. Coexistence mediated by recruitment fluctuations: a field guide to the storage effect. American Naturalist 125: 769-787.

Winemiller, K.O. and K.A. Rose. 1992. Patterns of life-history diversification in North American fishes: implications for population regulation. Canadian Journal of Fisheries and Aquatic Sciences 49: 2196-2218.

Worm, B., R. Hilborn, J.K. Baum, T.A. Branch, J.S. Collie, C. Costello, M.J. Fogarty, E.A. Fulton, J.A. Hutchings, S. Jennings, O.P. Jensen, H.K. Lotze, P.M. Mace, T.R. McClanahan, C. Minto, S.R. Palumbi, A.M. Parma, D. Richard, A.A. Rosenberg, R. Watson, and D. Zeller. 2009. Rebuilding global fisheries. Science 325:578-585.

Wright, P.J. and E.A. Trippel. 2009. Fishery-induced demographic changes in the timing of spawning: consequences for reproductive success. Fish and Fisheries 10: 283-304.

Tables

Table 2.1. Size classes, associated curved fork length (CFL; cm) for US Atlantic bluefin tuna, and fleet that targets each. Commercial limits are not presented because they are numerous and changing, varying by gear type, season, region, and fishery performance (Source: www.hmspermits.noaa.gov; www.iccat.int/en/RecsRegs.asp).

Size Class	*CFL(cm)*	*Fleet*	*Limits*	*Area*	*Season*
Young School	< 27”	No landings allowed			
School	27 < 47”	Recreational	1/vessel/day	All, excluding Gulf of Mexico	Year-round
Large School	47 < 59”	Recreational			
Small Medium	59 < 73”	Recreational			
Large Medium	73 < 81”	Commercial/Recreational	Rec: 1/vessel/year	All areas	Comm: 1 Jan-31 Mar; 1 Jun-31 Dec
Giant	81” +	Commercial/Recreational			

Table 2.2. Distribution of Atlantic bluefin tuna otolith samples by size (cm; curved fork length), region, and sample.

	1974-1978 (N=350)			**1996-2002 (N=234)**		**2009-2014 (N=1359)**		
Size (cm)	*New England*	*Mid-Atlantic*	*Gulf of Mexico*	*New England*	*Mid-Atlantic*	*New England*	*Mid-Atlantic*	*Gulf of Mexico*
50-100	38	54		28	26	5	147	
100-200	1	48	1	45	53	261	641	1
200-250	48		27	65		29	56	92
250-300	58		75	17		14	3	110

Table 2.3. Selectivity of Atlantic bluefin tuna age classes from 1970-2013, calculated from age-specific fishing mortality estimates generated in ICCAT's 2014 Atlantic bluefin tuna stock assessment via virtual population analysis (SCRS 2014). Age-16 references all ages >15 years.

Year	*Age-1*	*Age-2*	*Age-3*	*Age-4*	*Age-5*	*Age-6*	*Age-7*	*Age-8*
1970	0.209	0.911	1.000	0.569	0.208	0.037	0.014	0.004
1971	0.239	0.996	0.805	1.000	0.022	0.033	0.040	0.057
1972	0.301	1.000	0.834	0.148	0.276	0.104	0.006	0.025
1973	0.074	1.000	0.749	0.305	0.215	0.293	0.050	0.066
1974	0.593	0.801	1.000	0.446	0.433	0.377	0.212	0.251
1975	0.560	1.000	0.136	0.363	0.034	0.049	0.036	0.039
1976	0.076	0.379	1.000	0.064	0.099	0.047	0.017	0.017
1977	0.030	0.509	0.311	1.000	0.320	0.152	0.178	0.067
1978	0.213	0.407	1.000	0.338	0.728	0.613	0.148	0.056
1979	0.109	0.554	0.891	0.719	1.000	0.235	0.337	0.270
1980	0.150	0.779	0.697	0.650	0.459	0.211	0.354	0.718
1981	0.240	0.467	1.000	0.285	0.514	0.414	0.367	0.348
1982	0.511	0.670	0.351	0.170	0.085	0.202	0.287	0.266
1983	0.189	0.205	0.342	0.105	0.116	0.179	0.184	0.384
1984	0.090	0.646	0.222	0.264	0.431	0.472	0.306	0.181
1985	0.038	0.361	1.000	0.236	0.538	0.740	0.510	0.197
1986	0.047	0.360	0.533	0.308	0.187	0.215	0.271	0.206
1987	0.170	1.000	0.891	0.618	0.661	0.782	0.358	0.497
1988	0.194	0.687	1.000	0.413	0.478	0.602	0.706	0.463
1989	0.043	0.779	0.178	0.460	0.417	0.319	0.460	0.791
1990	0.120	0.154	1.000	0.166	0.274	0.295	0.203	0.311
1991	0.282	1.000	0.771	0.329	0.306	0.318	0.441	0.535
1992	0.040	0.433	0.149	0.085	0.129	0.214	0.189	0.418
1993	0.041	0.110	0.538	0.441	0.297	0.255	0.441	0.448
1994	0.166	0.079	0.146	0.311	0.377	0.278	0.232	0.483
1995	0.059	0.125	0.408	0.414	0.500	0.796	0.237	0.145
1996	0.037	0.656	0.172	0.687	0.534	0.221	0.301	0.472
1997	0.023	0.085	0.528	0.108	0.227	0.273	0.301	0.449
1998	0.023	0.087	0.326	0.366	0.087	0.238	0.169	0.395
1999	0.005	0.036	0.197	0.187	0.202	0.114	0.166	0.440
2000	0.006	0.017	0.084	0.152	0.483	0.472	0.303	0.382
2001	0.093	0.027	0.180	0.404	0.148	0.208	0.317	0.492
2002	0.047	0.414	0.346	0.398	0.513	0.225	0.178	0.644
2003	0.014	0.232	0.580	0.529	0.275	0.283	0.094	0.399
2004	0.059	0.186	1.000	0.549	0.667	0.706	0.451	0.686

2005	0.108	0.369	0.189	0.423	0.252	0.225	0.189	0.333
2006	0.027	0.118	0.109	0.155	0.491	0.573	0.345	0.345
2007	0.006	0.024	1.000	0.683	0.150	0.287	0.275	0.168
2008	0.010	0.100	0.380	0.680	1.000	0.220	0.580	0.860
2009	0.011	0.044	0.367	0.267	0.433	1.000	0.278	0.311
2010	0.012	0.253	0.193	0.398	0.181	0.361	0.205	0.434
2011	0.000	0.111	0.444	0.444	0.543	0.432	0.383	1.000
2012	0.013	0.169	0.442	0.416	0.156	0.195	0.299	0.623
2013	0.015	0.031	0.323	0.415	0.092	0.262	0.277	0.569
Average All	0.120	0.418	0.541	0.397	0.353	0.330	0.266	0.369
Average 70s	0.294	0.619	0.689	0.442	0.323	0.248	0.118	0.086
Average 90s	0.033	0.189	0.262	0.329	0.313	0.250	0.248	0.468
Average 10s	0.010	0.122	0.354	0.388	0.281	0.450	0.288	0.587

Year	*Age-9*	*Age-10*	*Age-11*	*Age-12*	*Age-13*	*Age-14*	*Age-15*	*Age-16*
1970	0.001	0.007	0.020	0.017	0.025	0.034	0.041	0.041
1971	0.035	0.019	0.024	0.042	0.045	0.047	0.051	0.051
1972	0.028	0.016	0.008	0.022	0.068	0.084	0.073	0.073
1973	0.100	0.078	0.020	0.032	0.050	0.100	0.070	0.070
1974	0.156	0.126	0.212	0.104	0.100	0.424	0.554	0.554
1975	0.068	0.097	0.126	0.124	0.102	0.092	0.144	0.144
1976	0.129	0.131	0.072	0.099	0.268	0.258	0.205	0.205
1977	0.067	0.178	0.300	0.230	0.155	0.294	0.330	0.330
1978	0.089	0.098	0.115	0.216	0.243	0.203	0.620	0.620
1979	0.088	0.098	0.179	0.326	0.667	0.730	0.747	0.747
1980	0.602	0.180	0.194	0.354	0.561	0.820	1.000	1.000
1981	0.390	0.481	0.260	0.367	0.544	0.779	0.903	0.903
1982	0.223	0.415	0.638	0.532	0.755	0.798	1.000	1.000
1983	0.384	0.347	0.342	0.342	0.400	0.732	1.000	1.000
1984	0.292	0.424	0.521	0.611	0.653	0.771	1.000	1.000
1985	0.159	0.202	0.250	0.389	0.606	0.688	0.885	0.885
1986	0.136	0.145	0.164	0.238	0.472	0.617	1.000	1.000
1987	0.491	0.515	0.303	0.345	0.455	0.630	0.782	0.782
1988	0.413	0.478	0.463	0.373	0.468	0.557	0.721	0.721
1989	0.755	0.663	0.675	0.730	0.669	0.877	1.000	1.000
1990	0.531	0.639	0.469	0.481	0.432	0.423	0.656	0.656
1991	0.659	0.882	0.876	0.888	0.824	0.753	0.806	0.806
1992	0.577	0.428	0.632	0.886	0.960	1.000	0.692	0.692
1993	0.779	1.000	0.669	0.690	0.786	0.759	0.807	0.807
1994	1.000	0.589	0.715	0.781	0.695	0.828	0.662	0.662

1995	0.342	0.941	0.697	0.612	0.638	0.757	1.000	1.000
1996	0.215	0.276	0.736	0.748	0.773	0.755	1.000	1.000
1997	0.438	0.335	0.295	0.523	0.733	0.955	1.000	1.000
1998	0.750	0.797	0.506	0.442	0.773	1.000	0.959	0.959
1999	0.430	0.684	0.679	0.715	0.762	1.000	0.964	0.964
2000	0.416	0.500	0.556	0.579	0.663	0.831	1.000	1.000
2001	0.251	0.377	0.612	0.891	0.825	0.831	1.000	1.000
2002	0.691	0.649	0.529	0.602	1.000	0.874	0.969	0.969
2003	0.841	0.797	0.623	0.362	0.652	0.949	1.000	1.000
2004	0.500	0.676	0.637	0.716	0.657	0.637	0.961	0.961
2005	0.423	0.387	0.757	1.000	0.928	0.640	0.874	0.874
2006	0.573	0.791	0.618	0.745	0.700	0.718	1.000	1.000
2007	0.144	0.114	0.240	0.216	0.263	0.263	0.371	0.371
2008	0.600	0.430	0.440	0.420	0.400	0.420	0.730	0.730
2009	0.633	0.600	0.467	0.411	0.456	0.556	0.856	0.856
2010	0.410	0.855	1.000	0.542	0.494	0.783	0.904	0.904
2011	0.617	0.432	0.667	0.704	0.580	0.605	0.778	0.778
2012	0.571	0.584	1.000	0.649	0.727	0.532	0.740	0.740
2013	0.738	0.385	0.477	1.000	1.000	0.738	0.677	0.677
Average All	0.403	0.428	0.450	0.479	0.546	0.617	0.739	0.739
Average 70s	0.102	0.126	0.165	0.155	0.173	0.254	0.371	0.371
Average 90s	0.456	0.517	0.559	0.643	0.790	0.892	0.985	0.985
Average 10s	0.594	0.571	0.722	0.661	0.651	0.643	0.791	0.791

Table 2.4. von Bertalanffy parameters of growth curves [L_{inf} (asymptotic length; cm CFL), K (rate at which asymptotic length is approached), and t_0 (length at age-0)] produced for Atlantic bluefin tuna samples landed in the 1970s, 1990s, and 2010s.

	1970s		***1990s***		***2010s***	
	Value	*SE*	*Value*	*SE*	*Value*	*SE*
L_{inf}	275.6	2.205	291.0	10.31	322.2	6.085
K	0.132	0.005	0.126	0.011	0.104	0.004
t_0	-0.47	0.101	-0.38	0.181	0.540	0.116

Table 2.5. Negative log likelihood contrasts for Atlantic bluefin tuna growth models, which include or exclude decadal effects. Full Model refers to models that incorporate separate decadal parameters; Reduced Model refers to models that use one set of parameters for both decades. Second-order Akaike Information Criteria (AIC_C) and AIC_C differences are reported for growth curves corresponding to the 1970s (N=350), 1990s (N=234), and 2010s (N=1359). Δ_I denotes the AIC_C difference between the full and reduced model.

	1970s v. 1990s	***1970s v. 2010s***	***1990s v. 2010s***
Full Model	3931.6	12012.5	11326.8
Reduced Model	3941.7	12272.6	11469.6
Δ_i	10.1	260.1	142.8

Table 2.6. von Bertalanffy parameters of growth curves [L_{inf} (asymptotic length; cm CFL), K (rate at which asymptotic length is approached), and t_0 (length at age-0)] produced for assigned western stock Atlantic bluefin tuna samples landed in the 1970s (N=325), 1990s (N=132), and 2010s (N=1185).

	1970s		***1990s***		***2010s***		***Restrepo***	
	Value	*SE*	*Value*	*SE*	*Value*	*SE*	*Value*	*SE*
L_{inf}	275.9	2.274	276.8	10.34	321.3	6.219	314.9	5.8
K	0.132	0.005	0.145	0.016	0.107	0.005	0.089	0.003
t_0	-0.46	0.104	-0.08	0.242	0.619	0.122	-1.13	0.035

Table 2.7. Negative log likelihood contrasts for assigned western stock Atlantic bluefin tuna growth models, which include or exclude decadal effects. Full Model refers to models that incorporate separate decadal parameters; Reduced Model refers to models that use one set of parameters for both decades. Second-order Akaike Information Criteria (AIC_C) and AIC_C differences are reported for growth curves corresponding to the 1970s (N=325), 1990s (N=132), and 2010s (N=1185). Δ_I denotes the AIC_C difference between the full and reduced model.

	1970s W v. 1990s W	***1970s W v. 2010s W***	***1990s W v. 2010s W***
Full Model	3045.2	10631.4	9399.8
Reduced Model	3052.2	10874.3	9469.4
Δ_i	7	242.9	69.6

Table 2.8. Estimated population mixing levels in Atlantic bluefin tuna samples from Gulf of Mexico, New England, and Mid-Atlantic fisheries in the 1970s, 1990s, and 2010s.

Year class	*Years sampled*	*Location*	*n*	*Population*	*MLE%*	*MLE SD*
1944-1974	1974-1978	New England, Mid-Atlantic, Gulf of Mexico	349	west	100	0.0
				east	0	
1947-1974	1975-1977	New England	145	west	100	0.2
				east	0	
1966-1974	1974-1977	Mid-Atlantic	102	west	100	0.0
				east	0	
1944-1967	1976 & 1978	Gulf of Mexico	102	west	100	1.2
				east	0	
1975-1997	1996-2002	New England, Mid-Atlantic	229	west	52	4.7
				east	48	
1975-1997	1996-2002	New England	153	west	59	5.6
				east	41	
1985-1997	1996-2000	Mid-Atlantic	76	west	37	7.7
				east	63	
1978-2011	2009-2014	New England, Mid-Atlantic, Gulf of Mexico	1375	west	96	1.2
				east	4	
1988-2009	2010-2014	New England	318	west	99	1.3
				east	1	
1993-2011	2010-2014	Mid-Atlantic	854	west	90	1.7
				east	10	
1978-2006	2009-2014	Gulf of Mexico	203	west	100	0.0
				east	0	

Table 2.9. Juvenile and adult mixing levels in Atlantic bluefin tuna samples from Gulf of Mexico, New England, and Mid-Atlantic fisheries from the 1970s, 1990s, and 2010s.

Year class	*Years sampled*	*Age group*	*Location*	*n*	*Population*	*MLE%*	*MLE SD*
1968-1974	1974-1977	Juvenile	New England, Mid-Atlantic, Gulf of Mexico	137	west	100	0.9
					east	0	
1972-1974	1975		New England	38	west	94	5.9
					east	6	
1968-1974	1974-1977		Mid-Atlantic	99	west	100	0.0
					east	0	
1944-1969	1975-1978	Adult	New England, Mid-Atlantic, Gulf of Mexico	212	west	100	0.0
					east	0	
1947-1967	1975-1977		New England	107	west	100	0.0
					east	0	
1944-1967	1976 & 1978		Gulf of Mexico	102	west	100	1.2
					east	0	
1989-1997	1996-2002	Juvenile	New England, Mid-Atlantic	116	west	35	5.8
					east	65	
1989-1997	1996-2002		New England	48	west	31	8.6
					east	69	
1990-1997	1996-2000		Mid-Atlantic	68	west	38	8.0
					east	62	
1975-1994	1996-2002	Adult	New England, Mid-Atlantic	113	west	74	6.6

					east	26	
1975-1994	1996-2002		New England	105	west	76	6.8
					east	24	
1985-1990	1997-1998		Mid-Atlantic	8	west	20	24.2
					east	80	
2003-2011	2010-2014	Juvenile	New England, Mid-Atlantic	873	west	93	1.8
					east	7	
2003-2009	2010-2014		New England	211	west	94	3.7
					east	6	
2004-2011	2010-2014		Mid-Atlantic	662	west	93	2.0
					east	7	
1978-2006	2009-2014	Adult	New England, Mid-Atlantic, Gulf of Mexico	502	west	98	1.3
					east	2	
1988-2006	2010-2014		New England	107	west	100	0.0
					east	0	
1993-2006	2011-2014		Mid-Atlantic	192	west	82	4.8
					east	18	
1978-2006	2009-2014		Gulf of Mexico	203	west	100	0.0
					east	0	

Table 2.10. Estimated population mixing levels in Atlantic bluefin tuna samples from fisheries in the 1970s, 1990s, and 2010s by size class.

Decade	*Size (cm)*	*n*	*Population*	*MLE%*	*MLE SD*
1970s	50-100	92	west	99	1.7
			east	1	
	100-200	50	west	100	0.8
			east	0	
	200-250	74	west	100	0.1
			east	0	
	250-300	133	west	100	0.0
			east	0	
1990s	50-100	54	west	27	8.2
			east	73	
	100-200	93	west	49	7.4
			east	51	
	200-250	64	west	68	9.3
			east	32	
	250-300	14	west	100	1.5
			east	0	
2010s	50-100	152	west	93	4.4
			east	7	
	100-200	903	west	92	1.7
			east	8	
	200-250	177	west	100	0.8
			east	0	
	250-300	127	west	100	1.2
			east	0	

Table 2.11. Estimates of Atlantic bluefin tuna stock mixing for strong year classes.

Year class	*Years sampled*	*Location*	*n*	*Population*	*MLE%*	*MLE SD*
1952	1975-1978	New England and Gulf of Mexico	20	west	100	0.0
				east	0	
1956	1975-1978	New England and Gulf of Mexico	22	west	100	0.0
				east	0	
1957	1975-1978	New England and Gulf of Mexico	18	west	100	0.0
				east	0	
1958	1975-1978	New England and Gulf of Mexico	14	west	100	0.0
				east	0	
1972	1975-1977	New England and Mid-Atlantic	23	west	95	7.2
				east	5	
1973	1975-1977	New England and Mid-Atlantic	60	west	98	2.8
				east	2	
1974	1975 & 1977	New England and Mid-Atlantic	27	west	100	0.8
				east	0	
1986	1996 & 2002	New England	17	west	47	18.5
				east	53	
1987	1996-2009	New England, Mid-Atlantic, and Gulf of Mexico	18	west	61	19.5
				east	39	
1988	1996-2012	New England, Mid-Atlantic, and Gulf of Mexico	28	west	98	4.9

				east	2	
1989	1996-2010	New England, Mid-Atlantic, and Gulf of Mexico	32	west	83	11.3
				east	17	
1995	1997-2013	New England, Mid-Atlantic, and Gulf of Mexico	43	west	65	9.4
				east	35	
1997	1998-2010	New England, Mid-Atlantic, and Gulf of Mexico	39	west	68	9.8
				east	32	
2001	2009-2014	New England, Mid-Atlantic, and Gulf of Mexico	56	west	100	0.6
				east	0	
2002	2010-2014	New England, Mid-Atlantic, and Gulf of Mexico	58	west	100	1.4
				east	0	
2003	2010-2014	New England, Mid-Atlantic, and Gulf of Mexico	88	west	98	2.2
				east	2	
2004	2010-2014	New England, Mid-Atlantic, and Gulf of Mexico	105	west	85	6.0
				east	15	
2005	2010-2014	New England, Mid-Atlantic, and Gulf of Mexico	170	west	92	4.1
				east	8	
2006	2011-2014	New England, Mid-Atlantic, and Gulf of Mexico	209	west	92	3.9
				east	8	

2007	2011-2014	New England and Mid-Atlantic	204	west	96	3.0
				east	4	
2008	2011-2014	New England and Mid-Atlantic	156	west	94	4.0
				east	6	

Figures

Figure 2.1. Map showing spawning grounds for western (red) and eastern (blue) stock Atlantic bluefin tuna. Yellow line denotes 45-degree Meridian used to delineate stock management boundaries.

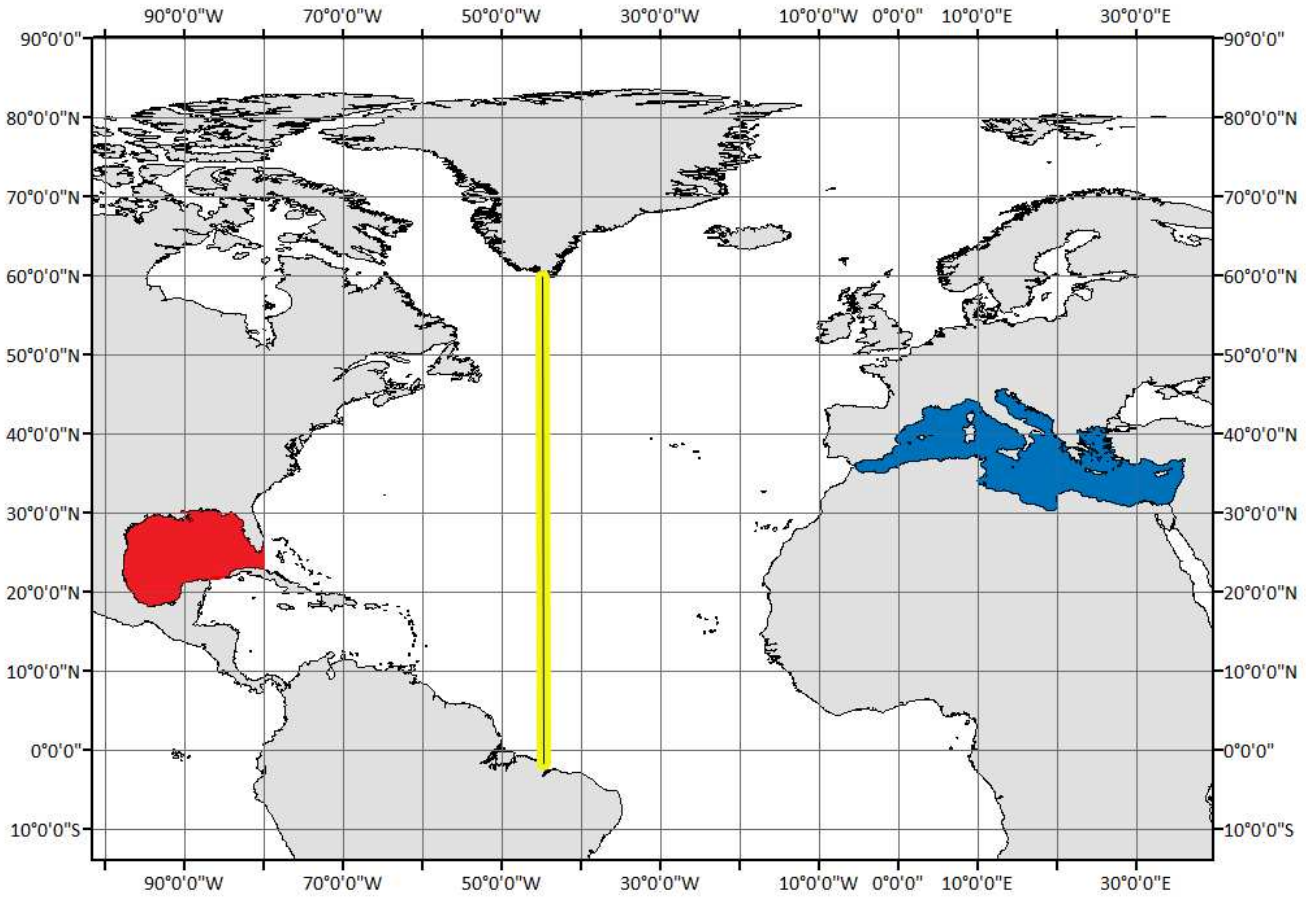

Figure 2.2. Landings (in tonnes) of Atlantic bluefin tuna in the Western (red) and Eastern (blue) North Atlantic from 1950-2013. The Eastern North Atlantic includes the Mediterranean Sea.

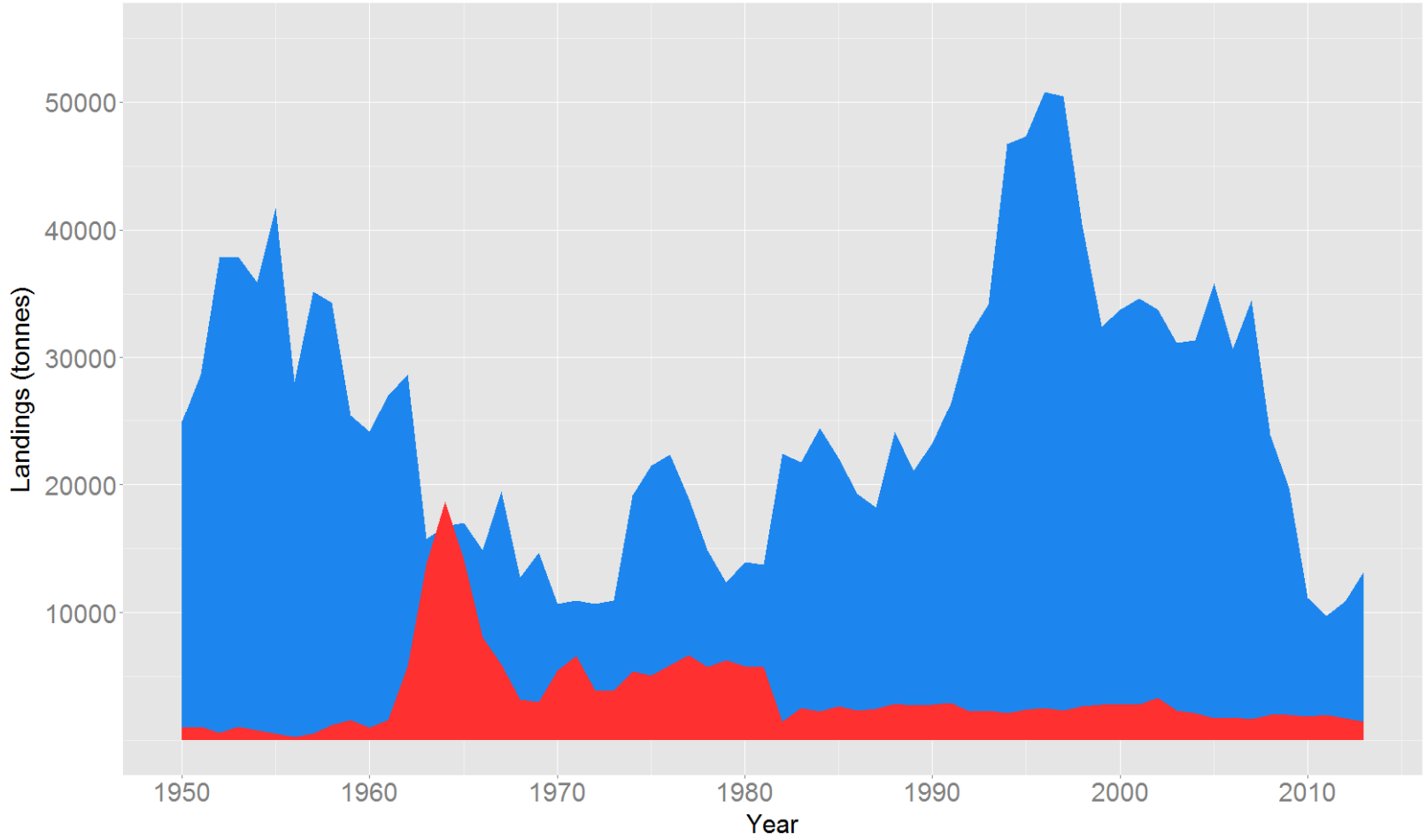

Figure 2.3. Catch-at-size data for Atlantic bluefin tuna from fisheries operating in the 1970s (1974-1978), 1990s (1996-2002), and 2010s (2009), obtained via the ICCAT database (https://www.iccat.int/en/accesingdb.htm).

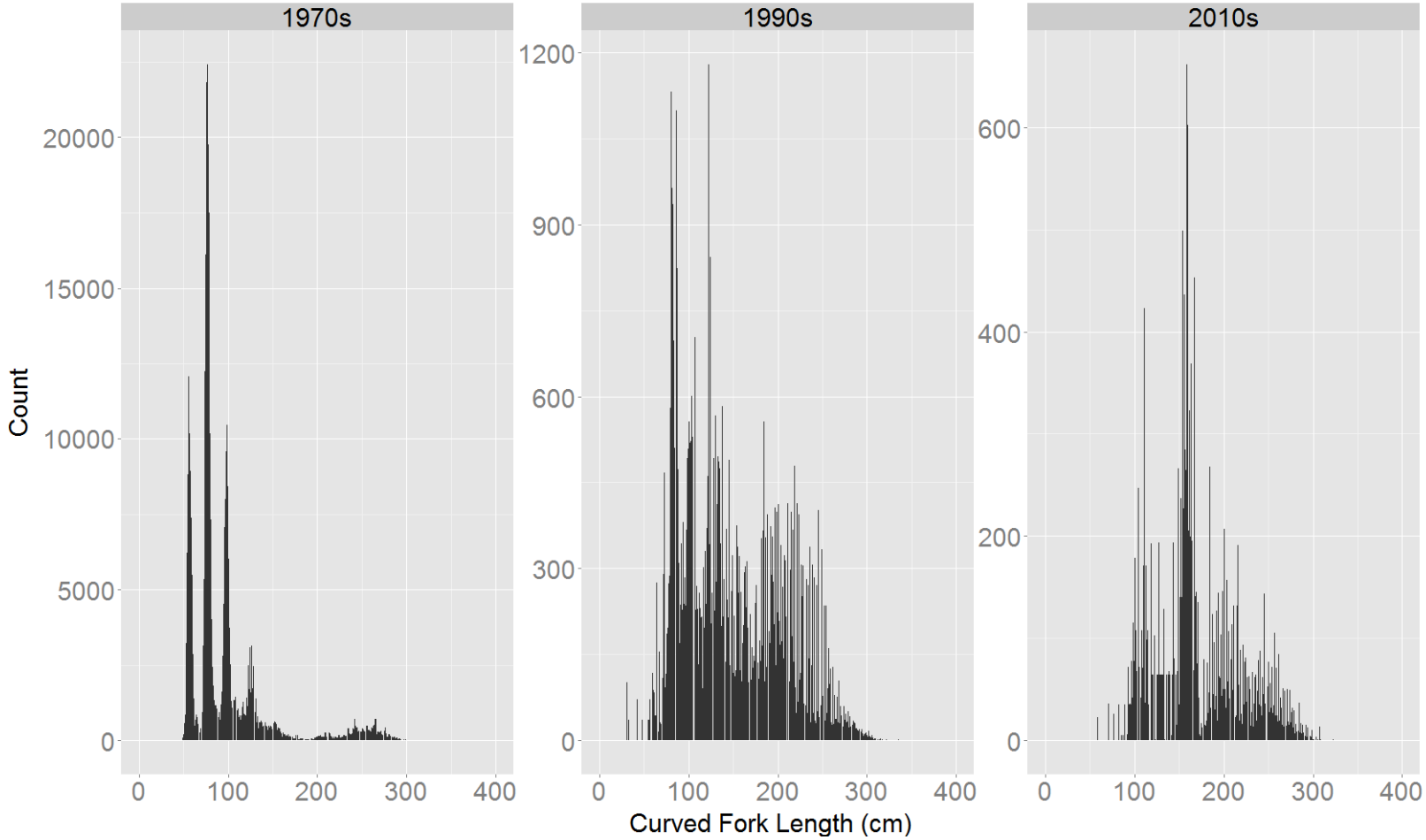

Figure 2.4. Size frequency data for Atlantic bluefin tuna individuals included in the 1970s (1974-1978), 1990s (1996-2002), and 2010s (2009-2014) samples obtained from NOAA.

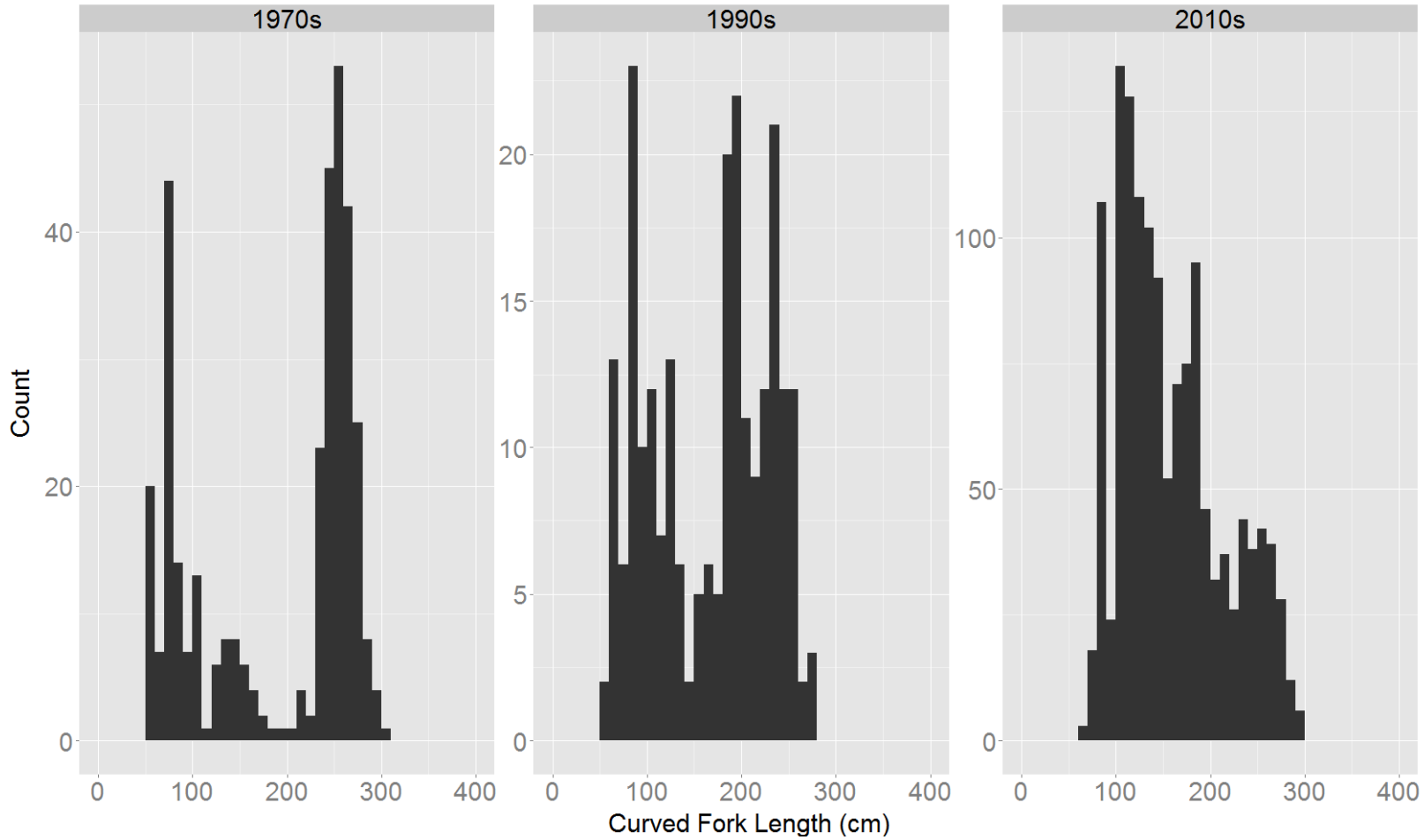

Figure 2.5. Atlantic bluefin tuna otolith $\delta^{13}C$ values (‰) plotted against estimated year class (estimated age subtracted from year of capture). Regression line and 1 standard error limits are shown.

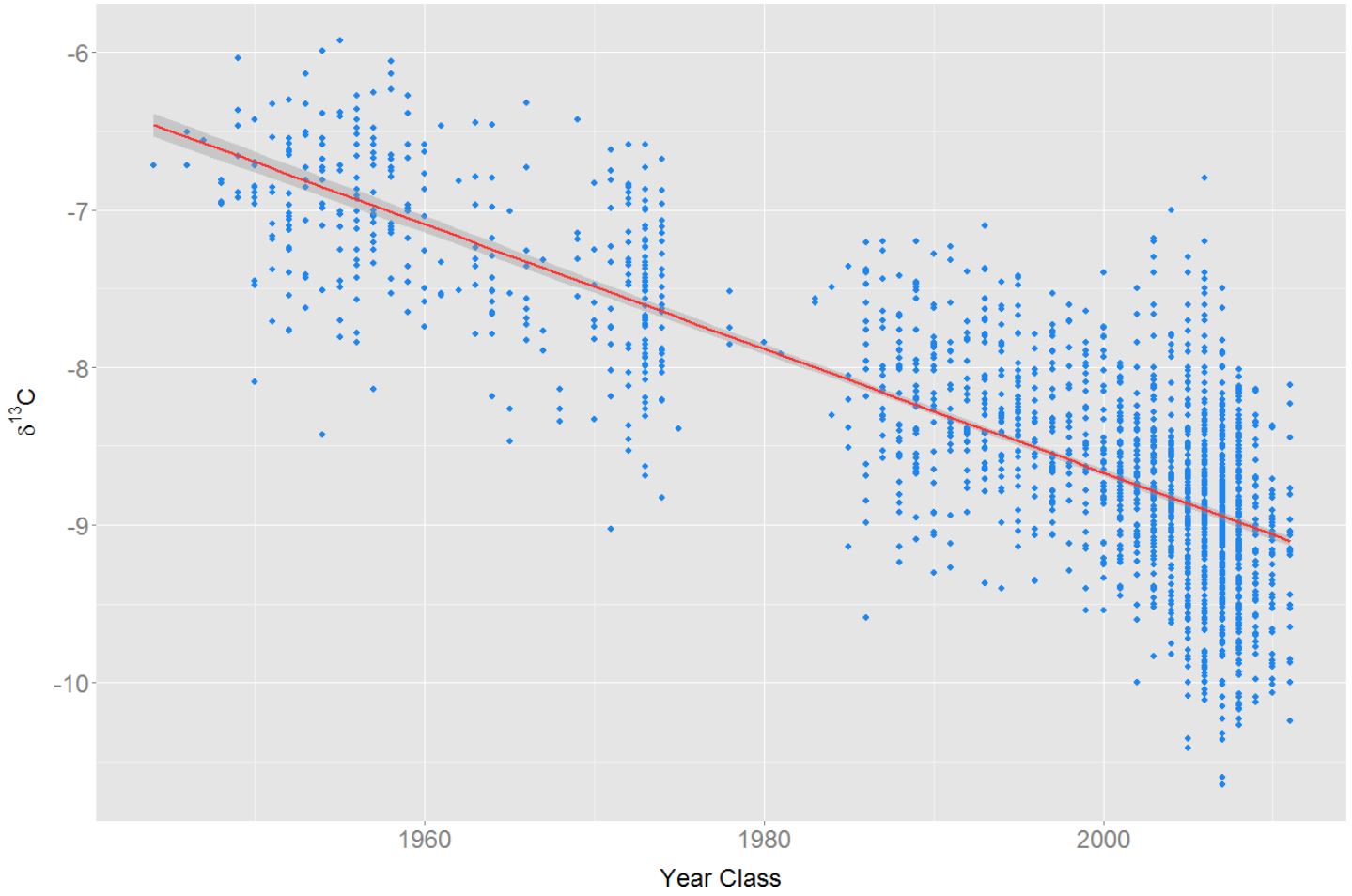

Figure 2.6. Corrected Atlantic bluefin tuna otolith δ^{13}Cvalues (‰) plotted against estimated year class (estimated age subtracted from year of capture). Regression line and 1 standard error limits are shown.

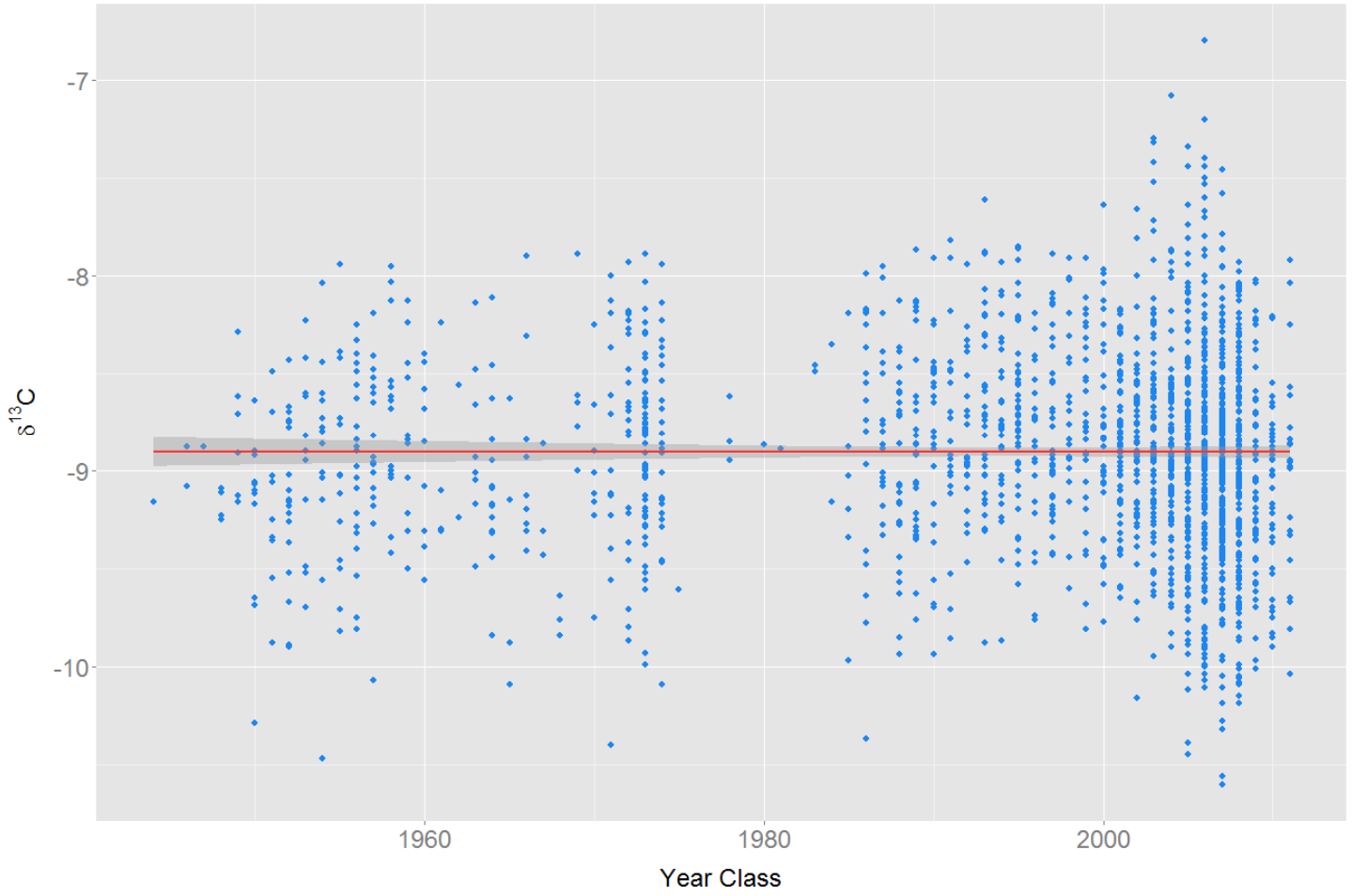

Figure 2.7. Atlantic bluefin tuna otolith $\delta^{18}O$ values (‰) plotted against estimated year class (estimated age subtracted from year of capture). Regression line and 1 standard error limits are shown.

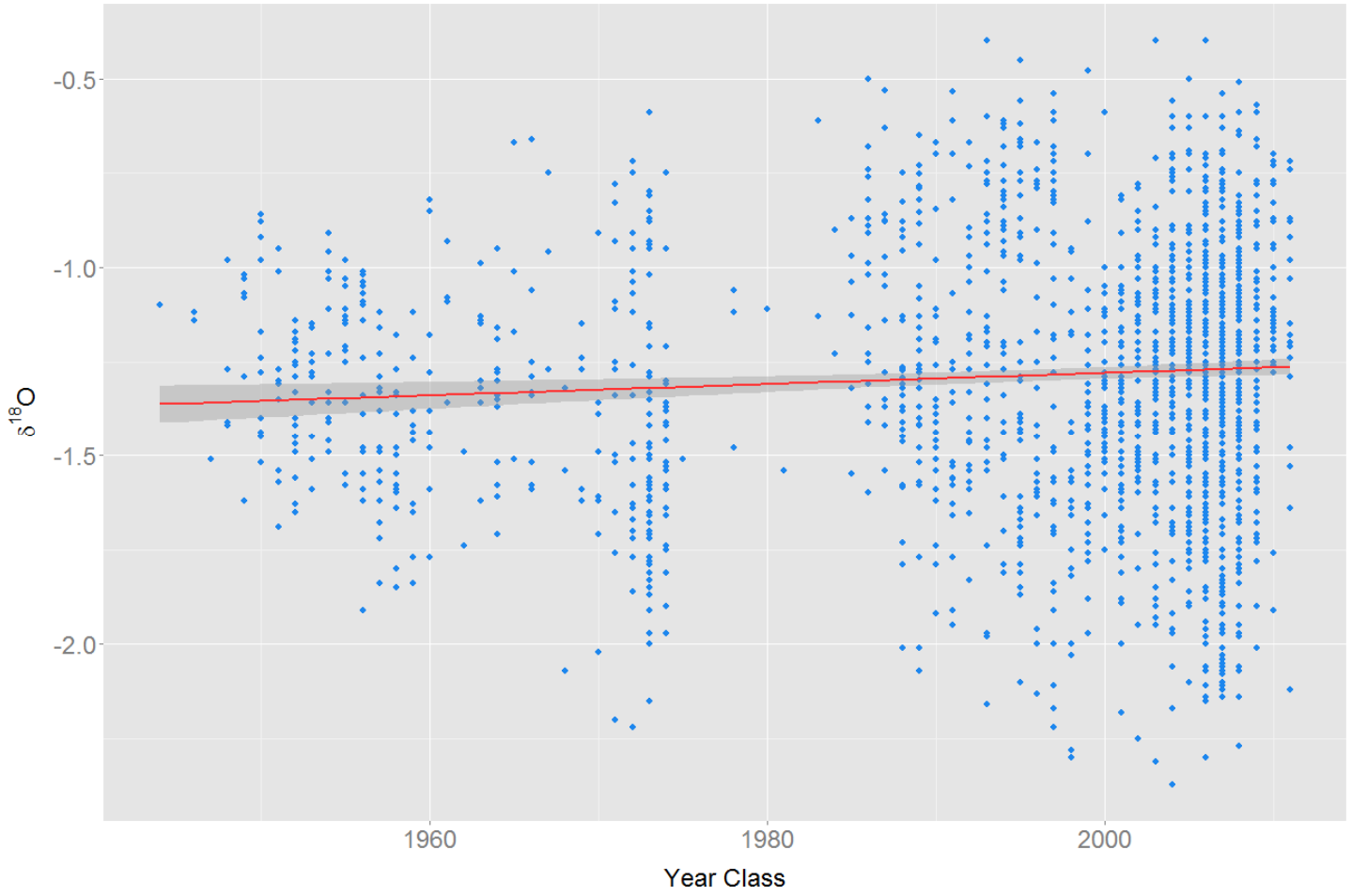

Figure 2.8. Global sea surface (30 psu; ≤ 15 m) $\delta^{18}O$ values (‰) from 1967-2008. Data obtained from National Aeronautics and Space Administration's (NASA) Global Seawater Oxygen-18 database (Schmidt et al. 1999; http://data.giss.nasa.gov/o18data/). Regression line and 1 standard error limits are shown.

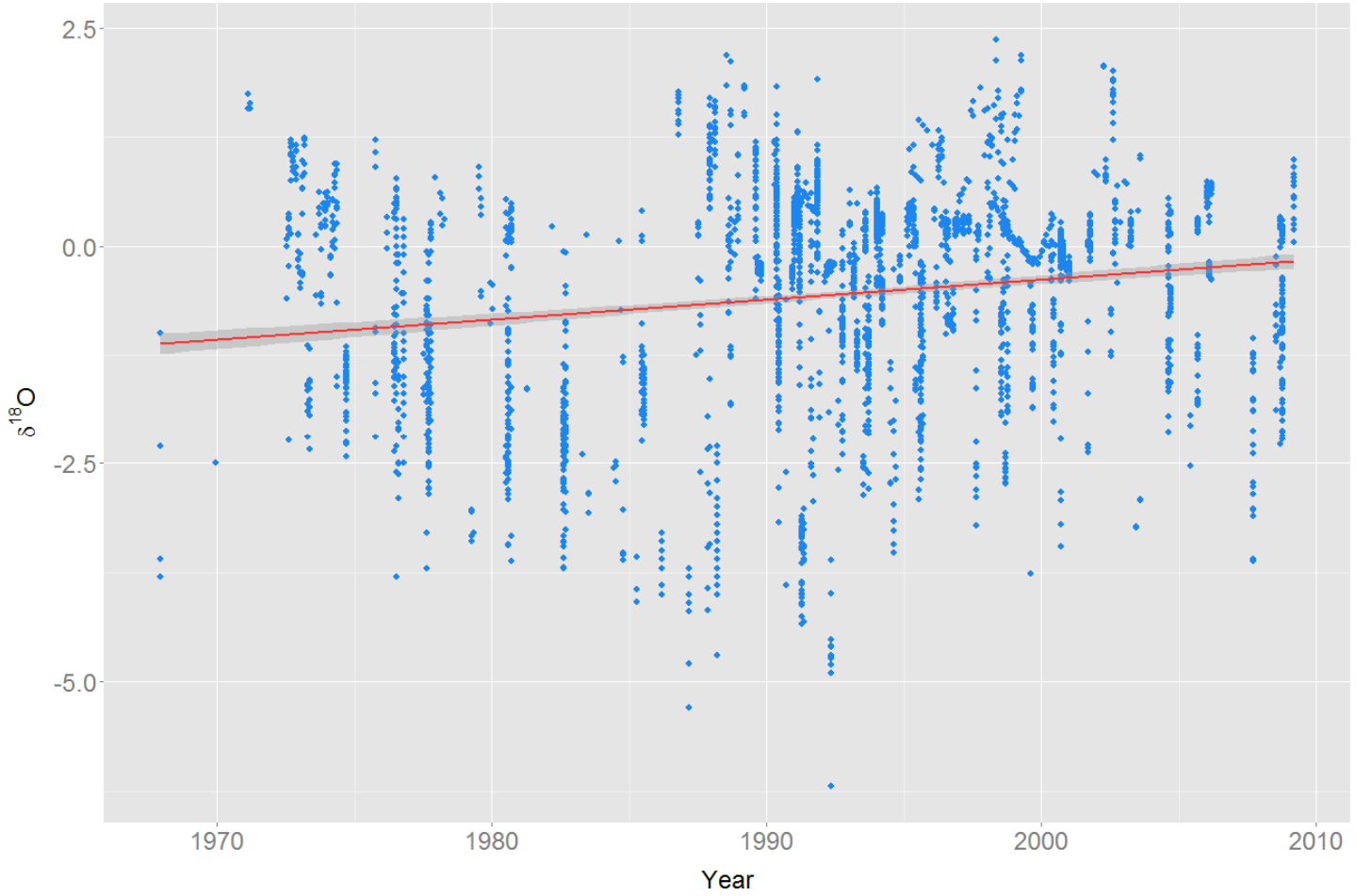

Figure 2.9. North Atlantic sea surface (30 psu; ≤ 15 m) $\delta^{18}O$ values (‰) from 1971-2004. Data obtained from National Aeronautics and Space Administration's (NASA) Global Seawater Oxygen-18 database (Schmidt et al. 1999; http://data.giss.nasa.gov/o18data/). Regression line and 1 standard error limits are shown.

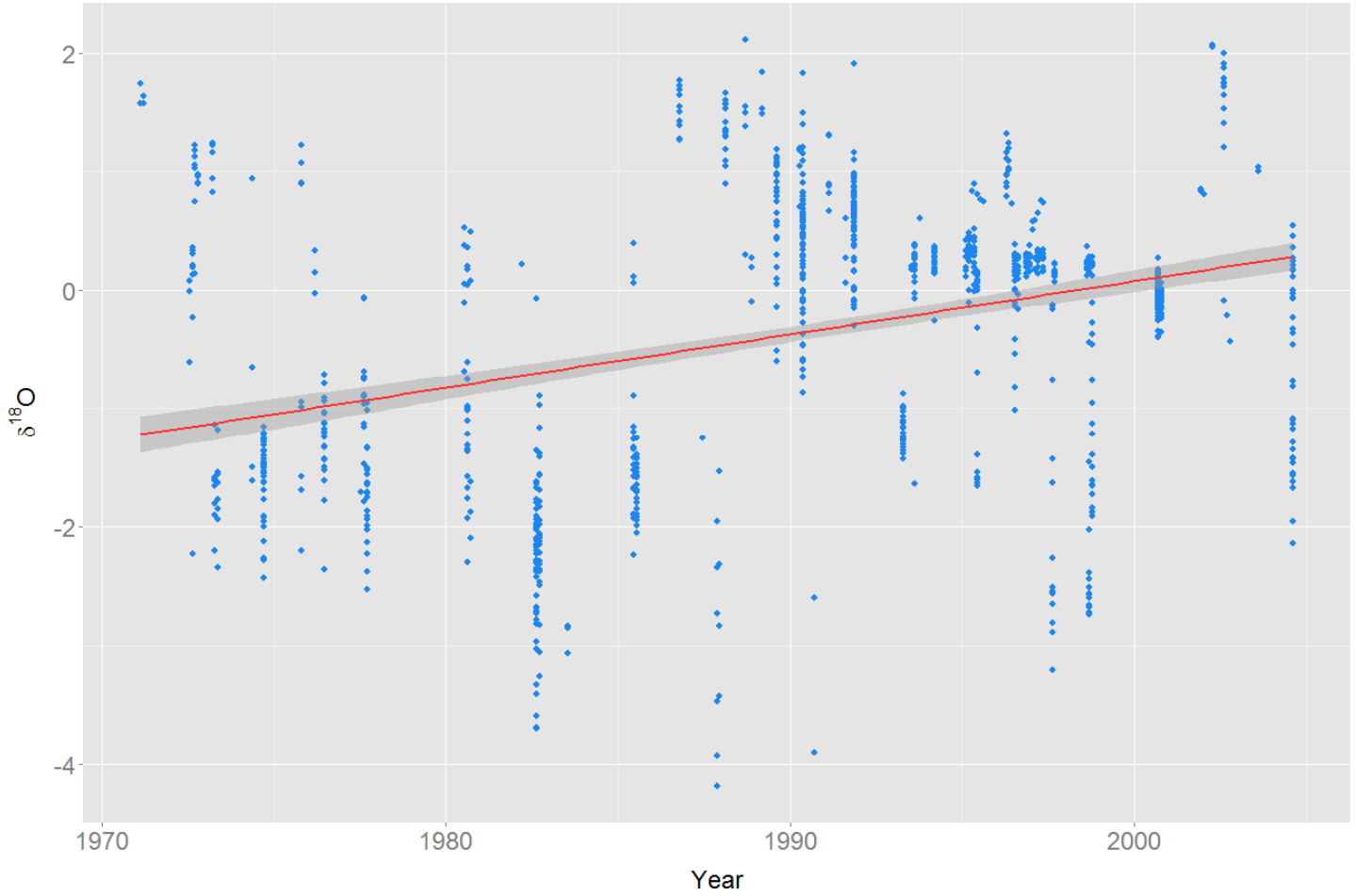

Figure 2.10. Western North Atlantic sea surface (30 psu; ≤ 15 m) $\delta^{18}O$ values (‰) from 1973-2003. Data obtained from National Aeronautics and Space Administration's (NASA) Global Seawater Oxygen-18 database (Schmidt et al. 1999; http://data.giss.nasa.gov/o18data/). Regression line and 1 standard error limits are shown.

Figure 2.11. Mediterranean Sea surface (30 psu; ≤ 15 m) $\delta^{18}O$ values (‰) from 1973-2003. Data obtained from National Aeronautics and Space Administration's (NASA) Global Seawater Oxygen-18 database (Schmidt et al. 1999; http://data.giss.nasa.gov/o18data/). Regression line and 1 standard error limits are shown.

Figure 2.12. Atlantic bluefin tuna otolith $\delta^{13}C$ and $\delta^{18}O$ (‰; relative to V-PDB) baseline dataset, composed of age-1 juveniles collected in respective nursery grounds in the US Mid-Atlantic Ocean (blue symbols) and Mediterranean Sea (red symbols) (1998-2011; N=264; data from Rooker et al. 2014). Dashed ellipses represent 90% confidence.

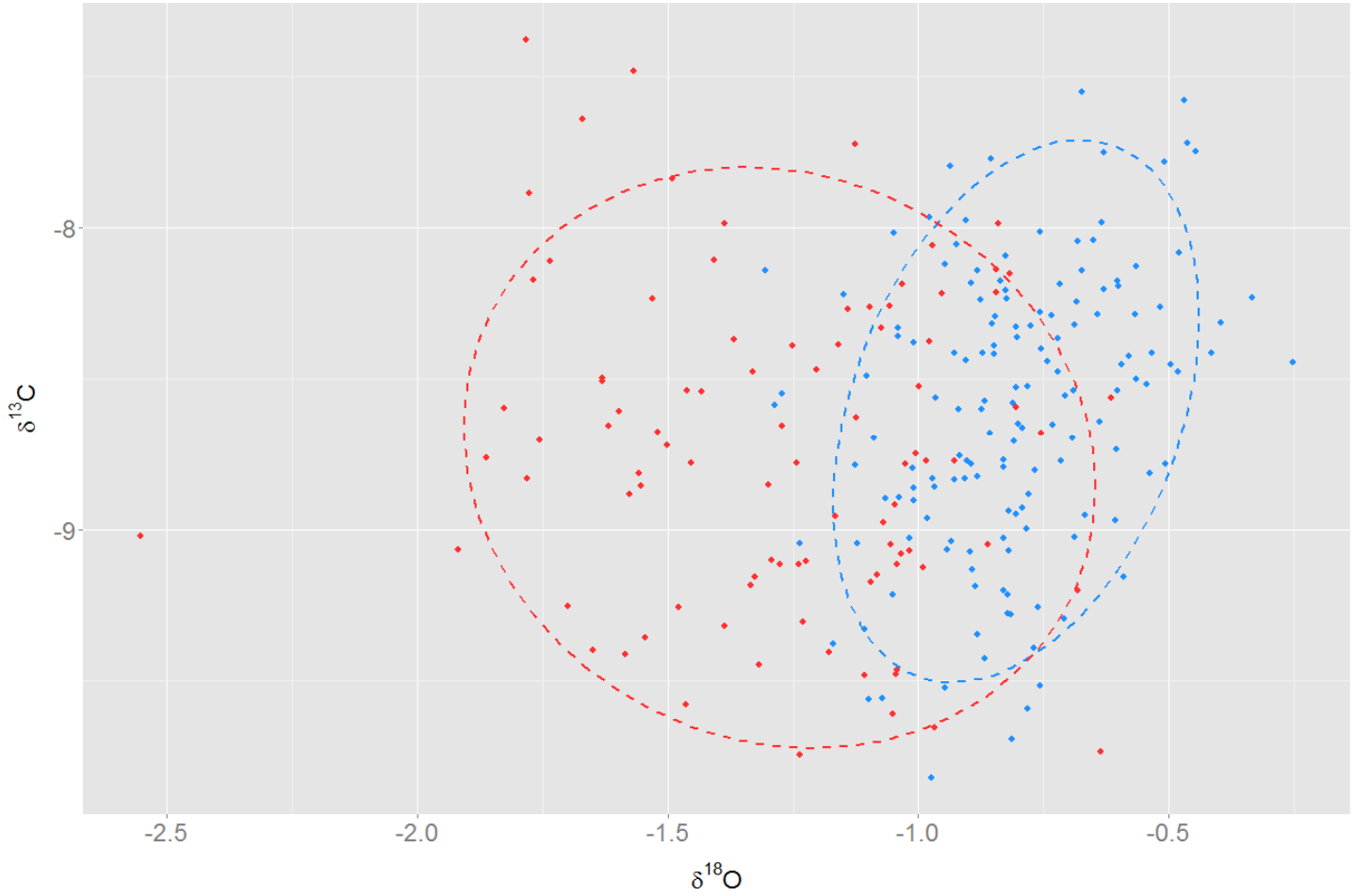

Figure 2.13. Annotated Atlantic bluefin tuna otolith image showing annuli (opaque bands; white dots), correct section type ("Y" section), measurement scale marker used for interpreting the first annulus.

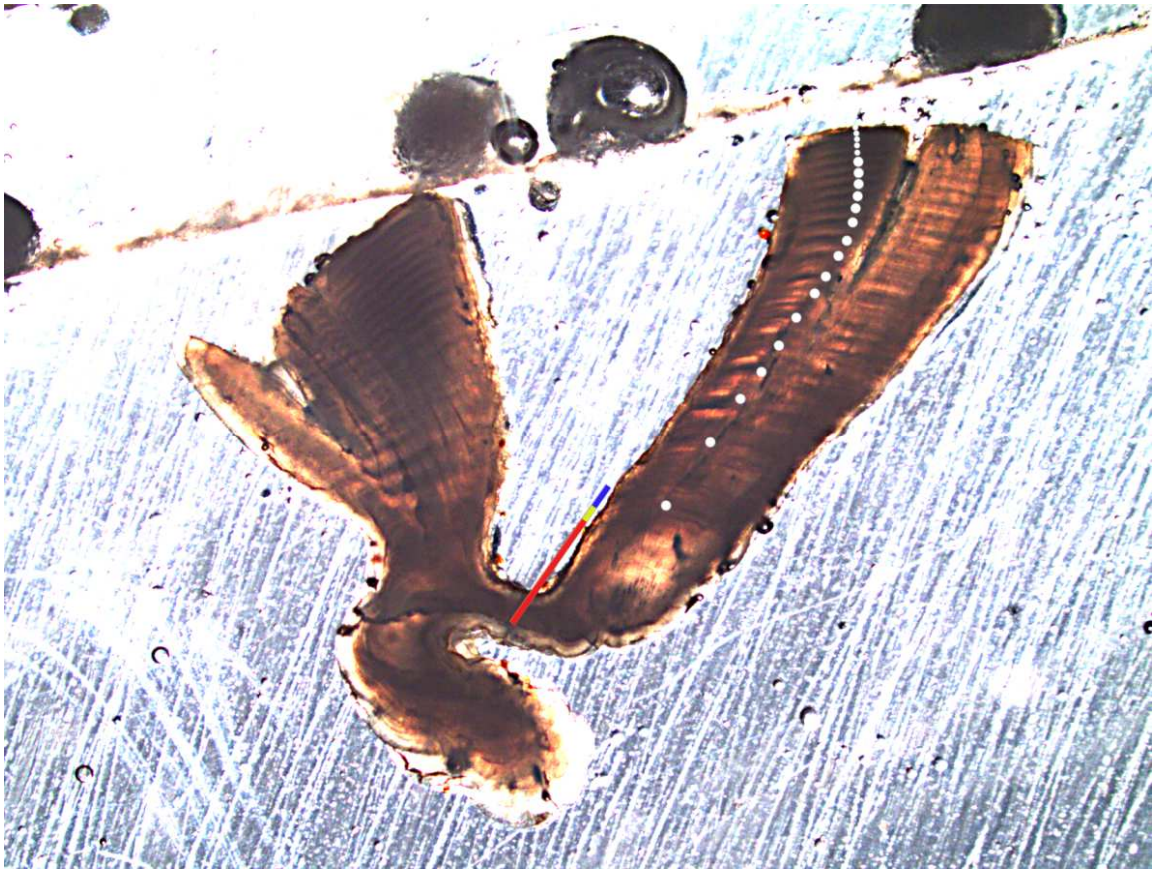

Figure 2.14. Annotated Atlantic bluefin tuna otolith images showing two section types (A: “V” section; B: “Y” section.

A)

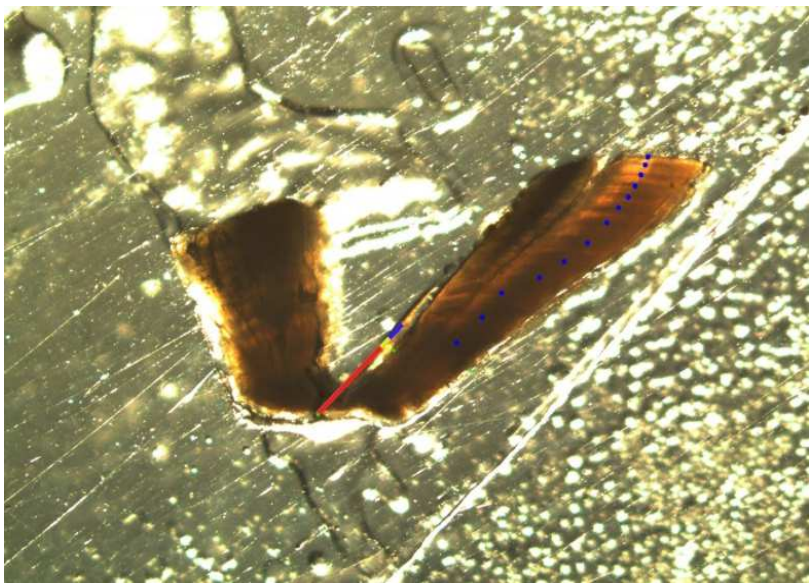

B)

Figure 2.15. Comparison of observed proportional length from ICCAT Atlantic bluefin tuna catch-at-size data (yellow bars) and proportional length from the ADMB model-derived proportional age matrix (blue bars).

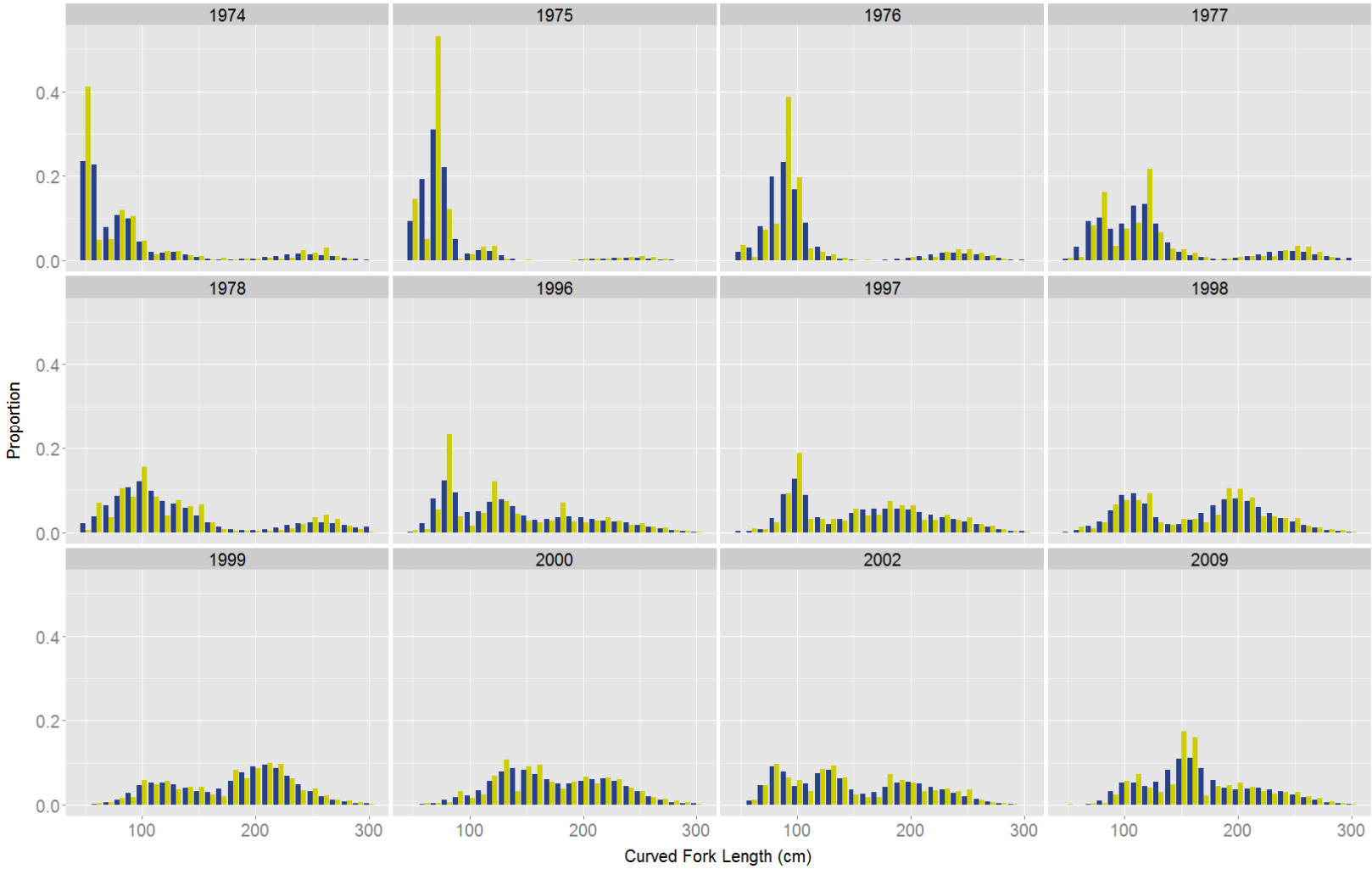

Figure 2.16. Cumulative frequencies of Atlantic bluefin tuna otolith $\delta^{18}O$ (‰) for known western (red) and eastern (blue) captured juveniles. A discriminatory threshold for the western stock was determined at the 90th percentile $\delta^{18}O$ value ($\delta^{18}O$ = -0.925) (dashed line).

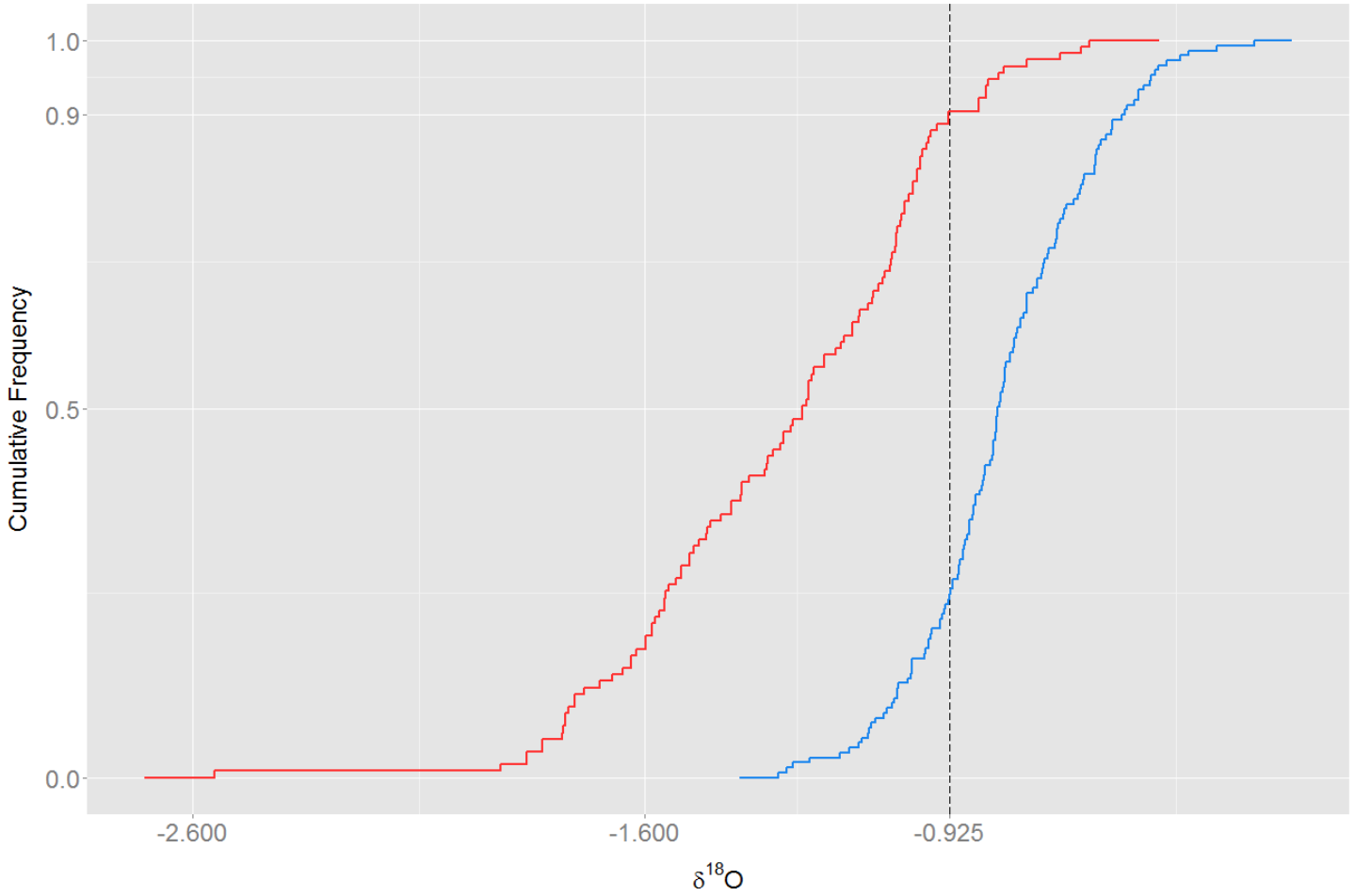

Figure 2.17. Relative size frequency distributions (cm, curved fork length) for Atlantic bluefin tuna individuals landed in the 1970s (blue; N=350), 1990s (yellow; N=234), and 2010s (green; N=1359). Bin width=10 cm.

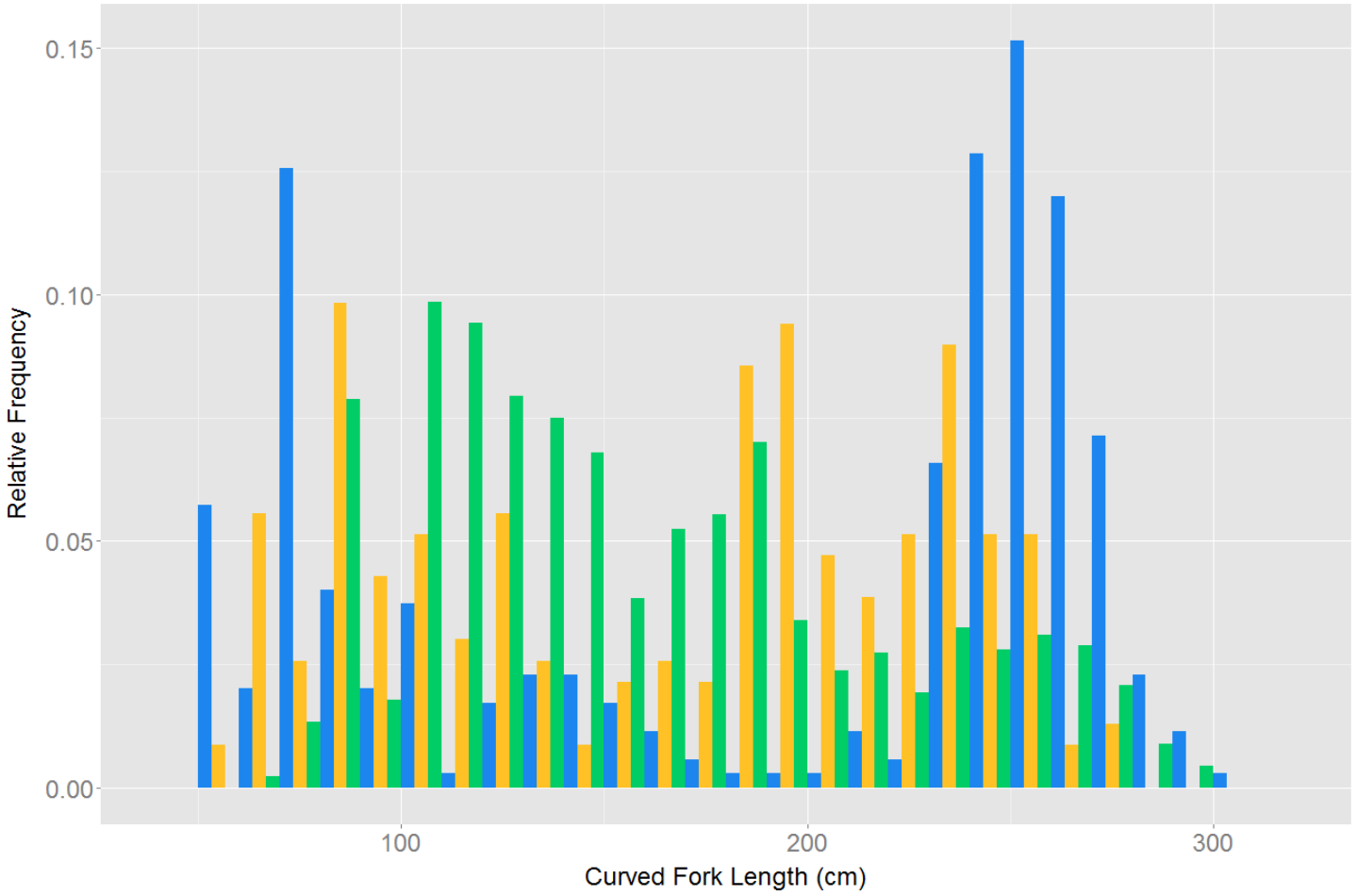

Figure 2.18. Relative age frequency distributions (years) for Atlantic bluefin tuna individuals landed in the 1970s (blue; N=350), 1990s (yellow; N=234), and 2010s (green; N=1359). Bin width=1 year.

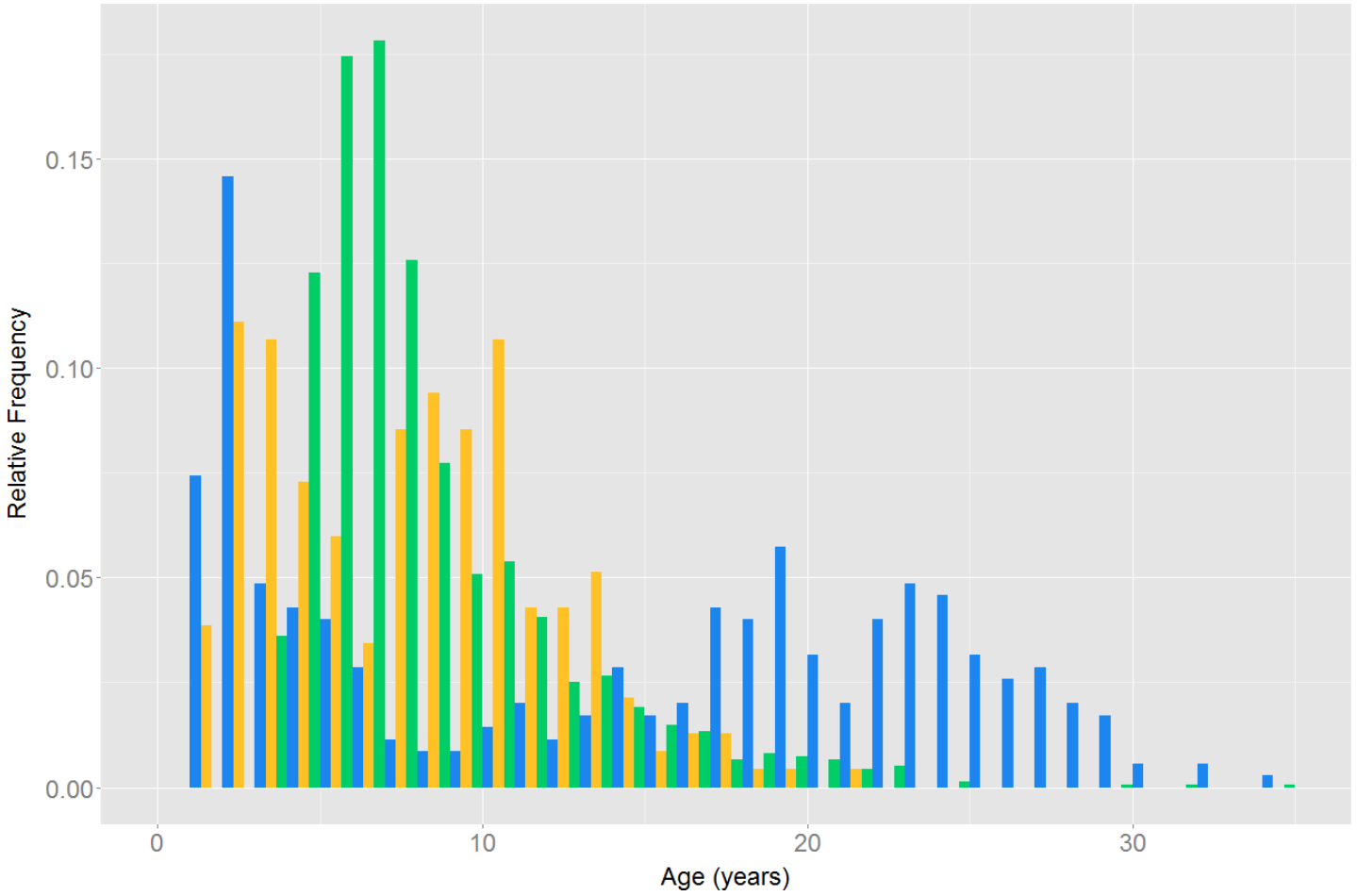

Figure 2.19. Relative age frequency distributions (years) for adult (age 8+) Atlantic bluefin tuna individuals landed in the 1970s (blue; N=350), 1990s (yellow; N=234), and 2010s (green; N=1359). Bin width=1 year.

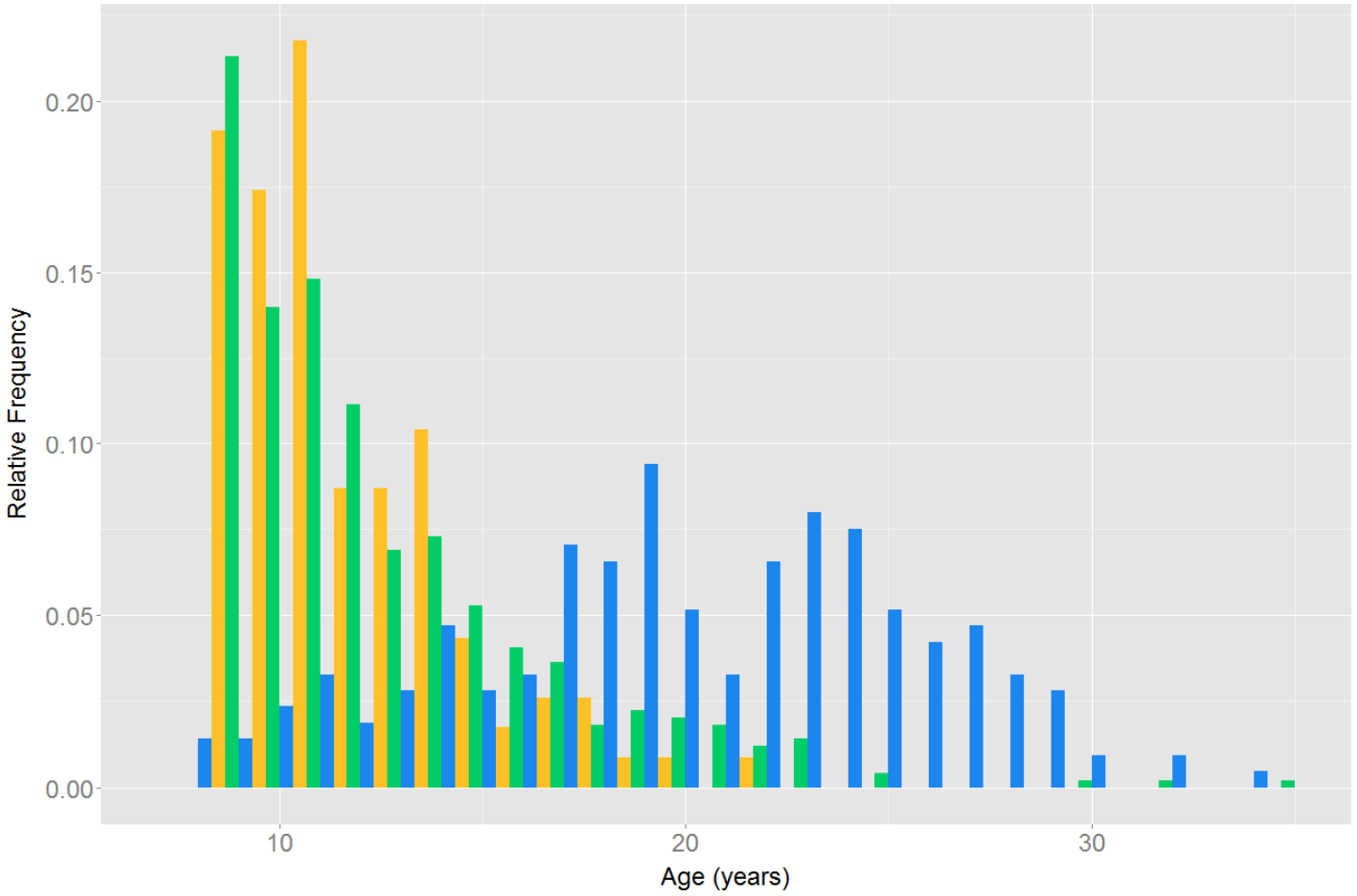

Figure 2.20. Cumulative frequencies of size for Atlantic bluefin tuna individuals landed in the 1970s (blue; N=350), 1990s (yellow; N=234), and 2010s (green; N=1359).

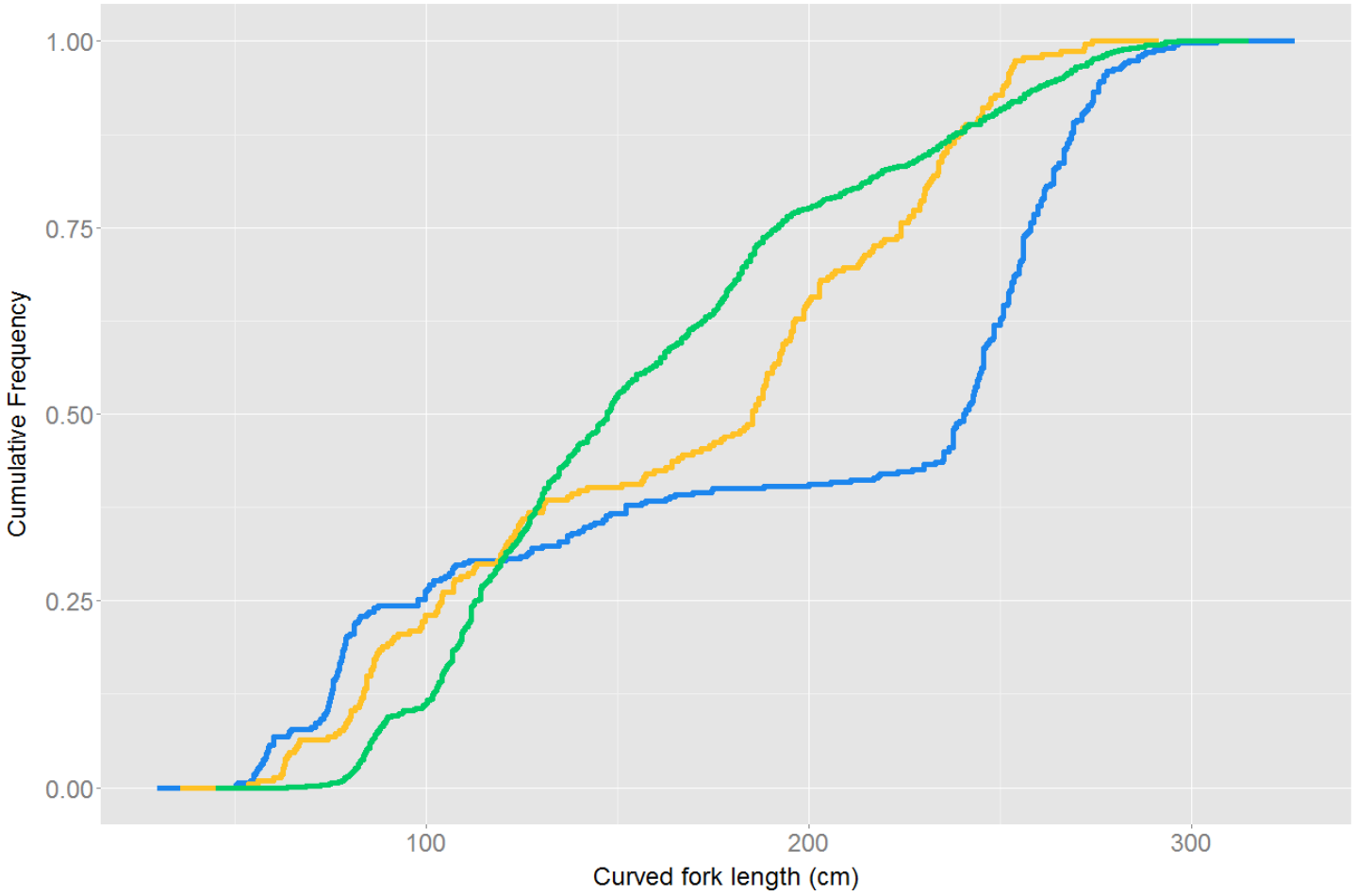

Figure 2.21. Cumulative frequencies of age for Atlantic bluefin tuna individuals landed in the 1970s (blue; N=350), 1990s (yellow; N=234), and 2010s (green; N=1359).

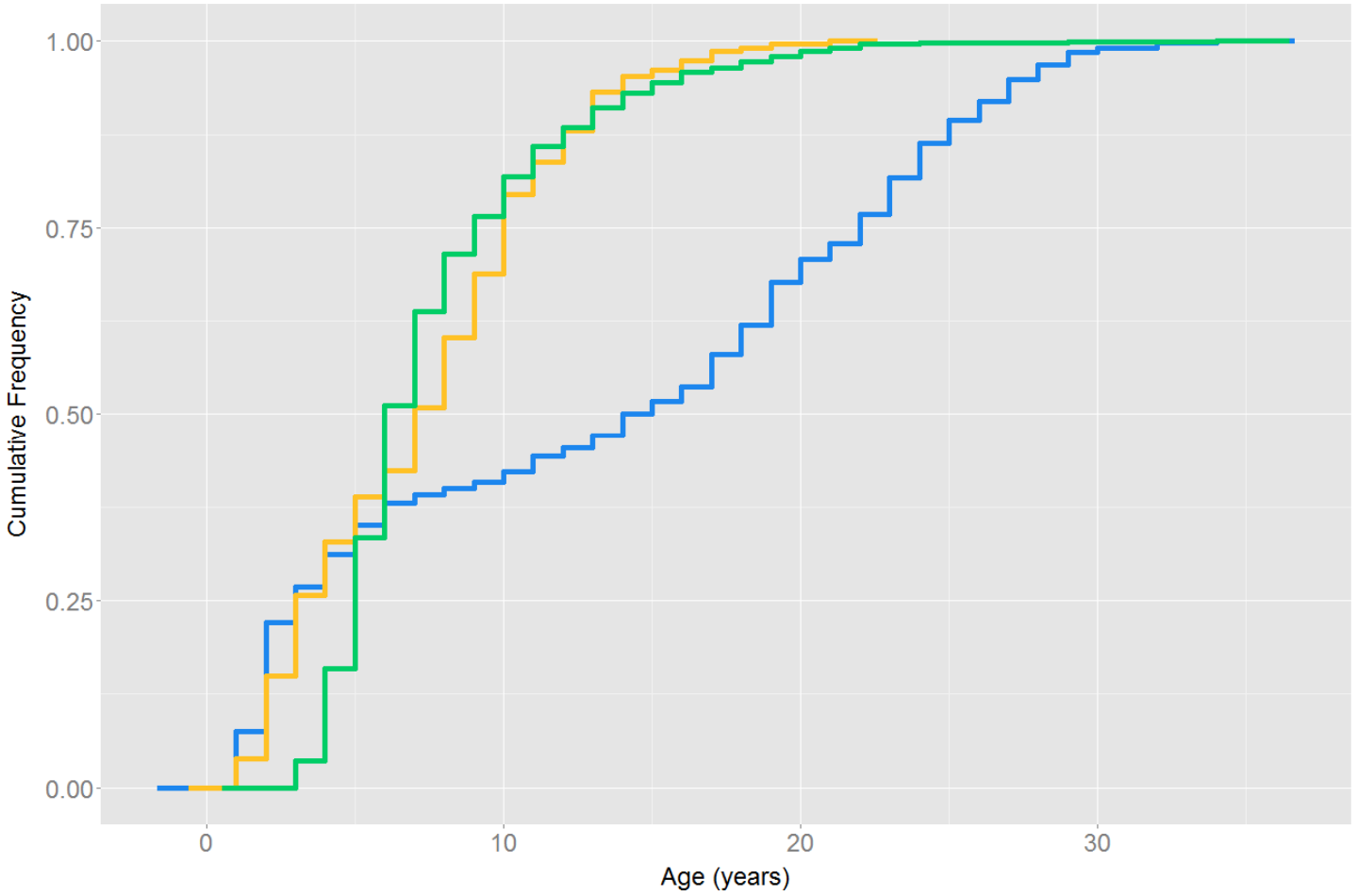

Figure 2.22. Age frequency distributions (years) for western stock-categorized Atlantic bluefin tuna individuals landed in the 1970s (blue; N=350), 1990s (yellow; N=234), and 2010s (green; N=1359). Bin width=1 year.

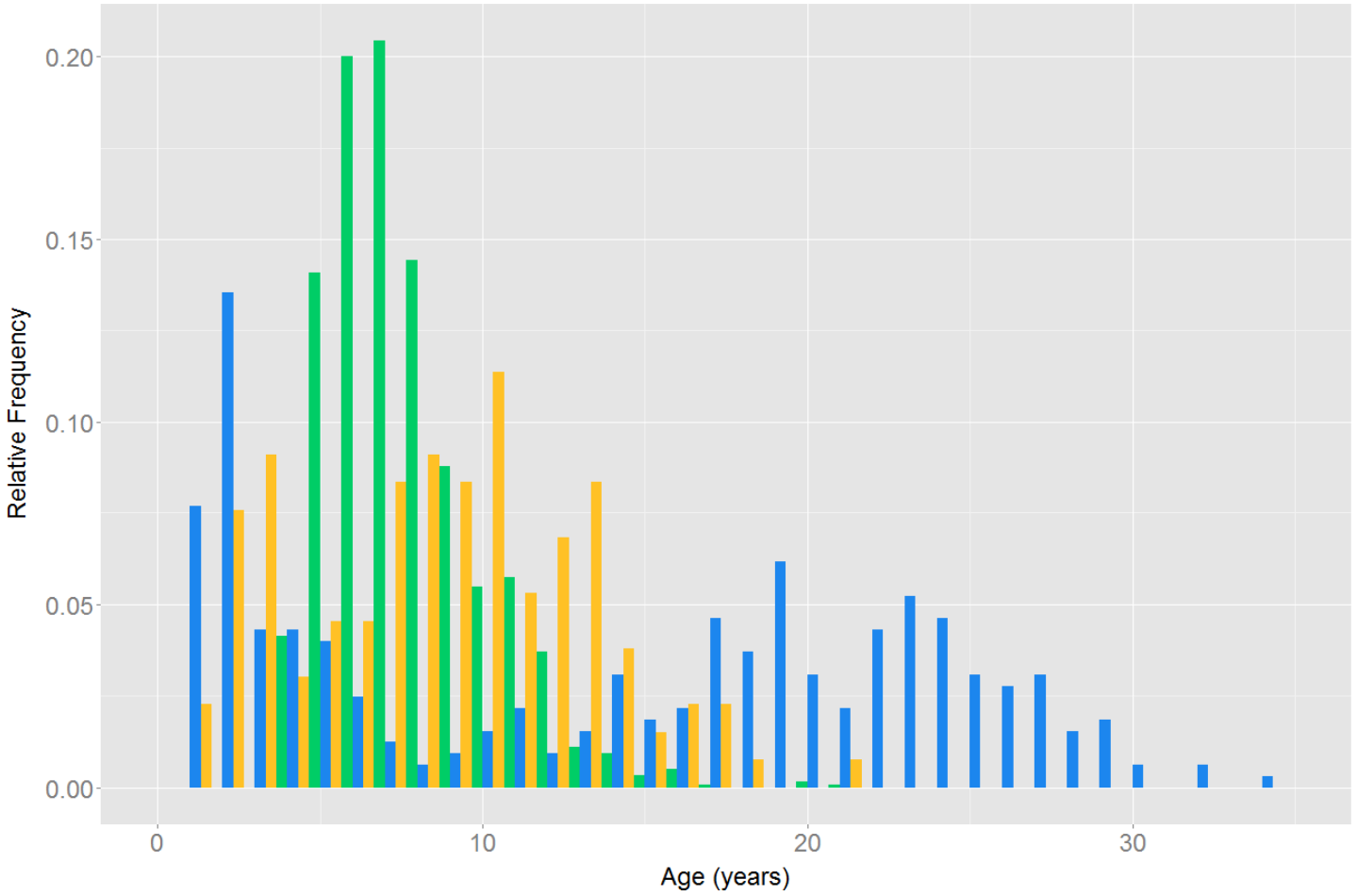

Figure 2.23. Year class frequency distributions for juvenile (<8 years) Atlantic bluefin tuna landed in the 1970s (blue), 1990s (yellow), and 2010s (green). Bin width=1 year.

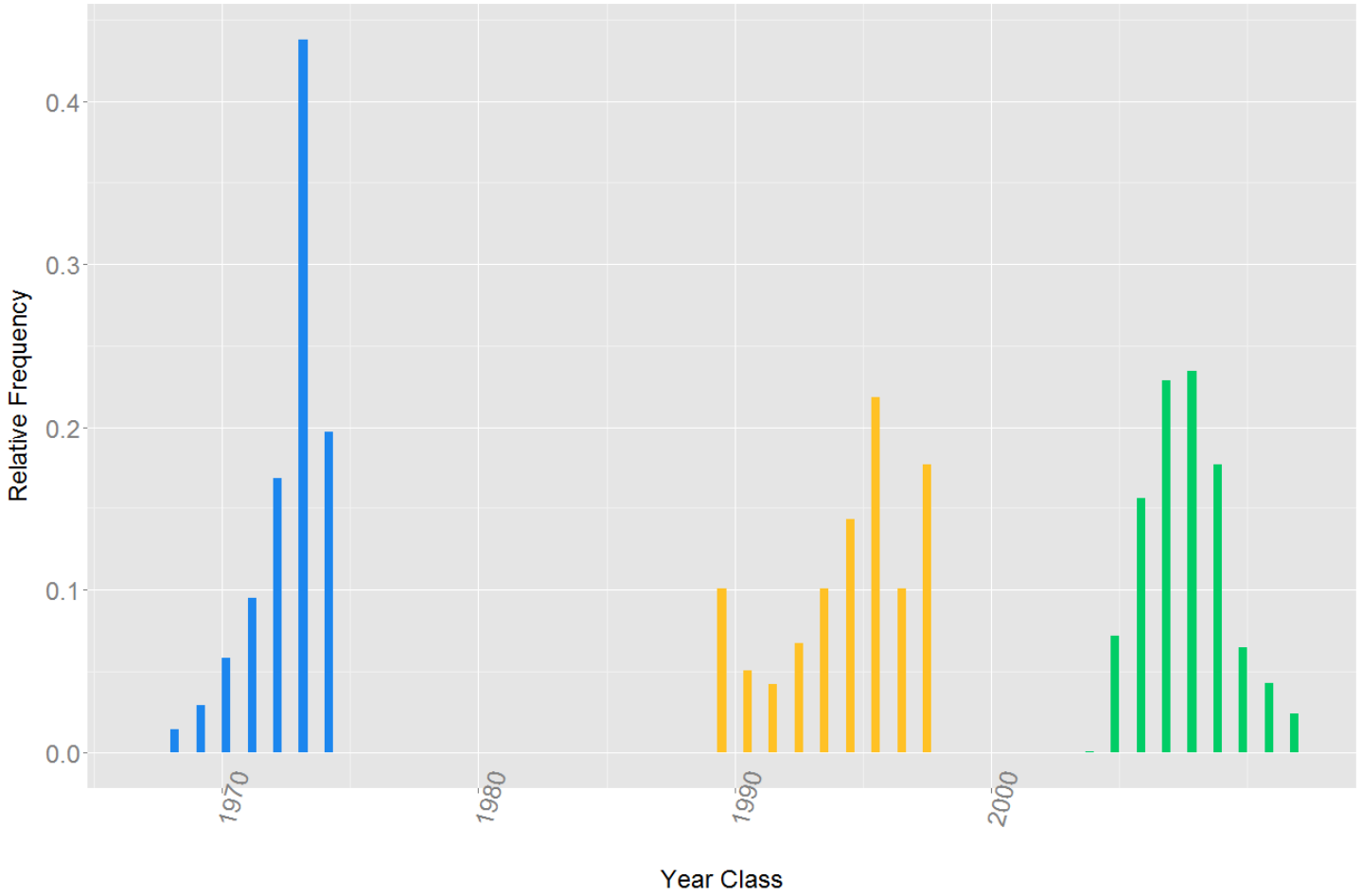

Figure 2.24. Year class frequency distributions for adult (> 7 years) Atlantic bluefin tuna landed in the 1970s (blue), 1990s (yellow), and 2010s (green). Bin width=1 year.

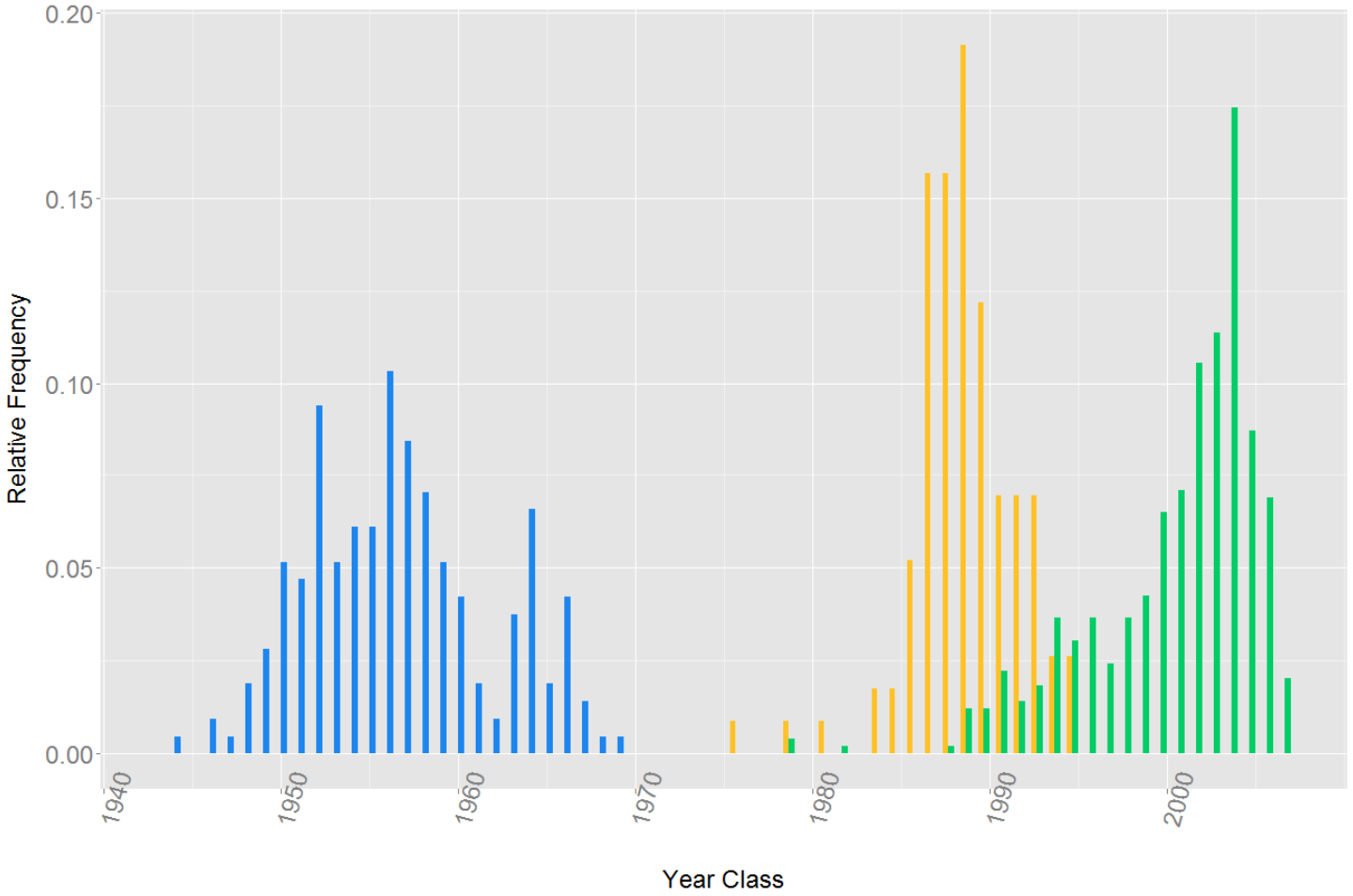

Figure 2.25. Age-specific selectivities for Atlantic bluefin tuna from 1970-2013, calculated from age-specific fishing morality rates estimated in the 2014 Atlantic bluefin tuna stock assessment's virtual population analysis performed by ICCAT (SCRS 2014). White boxes correspond to selectivity of 0, while dark blue boxes correspond to full selectivity (selectivity=1).

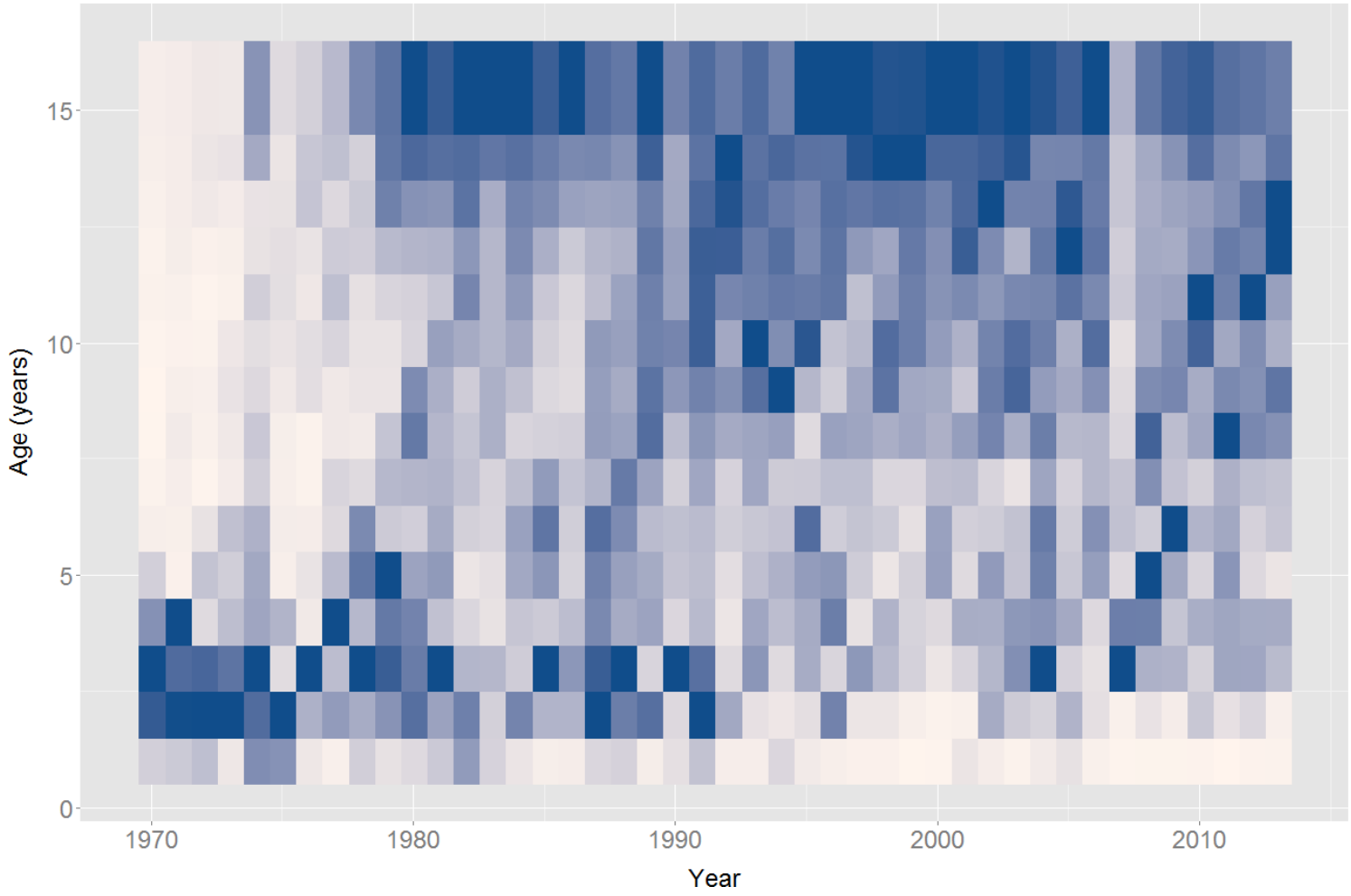

Figure 2.26. Age frequency of Atlantic bluefin tuna landed in the 1970s (blue), 1990s (yellow), and 2010s (green) adjusted with age-specific selectivities occurring during the time period of collection.

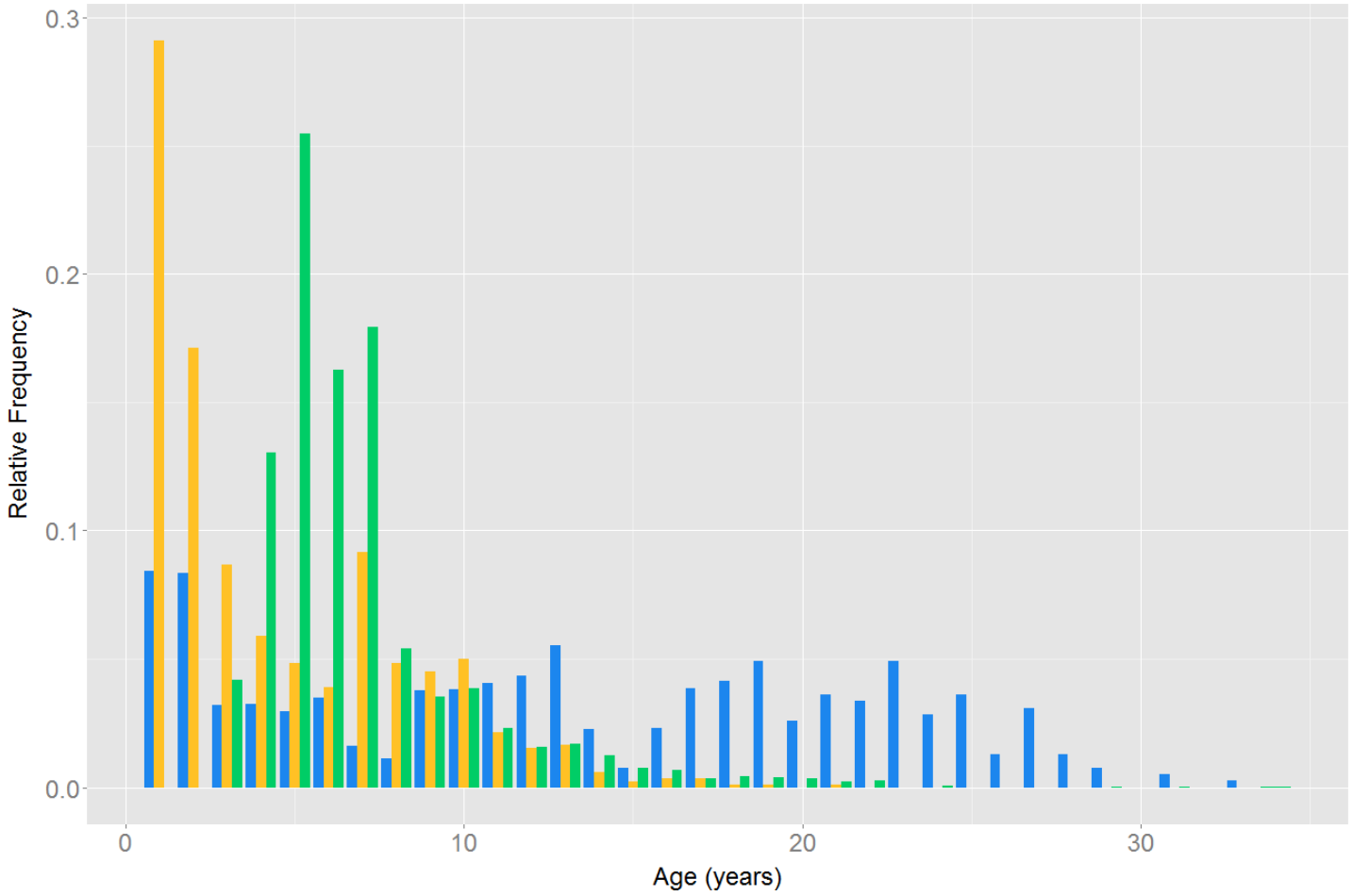

Figure 2.27. Total instantaneous mortality of Atlantic bluefin tuna in the 1970s (1974-1978), 1990s (1996-2000, 2002), and 2010s (2009) by decade. Mortality estimates were calculated using decadal selectivity-adjusted numbers-at-age.

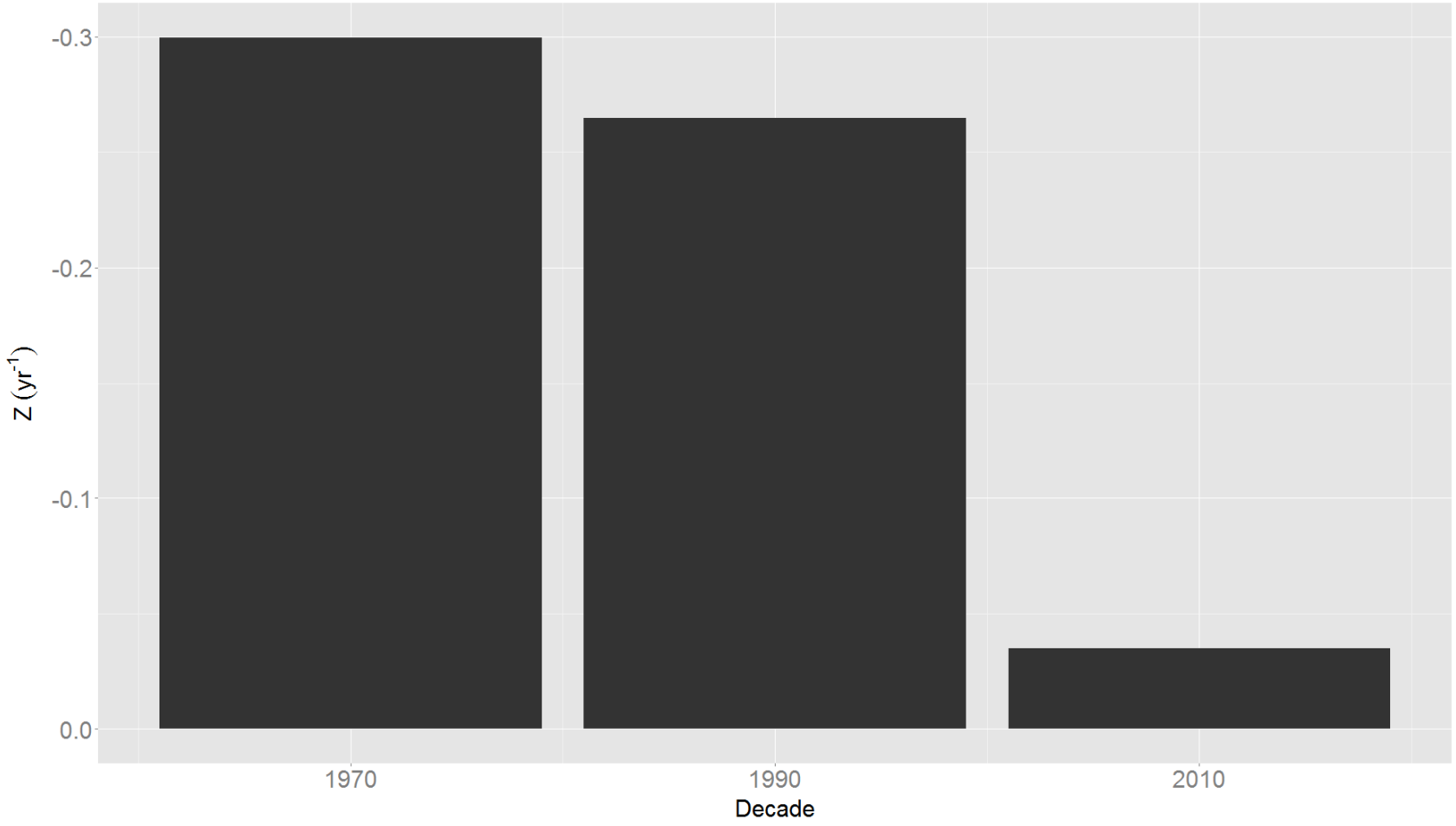

Figure 2.28. Length-at-age for Atlantic bluefin tuna individuals landed in the 1970s (blue; N=350), 1990s (yellow; N=234), and 2010s (green; N=1359). Lines connect mean length-at-age; clouds are 1 standard deviation (SD).

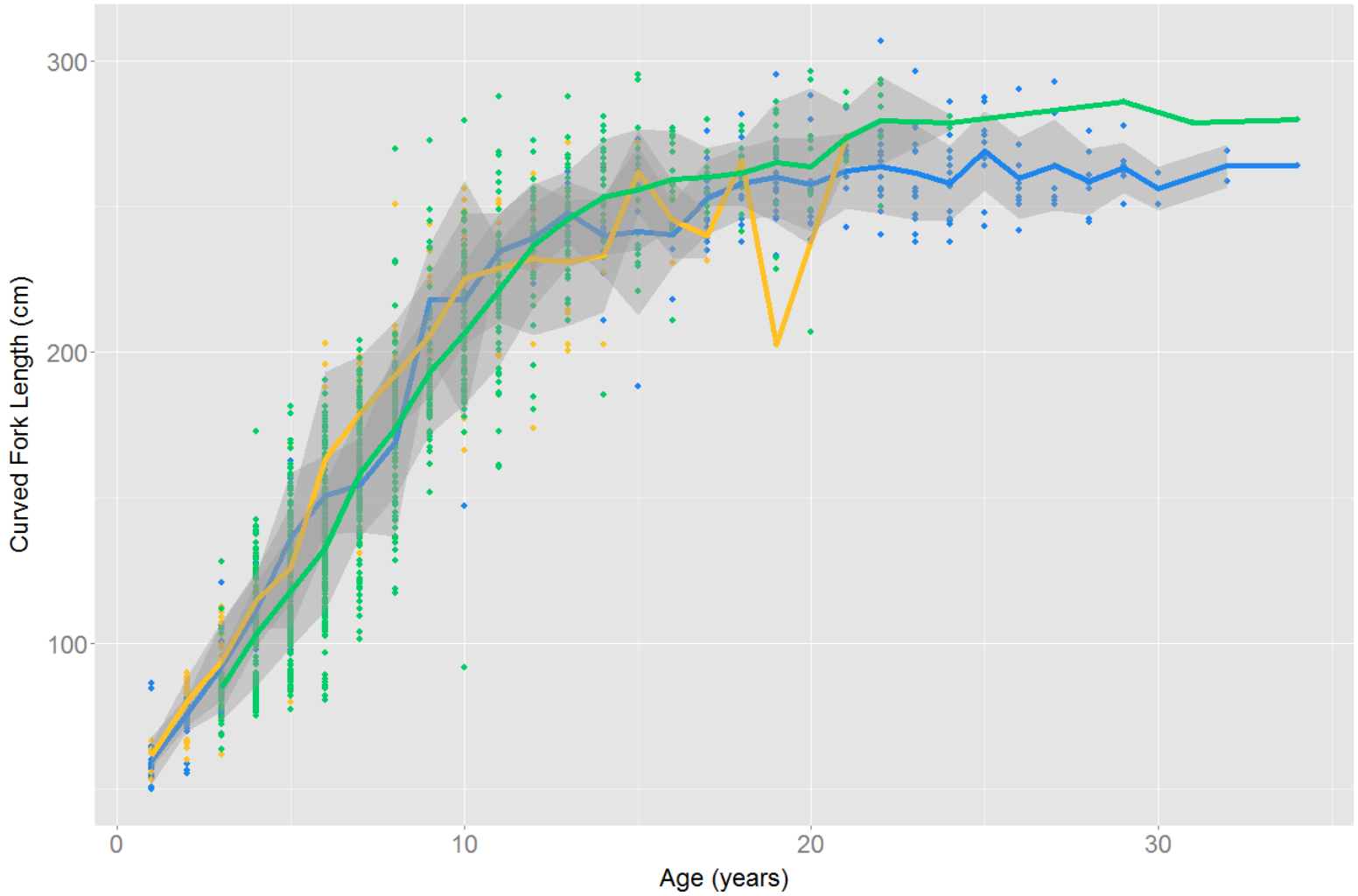

Figure 2.29. von Bertalanffy growth curves (predicted size-at-age) for Atlantic bluefin tuna individuals landed in the 1970s (blue; N=350), 1990s (yellow; N=234), and 2010s (green; N=1359).

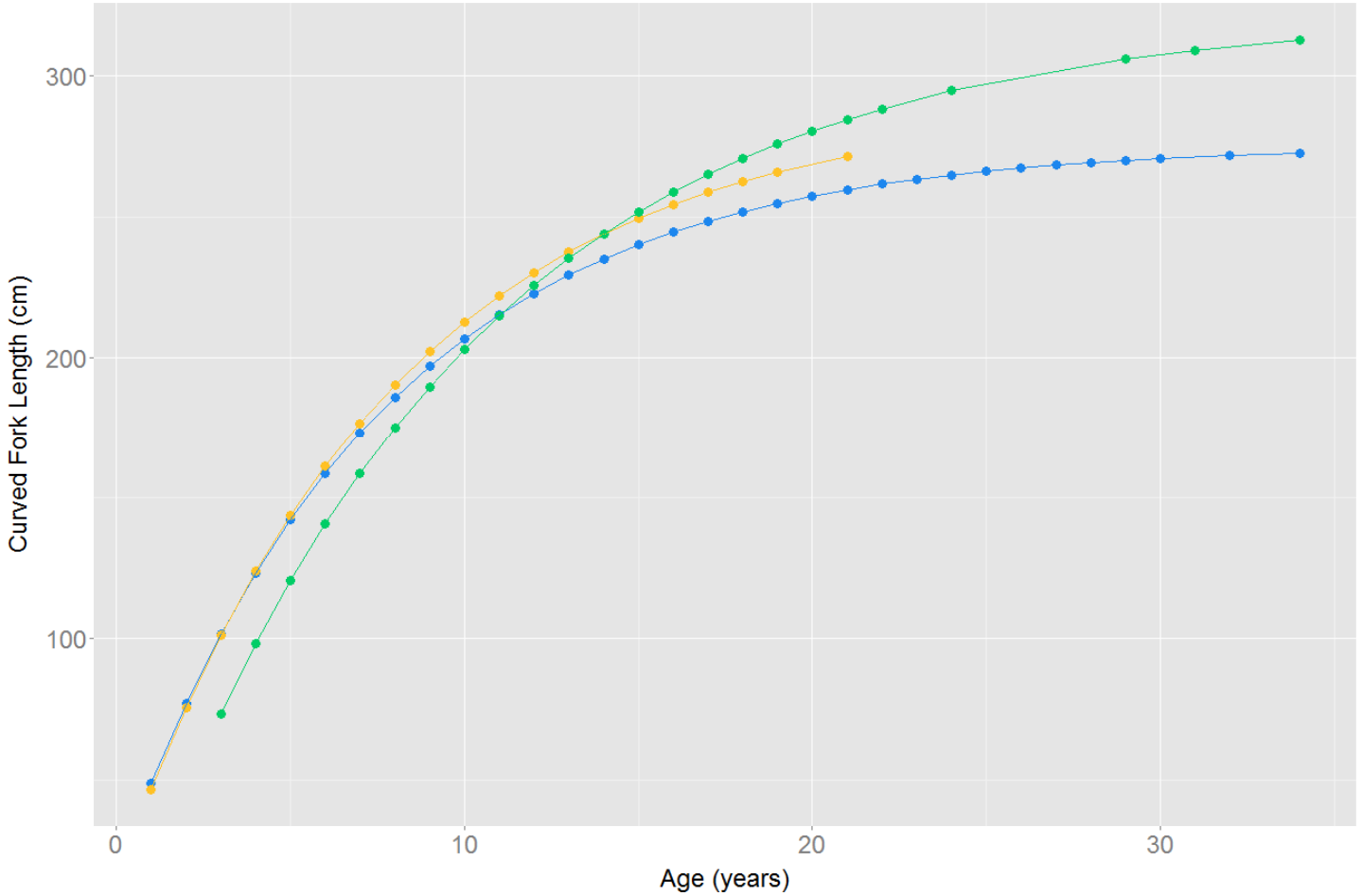

Figure 2.30. von Bertalanffy growth curves (predicted size-at-age) for Atlantic bluefin tuna individuals categorized as 1970s (blue), 1990s (yellow), and 2010s (green) western stock fish in comparison to the accepted growth curve for the western stock (red; Restrepo et al. 2010).

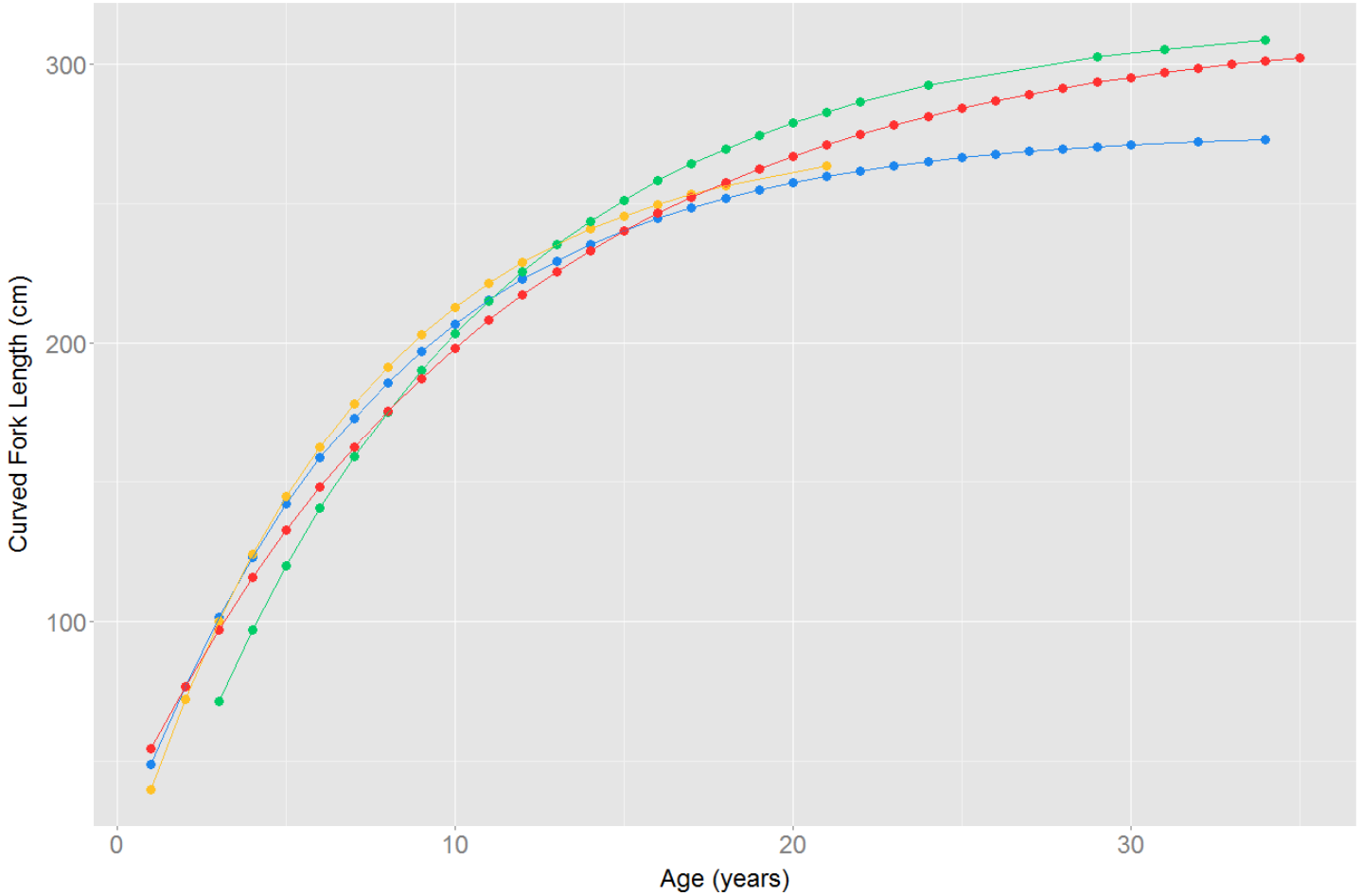

Figure 2.31. Abundance of western stock Atlantic bluefin tuna from 1970-2013 by age class, estimated by virtual population analysis (VPA) from the ICCAT stock assessment (SCRS 2014).

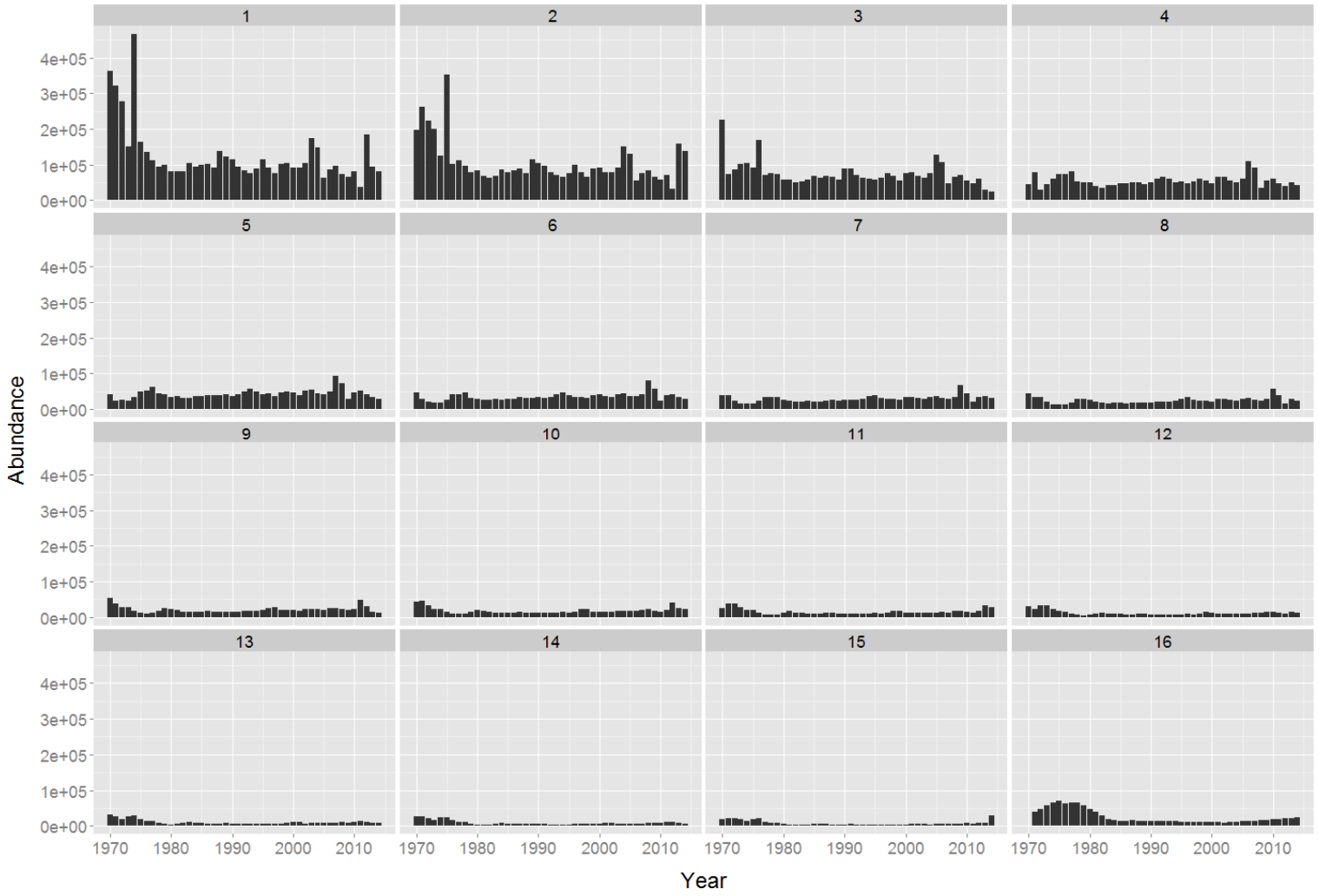

Appendix

Tables

Table A.1. Comparison of population mixing levels in Atlantic bluefin tuna samples from Gulf of Mexico, New England, and Mid-Atlantic fisheries in the 1970s, 1990s, and 2010s, estimated using the otolith $\delta^{13}C$ correction adjustment reported by Schloesser et al. (2009) to correct for the Suess Effect.

				Siskey		*Schloesser*	
Years sampled	*Location*	*n*	*Population*	*MLE%*	*MLE SD*	*MLE%*	*MLE SD*
1974-1978	New England, Mid-Atlantic, Gulf of Mexico	349	west	100	0.0	100	0.1
			east	0		0	
1996-2002	New England, Mid-Atlantic	229	west	52	4.7	50	4.7
			east	48		50	
2009-2014	New England, Mid-Atlantic, Gulf of Mexico	1375	west	96	1.2	96	1.2
			east	4		4	

Table A.2. Population mixing levels in Atlantic bluefin tuna samples from Gulf of Mexico, New England, and Mid-Atlantic fisheries in the 1970s, 1990s, and 2010s, with global, North Atlantic, Northwestern Atlantic, and Northeastern Atlantic seawater corrected $\delta^{18}O$ values.

				Uncorrected		*Global*		*North Atlantic*		*Northwest Atlantic*		*Northeast Atlantic*	
Years sampled	*Location*	*n*	*Population*	*MLE%*	*MLE SD*	*MLE%*	*MLE SD*	*MLE%*	*MLE SD*	*MLE%*	*MLE SD*	*MLE%*	*MLE SD*
1974-1978	New England, Mid-Atlantic, Gulf of Mexico	349	west	100	0.0	100	0.0	100	0.0	100	0.0	100	0.0
			east	0		0		0		0		0	
1996-2002	New England, Mid-Atlantic	229	west	52	4.7	52	4.7	52	4.7	52	4.7	52	4.7
			east	48		48		48		48		48	
2009-2014	New England, Mid-Atlantic, Gulf of Mexico	1375	west	96	1.2	96	1.2	96	1.2	96	1.2	96	1.2
			east	4		4		4		4		4	

Table A.3. Negative log likelihood contrasts for Atlantic bluefin tuna growth models, which include or exclude decadal effects. Full Model refers to models that incorporate separate decadal parameters; Reduced Model refers to models that use one set of parameters for both decades. Second-order Akaike Information Criteria (AIC_C) and AIC_C differences are reported for growth curves corresponding to the 1970s (N=350), 1990s (N=234), and 2010s (N=1359), including only age 1-16 individuals. Δ_I denotes the AIC_C difference between the full and reduced model.

	1970s v. 1990s	***1970s v. 2010s***	***1990s v. 2010s***
Full Model	2822.1	10506.2	10843.8
Reduced Model	2831.7	10577.7	10952.8
Δ_i	9.6	71.5	108.9

Table A.4. Negative log likelihood contrasts for assigned western stock Atlantic bluefin tuna growth models, which include or exclude decadal effects. Full Model refers to models that incorporate separate decadal parameters; Reduced Model refers to models that use one set of parameters for both decades. Second-order Akaike Information Criteria (AIC_C) and AIC_C differences are reported for growth curves corresponding to the 1970s (N=325), 1990s (N=132), and 2010s (N=1185), including only age 1-16 individuals. Δ_I denotes the AIC_C difference between the full and reduced model.

	1970s W v. 1990s W	***1970s W v. 2010s W***	***1990s W v. 2010s W***
Full Model	2011.2	9195.4	8960.6
Reduced Model	2021.8	9263.6	9013.6
Δ_i	10.6	68.2	53.0

List of References

Ailloud, L.E., M.V. Lauretta, J.M. Hoenig, J.F. Walter, and A. Fonteneau. 2014. Growth of Atlantic bluefin tuna determined from the ICCAT tagging database: a reconsideration of methods. ICCAT Collective Volume of Scientific Papers 70: 380-393.

Allendorf, F.W., P.R. England, G. Luikart, P.A. Ritchie, and N. Ryman. 2008. Genetic effects of harvest on wild animal populations. Trends in Ecology and Evolution 23: 327-337.

Allman, R. 2015. Unpublished data. NOAA Southeast Fisheries Science Center.

Anderson, C.N.K., C. Hsieh, S.A. Sandin, R. Hewitt, A. Hollowed, J. Beddington, R.M. May, and G. Sugihara. 2008. Why fishing magnifies fluctuations in fish abundance. Nature 452: 835-839.

Baglin, R.E. Jr. 1982. Reproductive biology of western Atlantic bluefin tuna. Fishery Bulletin 80: 121-134.

Bates, D., M. Maechler, B.M. Bolker, and S. Walker. 2014. lme4: Linear mixed-effects models using Eigen and S4. Journal of Statistical Software, URL: http://arxiv.org/abs/1406.5823.

Berkeley, S.A., M.A. Hixon, R.J. Larson, and M.S. Love. 2004. Fisheries sustainability ia protection of age structure and spatial distribution of fish populations. Fisheries 29: 23-32.

Birkeland, C., and P.K. Dayton. 2005. The importance in fishery management of leaving the big ones. Trends in Ecology and Evolution 20: 356-358.

Block, B. A., L. L. H. Teo, A. Walli, A. Boustany, M. J.W. Stokesbury, C. J. Farwell, K. C. Weng, H. Dewar, and T. D. Williams. 2005. Electronic tagging and population structure of Atlantic bluefin tuna. Nature 434:1121-1127.

Brenna, J.T., T.N. Corso, H.J. Tobias, and R.J. Caimi. 1997. High-precision continuous-flow isotope ratio mass spectrometry. Mass Spectrometry Reviews 16: 227-258.

Burnham, K.P. and D.R. Anderson. 2002. Model selection and multimodel inference: A practical information-theoretic approach. Second Edition.

Caddy, J.F., C.A. Dickson, and J.A. Butler. 1976. Age and growth of giant bluefin tuna (*Thunnus thynnus*) taken in Canadian waters in 1975. Journal of the Fisheries Research Board of Canada MS Rep. No. 1395.

Campana, S.E. 1999. Chemistry and composition of fish otoliths: pathways, mechanisms, and applications. Marine Ecology Progress Series 1888: 263-297.

Campana, S.E. 2001. Accuracy, precision and quality control in age determination, including a review of the use and abuse of age validation methods. Journal of Fish Biology 59: 197-242.

Carroll, M.T., J.L. Anderson, J. Martinez-Garmendia. 2001. Pricing US North Atlantic bluefin tuna and implications for management. Agribusiness 17: 243-254.

Conover, D.O., and S.B. Munch. 2002. Sustaining fisheries yields over evolutionary time scales. Science 297:94-96.

Conover, D.O., S.B. Munch, and S.A. Arnott. 2009. Reversal of evolutionary downsizing caused by selective harvest of large fish. Proceedings of the Royal Society: Biological Sciences 276: 2015-2020.

Cort, J.L., S. Deguara, T. Galaz, B. Mèlich, I. Artetxe, I. Arregi, J. Neilson, I. Andrushchenko, A. Hanke, M. Neves dos Santos, V. Estruch, M. Lutcavage, J. Knapp, G. Compeán-Jiménez, R. Solana-Sansores, A. Belmonte, D. Martínez, C. Picinetti, A. Di Natale, A. Kimoto, P. Addis, M. Velasco, J.M. de la Serna, D. Godoy, T. Ceyhan, A. López, O. Ribalta, N. Abid, M. Idrissi, and L. Nøttestad. 2013. Searching for the giant Atlantic bluefin tuna (*Thunnus thynnus*). ICCAT Collective Volume of Scientific Papers SCRS/2012/114.

Cui, L., and X. Wang. 2014. Determination of carbon and oxygen isotopes of geological samples with a complicated matrix: comparison of different analytical methods. Analytical Methods 6: 9173-9178.

Degens, E.T., W.G. Deuser, and R.L. Haedrich. 1969. Molecular structure and composition of fish otoliths. Marine Biology 2: 105-113.

Dickhut, R.M., A.D. Deshpande, A. Cincinelli, M.A. Cochran, S. Corsolini, R.W. Brill, D.H. Secor, and J.E. Graves. 2009. Atlantic bluefin tuna (*Thunnus* thynnus) population dynamics delineated by organochlorine tracers. Environmental Science & Technology 43: 8522-8527.

Dixon, P.A., M.J. Milicich, G. Sugihara. 1999. Episodic fluctuations in larval supply. Science 283: 1528-1530.

Edeline, E., S.M. Carlson, L.C. Stige, I.J. Winfield, J.M. Fletcher, J.B. James, T.O. Haugen, L.A. Bollestad, and N. Stenseth. 2007. Trait changes in a harvested population are driven by a dynamic tug-of-war between natural and harvest selection. Proceedings of the National Academy of Sciences 104: 15799-15804

Eggleston, D.B., E.A. Bochenek. 1990. Stomach contents and parasite infestation of school bluefin tuna *Thunnus thynnus* collected from the middle Atlantic Bight, Virginia. Fishery Bulletin 88: 389-395.

Elsdon, T.S., B.K. Wells, S.E. Campana, B.M. Gillanders, C.M. Jones, K.E. Limburg, D.H. Secor, S.R. Thorrold, and B.D. Walther. 2008. Otolith chemistry to describe movements and life-history parameters of fishes: hypotheses, assumptions, limitations and inferences. Oceanography and Marine Biology: An Annual Review 46: 297-330.

Estrada, J.A., M. Lutcavage, S.R. Thorrold. 2005. Diet and trophic position of Atlantic bluefin tuna (*Thunnus thynnus*) inferred from stable carbon and nitrogen isotope anlaysis. Marine Biology 147: 37-45.

Ferraz-Mello, S. 1981. Estimation of periods from unequally spaced observations. The Astronomical Journal 86: 619-624.

Fitzhugh, G.R., K.W. Shertzer, G.T. Kellison, and D.M. Wyanski. 2012. Review of size- and age-dependence in batch spawning implications for stock assessment of fish species exhibiting indeterminate fecundity. Fishery Bulletin 110: 413-425.

Fournier, D.A., H.J. Skaug, J. Ancheta, J. Ianelli, A. Magnusson, M.N. Maunder, A. Nielson, and J. Sibert. 2012. AD Model Builder: using automatic differentiation for statistical inference of highly parameterized complex nonlinear models. Optimization Methods and Software 27: 233-249.

Fromentin, J.M. 2009. Lessons from the past: investigating historical data from bluefin tuna fisheries. Fish and Fisheries 10: 197-216.

Fromentin, J.M., and J.E. Powers. 2005. Atlantic bluefin tuna: population dynamics, ecology, fisheries and management. Fish and Fisheries 6:281-306.

Fromentin, J.M., H. Arrizabalaga, V.R. Restrepo, and J. Ortiz de Urbina. 2007. Estimates of total mortality of Eastern Atlantic bluefin tuna abased on year-class curves. ICCAT Collective Volume of Scientific Papers 60: 928-936.

Fromentin, J.M., and V.R. Restrepo. 2009. A year-class curve analysis to estimate mortality of Atlantic bluefin tuna caught by the Norwegian fishery from 1956 to 1979. ICCAT Collective Volume of Scientific Papers 64: 480-490.

Fromentin, J.M., G. Reygondeau, S. Bonhommeau, and G. Beaugrand. 2014. Oceanographic changes and exploitation drive the spatiotemporal dynamics of Atlantic bluefin tuna. Fisheries Oceanography 23:147-156.

Garcia, S.M., J. Kolding, J. Rice, M.-J. Rochet. S. Zhou, T. Arimoto, J.E. Beyer, L. Borges, A. Bundy, D. Dunn, E.A. Fulton, M. Hall, M. Heino, R. Law, M. Makino, A.D. Rijnsdorp, F. Simard, and A.D.M. Smith. 2012. Reconsidering the consequences of selective fisheries. Science. 335:1045-1047.

Graves, J.E., A.S. Wozniak, R.M. Dickhut, M.A. Cochran, E.H. MacDonald, E. Bush, H. Arrizabalaga, and N. Goni. 2015. Transatlantic movements of juvenile Atlantic bluefin

tuna inferred from analyses of organochlorine tracers. Canadian Journal of Fisheries and Aquatic Sciences 72: 1-9.

Gunn, J.S., N.P. Clear, T.I. Carter, A.J. Rees, C.A. Stanley, J.H. Farley, J.M. Kalish. 2008. Age and growth in southern bluefin tuna, *Thunnus maccoyii* (Castelnau): Direct estimation from otoliths, scales, and vertebrae. Fisheries Research 92: 207-220.

Harris, P.J., and J.C. McGovern. 1997. Changes in the life history of red porgy, *Pagrus pagrus*, from the southeastern United States, 1972-1994. Fishery Bulletin 95: 732-747.

Hartley, H. 1949. Tests of significance in harmonic analysis. Biometrika 194-201.

Harvey, C.J., N. Tolimieri, and P.S. Levin. 2006. Changes in body size, abundance, and energy allocation in rockfish assemblages of the Northeast Pacific. Ecological Applications 16: 1502-1515.

Heinisch, G., H. Rosenfeld, J.M. Knapp, H. Gordin, and M.E. Lutcavage. 2014. Sexual maturity in western Atlantic bluefin tuna. Scientific Reports 4, 7205; DOI:10.1038/srep07205.

Hislop, J.R.G. 1988. The influence of maternal length and age on the size and weight of the eggs and the relative fecundity of the haddock, *Melanogrammus aeglefinus*, in British waters. Journal of Fish Biology 32: 923-930.

Hixon, M.A., D.W. Johnson, and S.M. Sogard. 2014. BOFFFFs: on the importance of conserving old-growth age structure in fishery populations. ICES Journal of Marine Science 71: 2171-2185.

Hoolihan, J.P., J. Luo, F.J. Abascal, S.E. Campana, G. De Metrio, H. Dewar, M.L. Domeier, L.A. Howey, M.E. Lutcavage, M.K. Musyl, J.D. Neilson, E.S. Orbesen, E.D. Prince, and J.R. Rooker. 2011. Evaluating post-release behaviour modification in large pelagic fish deployed with pop-up satellite archival tags. ICES Journal of Marine Sciences 68: 880-889.

Hsieh, C.H., S.M. Glaser, A.J. Lucas, and G. Sugihara. 2005. Distinguishing random environmental fluctuations from ecological catastrophes for the North Pacific Ocean. Nature 435: 336-340.

Hsieh, C.H., C.S. Reiss, J.R. Hunter, J.R. Beddington, R.M. May, and G. Sugihara. 2006. Fishing elevates variability in the abundance of exploited species. Nature 443: 859-862.

Hsieh, C.H., A. Yamauchi, T. Nakazawa, and W. Wang. 2010. Fishing effects on age and spatial structures undermine population stability of fishes. Aquatic Sciences 72: 165-178.

Hutchings, J. A. 2000. Collapse and recovery of marine fishes. Nature 406:882-885.

ICCAT. 2000. ICCAT Conversion Factors. http://www.iccat.int/documents/stats/convers.pdf.

Jennings, S., J.D. Reynolds, and S.C. Mills. 1998. Life history correlates of responses to fisheries exploitation. Proceedings of the Royal Society: Biological Sciences 265: 333-339.

Jennings, S., P.R. Greenstreet, and J.D. Reynolds. 1999. Structural change in an exploited fish community: a consequence of differential fishing effects on species with contrasting life histories. Journal of Animal Ecology 68: 617-627.

Jorgensen, C. K. Enberg, E.S. Dunlop, R. Arlinghaus, D.S. Boukal, K. Brander, B. Ernande, A. Gardmark, F. Johnson, S. Matsumara, H. Pardoe, K. Raab, A. Silva, A. Vainikka, U. Dieckmann, M. Heino, A.D. Rijnsdorp. 2007. Managing evolving fish stocks. Science 318: 1247-1248.

Kalish, J.M. 1989. Otolith microchemistry: validation of the effects of physiology, age and environment on otolith composition. Journal of Experimental Marine Biology and Ecology 132: 151-178.

Kalish, J.M. 1991. ^{13}C and ^{18}O isotopic disequilibria in fish otoliths: metabolic and kinetic effects. Marine Ecology Progress Series 75: 191-203.

Keeling, C.D. 1979. The Suess effect: ^{13}Carbon-^{14}Carbon interrelations. Environment International 2: 229-300.

Kerr, L.A., S.X. Cadrin, and D.H. Secor. 2012. Evaluating population effects and management implications of mixing between eastern and western Atlantic bluefin tuna stocks. ICES CM 2012/N:13.

Knapp, J.M., G. Aranda, A. Medina, and M. Lutcavage. 2014. Comparative assessment of the reproductive status of female Atlantic bluefin tuna from the Gulf of Mexico and the Mediterranean Sea. PLoS One 9: e98233.

Law, R. 2000. Fishing, selection, and phenotypic evolution. ICES Journal of Marine Science 57: 659-668.

Law, R. 2007. Fisheries-induced evolution: present status and future directions. Marine Ecology Progress Series 335: 249-251.

LeGrande, A.N., and G.A. Schmidt. 2006. Global gridded data set of the oxygen isotopic composition in seawater. Geophysical Research Letters 33: L12604.

Logan, J.M., E. Rodriquez-Marin, N. Goni, S. Barreiro, H. Arrizabalaga, W. Golet, and M. Lutcavage. 2011. Diet of young Atlantic bluefin tuna (*Thunnus thynnus*) in eastern and western Atlantic foraging grounds. Marine Biology 158: 73-85.

Lomb, N.R. 1976. Least-squares frequency analysis of unequally spaced data. Astrophysics and Space Science 39: 447-462.

MacKenzie, B.R., M.R. Payne, J. Boje, J.L. Hoyer, and H. Siegstad. 2014. A cascade of warming impacts brings bluefin tuna to Greenland waters. Global Change Biology 20: 2484-2491.

Marcek, B.J., and J.E. Graves. 2014. An estimate of post-release mortality of school-size bluefin tuna in the U.S. recreational troll fishery. North American Journal of Fisheries Management 34: 602-608.

Marteinsdottir, G. and A. Steinarsson. 1998. Maternal influence on the size and viability of Iceland cod *Gadus morhua* egs and larvae. Journal of Fish Biology 52: 1241-1258.

Mather, F.J., J.M. Mason, and A.C. Jones. 1995. Historical document: life history and fisheries of Atlantic bluefin tuna. National Oceanic and Atmospheric Agency Technical Memorandum NMFS-SEFSC 370.

McCrea, J.M. 1950. On the isotopic chemistry of carbonates and a paleotemperature scale. The Journal of Chemical Physics 18: 849-857.

Millar, R.B. 1990. A versatile computer program for mixed stock fishery composition estimation. Canadian Technical Report of Fishery and Aquatic Science No. 1753.

Millar, R.B. 2015. A better estimator of mortality rate from age-frequency data. Canadian Journal of Fisheries and Aquatic Sciences 72: 364-375.

Mulligan, T.J, and B.M. Leaman. 1992. Length-at-age analysis: can you get what you see? Canadian Journal of Fisheries and Aquatic Sciences 49: 632-643.

Mullon, C., J.G. Field, O. Thebaud, P. Cury, and C. Chaboud. 2012. Keeping the big fish: economic and ecological tradeoffs in size-based fisheries management. Journal of Bioeconomics 14: 267-285.

Myers, R.A., J.A. Hutchings, and N.J. Barrowman. 1996. Hypotheses for the decline of cod in the North Atlantic. Marine Ecology Progress Series 138: 293-308.

Myers, R.A, J.A. Hutchings, and N.J. Barrowman. 1997. Why do fish stocks collapse? The example of cod in Atlantic Canada. Ecological Applications 7: 91-106.

Myers, R.A., and B. Worm. 2003. Rapid worldwide depletion of predatory fish communities. Nature 423:280-283.

Mylonas, C.C., F. De La Gandara, A. Corriero, and A.B. Rios. 2010. Atlantic bluefin tuna (*Thunnus thynnus*) farming and fattening in the Mediterranean Sea. Reviews in Fisheries Science 18: 266-280.

Neilson, J.D., and S.E. Campana. 2008. A validated description of age and growth of western Atlantic bluefin tuna (*Thunnus thynnus*). Canadian Journal of Fisheries and Aquatic Sciences 65: 1523-1527.

Neilson, J.D., S. Smith, M. Ortiz, and B. Lester. 2009. Indices of stock status obtained from the Canadian bluefin tuna fishery. ICCAT Collective Volume Science Papers 64: 380-404.

Nemerson, D., S. Berkeley, and C. Safina. 2000. Spawning site fidelity in Atlantic bluefin tuna, *Thunnus thynnus*: the use of size-frequency analysis to test for the presence of migrant east Atlantic bluefin tuna on Gulf of Mexico spawning grounds. Fishery Bulletin 98: 118-126.

Overholtz, W.J. 1989. Density-dependent growth in the Northwest Atlantic stock of Atlantic mackerel (*Scomber scombrus*). Journal of Northwest Atlantic Fisheries Science 9: 115-121.

Overholtz, W.J. and K.D. Friedland. 2002. Recovery of the Gulf of Maine—Georges Bank Atlantic herring (*Clupea harengus*) complex: perspectives based on bottom trawl survey data. Fishery Bulletin 100: 593-608.

Overholtz, W.J. 2006. Estimates of consumption of Atlantic herring (*Clupea harengus*) by bluefin tuna (*Thunnus thynnus*) during 1970-2002: an approach incorporating uncertainty. Journal of Northwest Atlantic Fisheries Science 36: 55-63.

Patterson, W.P., G.R. Smith, and K.C. Lohmann. 1993. Continental paleothermometry and seasonality using the isotopic composition of aragonitic otoliths of freshwater fishes. *Climate change in continental isotopic records*: 191-202.

Paul, D., and G. Skrzypek. 2007. Assessment of carbonate-phosphoric acid analytical technique performed using GasBench II in continuous flow isotope ratio mass spectrometry. International Journal of Mass Spectrometry 262: 180-186.

Pauly, D. 1983. Some simple methods for the 1983 assessment of tropical fish stocks. FAO Fish.Tech.Pap 234: 52..

Pikitch, E.K., C. Santora, E.A. Babcock, A. Bakun, R. Bonfil, D.O. Conover, P. Dayton, P. Doukakis, D. Fluharty, B. Heneman, E.D. Houde, J. Link, P.A. Livingston, M. Mangel, M.K. McAllister, J. Pope, and K.J Sainsbury. 2004. Ecosystem-based fishery management. Science 305:346-347.

Porch, C.E. 2005. The sustainability of western Atlantic bluefin tuna: a warm-blooded fish in a hot-blooded fishery. Bulletin of Marine Science 76: 363-384.

Radtke, R.L. 1984. Cod fish otoliths: information storage structures. In *The propagation of Cod* Gadus morhua *L*. (E. Dahl, D.S. Danielssen, E. Moksness, and P. Solemdal) 273-298.

Radtke, R.L., and B. Morales-Nin. 1989. Mediterranean juvenile bluefin tuna: life history patterns. Journal of Fish Biology 35:485-496.

Radtke, R.L., D.W. Townsend, S.D. Folsom, and M.A. Morrison. 1990. Strontium:calcium concentration ratios in otoliths of herring larvae as indicators of environmental histories. Environmental Biology of Fishes 27: 51-61.

Radtke, R.L., W. Showers, E. Moksness, and P. Lenz. 1996. Environmental information stored in otoliths: insights from stable isotopes. Marine Biology 127: 161-170.

Ravier, C. and J.-M. Fromentin. 2001. Long-term fluctuations in the Eastern Atlantic and Mediterranean bluefin tuna population. ICES Journal of Marine Science 58: 1299-1317.

Ravier, C. and J.-M. Fromentin. 2004. Are the long-term fluctuations in Atlantic bluefin tuna (*Thunnus thynnus*) population related to environmental changes? Fisheries Oceanography 13: 145-160.

Restrepo, V.R., G.A. Diaz, J.F. Walter, J.D. Neilson, S.E. Campana, D. Secor, and R.L. Wingate. 2010. Updated estimate of the growth curve of Western Atlantic bluefin tuna. Aquatic Living Resources 23: 335-342.

Ricker, W.E. 1981. Changes in the average size and average age of Pacific salmon. Canadian Journal of Fisheries and Aquatic Sciences 38: 1636-1656.

Rivas, L.R. 1976. Variation in sex ratio, size differences between sexes, and change in size and age composition in western North Atlantic giant bluefin tuna (*Thunnus thynnus*). ICCAT Collective Volume of Scientific Papers 5: 297-301.

Rodriguez-Marin, E. N. Clear, J.L. Cort, P. Megalofonou, J.D. Neilson, M. Neves dos Santos, D. Olafsdottir, C. Rodriguez-Cabello, M. Ruiz, and J. Valeiras. 2006. Report of the 2006 ICCAT workshop for bluefin tuna direct ageing. ICCAT Collective Volume Science Papers 60(4): 1349-1392.

Rooker, J.R., D.H. Secor, G. De Metrio, and E. Rodriquez-Marin. 2006. Evaluation of population structure and mixing rates of Atlantic bluefin tuna from chemical signatures in otoliths. ICCAT Collective Volume Science Papers 59: 813-818.

Rooker, J.R., J.R. Alvarado-Bremer, B.A. Block, J.L. Cort, H. Dewar, G. DeMetrio, R.T. Kraus, E.D. Prince, E. Rodriquez-Marin, D.H. Secor. 2007. Life history and stock structure of Atlantic bluefin tuna (*Thunnus thynnus*). Reviews in Fisheries Science 15:265-310.

Rooker, J.R., D.H. Secor, G. D. DeMetrio, R. Schloesser, B.A. Block, and J.D. Neilson. 2008. Natal homing and connectivity in Atlantic bluefin tuna populations. Science 322: 742-744.

Rooker, J.R., H. Arrizabalaga, I. Fraile, D.H. Secor, D.L. Dettman, N. Abid, P. Addis, S. Deguara, F.S. Karakulak, A. Kimoto, O. Sakai, D. Macias, M.N. Santos. 2014. Crossing the line: migratory and homing behaviors of Atlantic bluefin tuna. Marine Ecology Progress Series 504: 265-276.

Rouyer, T., A. Sadykov, J. Ohlberger, and N.C. Stenseth. 2012. Does increasing mortality change the response of fish populations to environmental fluctuations? Ecology Letters 15: 658-665.

Ruf, T. 1999. The Lomb-Scargle periodogram in biological rhythm research: analysis of incomplete and unequally spaced time-series. Biological Rhythm Research 30: 178-201.

Safina, C., and D.H. Klinger. 2008. Collapse of bluefin tuna in the Western Atlantic. Conservation Biology 22: 243-246.

Scargle, J.D. 1982. Studies in astronomical time series analysis. II. Statistical aspects of spectral analysis of unevenly spaced data. The Astrophysical Journal 263: 835-853.

Schloesser, R.W., J.R. Rooker, P. Louchuoarn, J.D. Neilson, and D.H. Secor. 2009. Interdecadal variation in seawater for $\delta^{13}C$ and $\delta^{18}O$ recorded in fish otoliths. Limnology and Oceanography 54(5): 1665-1668.

Schloesser, R.W., J.D. Neilson, D.H. Secor, and J.R. Rooker. 2010. Natal origin of Atlantic bluefin tuna (*Thunnus thynnus*) from Canadian waters based on otolith for $\delta^{13}C$ and $\delta^{18}O$. Canadian Journal of Fisheries and Aquatic Science 67: 563-569.

Schmidt, G.A., G.R. Bigg, and R.J. Rohling. 1999. Global Seawater Oxygen-18 Database – v1.21. http://data.giss.nasa.gov/o18data/

Schneider, R.C., and S.V. Smith. 1982. Skeletal Sr content and density in *Porites* spp. In relation to environmental factors. Marine Biology 66: 121-131.

SCRS (Standing Committee on Research and Statistics, International Commission for the Conservation of Atlantic Tunas). 2012. Report of the 2012 Atlantic bluefin tuna stock assessment session. Madrid. Available from http://www.iccat.es/en/assess.html.

SCRS (Standing Committee on Research and Statistics, International Commission for the Conservation of Atlantic Tunas). 2014. Report of the 2014 Atlantic bluefin tuna stock assessment session. Madrid. Available from http://www.iccat.es/en/assess.html.

Secor, D.H. 2000. Longevity and resilience of Chesapeake Bay striped bass. ICES Journal of Marine Science 57: 808-815.

Secor, D.H. 2000. Spawning in the nick of time? Effect of adult demographics on spawning behavior and recruitment in Chesapeake Bay striped bass. ICES Journal of Marine Science 57: 403-411.

Secor, D.H. 2007. The year-class phenomenon and the storage effect in marine fishes. Journal of Sea Research 57:91-103.

Secor, D.H. 2010. Is otolith science transformative? New views on fish migration. Environmental Biology of Fishes 89: 209-220.

Secor, D.H. 2014. Synopsis of regional mixing levels for Atlantic bluefin tuna estimated from otolith stable isotope analysis, 2007-2014. ICCAT Collective Volume Science Papers.

Secor, D.H. 2015. Migration ecology of marine fishes. Johns Hopkins University Press, Baltimore.

Secor, D.H., S.E. Campana, V.S. Zdanowicz, J.W.H. Lam, L. Yang, and J.R. Rooker. 2002. Inter-laboratory comparison of Atlantic and Mediterranean bluefin tuna otolith microconstituents. ICES Journal of Marine Science 59: 1294-1304.

Secor, D.H., R. Allman, D. Busawon, B. Gahagan, W. Golet, E. Koob, P. Lastra Luque, and M. Siskey. 2014. Standardization of otolith-based ageing protocols for Atlantic bluefin tuna. ICCAT Collective Volume of Scientific Papers SCRS/2013/084.

Secor, D.H., D. Busawon, B. Gahagan, W. Golet, E. Koob, J. Neilson, and M. Siskey. 2014. Conversion factors for Atlantic bluefin tuna fork length from measures of snout length and otolith mass. ICCAT Collective Volume of Scientific Papers 70: 364-367.

Secor, D.H., J.R. Rooker, B.I. Gahagan, M.R. Siskey, and R. W. Wingate. 2015. Depressed resilience of bluefin tuna in the Western Atlantic and age truncation. Conservation Biology 29: 400-408.

Sinclair, A.F., D.P. Swain, and J.M. Hanson. 2002. Disentangling the effects of size-selective mortality, density, and temperature on length-at-age. Canadian Journal of Fisheries and Aquatic Sciences 59: 372-382.

Smith, S.V., R.W. Buddemeier, R.C. Redalje, and J.E. Houck. 1979. Strontium-calcium thermometry in coral skeletons. Science 204: 404-406.

Solomon, C.T., P.K. Weber, J.J. Cech Jr., B.L. Ingram, M.E. Conrad, M.V. Machavaram, A.R. Pogodina, and R.L. Franklin. 2006. Experimental determination of the sources of otolith carbon and associated isotopic fractionation. Canadian Journal of Fisheries and Aquatic Sciences 63: 79-89.

Spotl, C. and T.W. Vennemann. 2003. Continuous-flow isotope ratio mass spectrometric analysis of carbonate minerals. Rapid Communications in Mass Spectrometry 17: 1004-1006.

Stokesbury, M.J.W., J.D. Neilson, E. Susko, and S.J. Cooke. 2011. Estimating mortality of Atlantic bluefin tuna (*Thunnus thynnus*) in an experimental recreational catch-and-release fishery. Biological Conservation 144: 2684-2691.

Swain, D.P., A.F. Sinclair, and J.M. Hanson. 2007. Evolutionary response to size-selective mortality in an exploited fish population. Proceedings of the Royal Society B 274: 1015-1022.

Swart, P.K, S.J. Burns, and J.J. Leder. 1991. Fractionation of the stable isotopes of oxygen and carbon in carbon dioxide during the reaction of calcite with phosphoric acid as a function of temperature and technique. Chemical Geology (Isotope Geoscience Section) 86: 89-96.

Tanaka, S. 2006. Maturation of bluefin tuna in the Sea of Japan. ISC PBF-WG/06/Doc.9.

Taylor, N.G., M.K. McAllister, G.L. Lawson, T. Carruthers, B.A. Block. 2011. Atlantic bluefin tuna: a novel multistock spatial model for assessing population biomass. PLoS One 6: e27693.

Thorrold, S.R., C.M. Jones, and S.E. Campana. 1997. Response of otolith microchemistry to environmental variations experienced by larval and juvenile Atlantic croaker (*Micropogonias undulatus*). Limnology and Oceanography 42: 102-111.

Trippel, E.A. 1995. Age at maturity as a stress indicator in fisheries. BioScience 45: 759-771.

Verburg, P. 2007. The need to correct for the Suess effect in the application of $\delta^{13}C$ in sediment of autotrophic Lake Tanganyika as a productivity proxy in the Anthropocene. Journal of Paleolimnology 37: 591-602.

Walli, A., S.L.H. Teo, A. Boustany, C.J. Farwell, T. Williams, H. Dewar, E. Prince, and B.A. Block. 2009. Seasonal movements, aggregations and diving behavior of Atlantic bluefin tuna (*Thunnus thynnus*) revealed with archival tags. PLoS One 4: e6151.

Warner, R.R. and P.L. Chesson. 1985. Coexistence mediated by recruitment fluctuations: a field guide to the storage effect. American Naturalist 125: 769-787.

Winemiller, K.O. and K.A. Rose. 1992. Patterns of life-history diversification in North American fishes: implications for population regulation. Canadian Journal of Fisheries and Aquatic Sciences 49: 2196-2218.

Worm, B., R. Hilborn, J.K. Baum, T.A. Branch, J.S. Collie, C. Costello, M.J. Fogarty, E.A. Fulton, J.A. Hutchings, S. Jennings, O.P. Jensen, H.K. Lotze, P.M. Mace, T.R. McClanahan, C. Minto, S.R. Palumbi, A.M. Parma, D. Richard, A.A. Rosenberg, R. Watson, and D. Zeller. 2009. Rebuilding global fisheries. Science 325:578-585.

Wright, P.J. and E.A. Trippel. 2009. Fishery-induced demographic changes in the timing of spawning: consequences for reproductive success. Fish and Fisheries 10: 283-304.